WAVE REFLECTION AND TRANSMISSION IN CHANNELS OF GRADUALLY VARYING DEPTH

by

A. T. Ippen, A. M. Z. Alam and E. L. Bourodimos

HYDRODYNAMICS LABORATORY

Report No. 72

DEPARTMENT OF CIVIL ENGINEERING

SCHOOL OF ENGINEERING
MASSACHUSETTS INSTITUTE OF TECHNOLOGY
Cambridge 39, Massachusetts

July, 1964

R64-31

HYDRODYNAMICS LABORATORY

Department of Civil Engineering

Massachusetts Institute of Technology

WAVE REFLECTION AND TRANSMISSION IN CHANNELS

OF GRADUALLY VARYING DEPTH

by

A.T. Ippen, A.M.Z. Alam and E.L. Bourodimos

July 1964

Report No. 72

ACKNOWLEDGEMENTS

ABSTRACT

This report presents the results of a study on the reflection and transmission of water waves in a rectangular channel with transitions of linearly varying depths. Two channel sections of uniform depths are joined by sections of slopes 1:0.58, 1:2.75 and 1:16 in the three sets of experiments. Wave conditions were systematically varied to cover the range of deep-water to shallow-water waves in the deeper approach channel. The pertinent parameters considered for each slope were relative depth (ratio of upstream to downstream depth), ratio of group velocities and wave steepness. Since a comprehensive theory does not exist, the classical small wave amplitude theory for abrupt transitions was employed to correlate the results of the study. Comparisons with other theories developed recently were made where applicable.

Some of the important conclusions are:

1. For short and intermediate waves reflection coefficients become generally larger than predicted as the slope of the transition decreases.

2. For short and intermediate waves transmission coefficients generally agree with predictions for group velocity ratios near unity, but tend to lower values for lower ratios of group velocity as the slope of the transition decreases.

3. For short and intermediate waves wave steepness has a relatively small influence on reflection and transmission coefficients.

4. For shallow water waves the reflection coefficients were found independent of relative depth ratios contrary to prediction but decreased markedly with increasing wave steepness for the smallest slope.

5. For shallow water waves the transmission coefficients followed the predicted trend, but became relatively lower for increasing relative depth ratios. Increasing wave steepness had the effect of increasing the transmission coefficients for the smallest slope.

TABLE OF CONTENTS

TABLE OF CONTENTS (cont'd)

LIST OF TABLES

LIST OF FIGURES

LIST OF FIGURES (cont'd)

LIST OF NOTATIONS

A	cross-sectional area of flow, ft^2
a_i, a_r, a_t	amplitude of incident, reflected, and transmitted waves, respectively, ft or cm
a	measured wave amplitude, ft or cm
a'	transformed wave amplitude valid for comparison with theory, ft or cm
a_o	deep water wave amplitude, ft or cm
b	width of wave channel, ft
C	wave velocity or celerity, ft/sec
C_o	deep water wave velocity or celerity, ft/sec
C_G	group velocity, ft/sec
E	average wave energy per unit surface area $= \gamma\dfrac{a^2}{2}$
e	base of natural logarithm
g	gravitational acceleration, ft/sec^2
H	wave height $= 2a$, ft
H_o	deep water wave height $= 2a_o$, ft
h	mean water depth, ft
J_n	Bessel function of first kind, $n = 0,1$
$K_r = \dfrac{a_r}{a_i}$	reflection coefficient, dimensionless
$K_t = \dfrac{a_t}{a_i}$	transmission coefficient, dimensionless
k	wave number $= 2\pi/L$, ft^{-1}
L	wavelength, ft
L_o	deep water wave length, ft
ℓ	length dimension, defined where used, ft.

n_n	dimensionless parameter for wave group velocity
n	positive set of integers: 0,1,2,3,etc.
p	pressure intensity, lb/ft^2
Q	volume rate of flux, ft^3/sec
t	time, sec
T	wave period, sec
u	horizontal velocity, ft/sec
x	horizontal coordinate, ft
Y_n	Bessel function of second kind, $n = 0,1$
Z	vertical coordinate, positive upward, ft
β	parameter defined as $(\sigma^2 x_2)/(gh_3)$, ft^{-1}
Δ	term involving Bessel functions, as defined
δ	angular phase shift, radians
ρ	mass density of fluid, $slugs/ft^3$
η, η_n	displacement of instantaneous water surface, ft
η_i, η_r, η_t	instantaneous displacement of water surface above or below mean water level for incident, reflected, and transmitted waves, respectively, ft
μ	term involving Bessel functions, as defined
ν	term involving Bessel functions, as defined
σ	angular frequency $= 2\pi/T$, sec^{-1}
π	numerical constant $= 3.1416$

I. STATEMENT AND BACKGROUND OF PROBLEM

1.1 General Discussion of Wave Reflection and Transmission Phenomena

The general problem of modification of a train of water waves by a
channel of varying cross section with distance is one with several interesting
and useful applications. Examples of this general class of problems are
ocean waves moving onto the continental shelf, the shoaling of waves on
the beach, and the transmission of waves into estuaries of various
configurations. This problem is central to the whole field of coastal
engineering because the transformations waves undergo as they approach a
shoreline determine the type and degree of breakwater and harbor protection
required. Also the increased use of embayment and estuary shorelines by
man makes it necessary to predict accurately the amplitudes of waves
incident upon the shoreline, particularly so in regions occasionally subject
to hurricanes and tidal waves causing loss of life and property.

1.2 Review of Previous Work

The one-dimensional propagation of waves in a continuous medium has
been studied extensively since the 19th century (1) and the reflection and
transmission coefficients of waves are given for the case of an abrupt change
of channel geometry, and also for certain particular types of the variation
of the geometry.

Stoker (2) has presented the behavior of a train of waves moving over
a sloping beach and also dealt with the resulting phenomena, e.g., waves
of translation, breaking of waves, long-shore currents, etc.

The effects of an abrupt change in channel geometry on waves are given
by Lamb (3). From energy and continuity considerations, reflection and
transmission coefficients are derived in terms of wave properties and channel
geometry. A formula for the reflection coefficient from a smooth beach of
constant slope has been given by Miche (4) which seems to predict the
approximate value. The Miche formula has been verified in part, by
experimental measurements by Ursell, Dean, and Yu (5). Theory and experiment
have been found to be in reasonable agreement.

Kajiura (7) has studied the partial reflection of water waves passing
over a channel of continuously and non-linearly varying depth. Considering
that the waves are of small amplitude, he has shown that for long waves
the effect of the transition on reflection becomes smaller with an
increasing ratio of the length of transition to the incident wavelength.
For small values of the ratio of the length of transition to the incident
wavelength (less than 1/20) the reflection and the transmission coefficients
can be reasonably predicted by the well known formula for an abrupt transition.
He also concluded that for weak reflection the transmitted wave can be
approximated by Green's Formula, even though part of the energy is continuously
reflected.

1

Perroud (8) treated the same problem under the assumptions of shallow water waves propagating into channels of linearly or exponentially varying cross-section including the effect of linear frictional resistance, the coefficient of which is assumed constant throughout the channel. This assumption of frictional resistance leads to an exponentially decreasing law of the amplitude as known for a uniform channel. Hence this approach is merely an extension of the latter solution without furthering the physical insight into the problem.

Evangelisti (9) has studied the problem of propagation of shallow water waves in a straight channel with the assumptions of monotonous variations of breadth and width $b(x) = K_1 X^\alpha$ and $h(x) = K_2 X^\beta$ respectively ignoring the influence of friction (nonviscous fluid). (K_1, K_2, α, β arbitrary constants). He presented a solution of the wave propagated in such a channel in terms of Hankel functions. This general solution without considering damping permits calculation of the corrections over the solution for the case of small amplitude variations within a wave length. His solution reduces to the well-known Green's law for the latter condition.

Dean (10) has studied theoretically the reflection and transmission phenomena under the assumption of shallow water waves and small amplitude linearized theory, without friction and energy dissipation in channels of a) linearly varying depth, b) linearly varying width, c) combination of a and b. He presented the reflection and transmission coefficient for each case in terms of Bessel functions and channel geometry.

Some of the reflection and transmission coefficients for shallow water waves obtained in the present study are compared with those predicted by Dean (10).

It is found that the reflection coefficients differ considerably from the theoretical values whereas the transmission coefficients follow the trend predicted by the theory, while differing in magnitude. The experimental reflection coefficients for shallow water waves are found to decrease significantly with increasing wave steepness while the transmission coefficients increase with increasing wave steepness for the slope of 1:16.

1.3 The Present Study

The travel of water waves over a bottom of variable depth is affected by refraction, reflection and transmission. Complications are further augmented by energy dissipation. For very small slopes waves may be refracted on the assumption of zero reflection considering negligible dissipation or assuming suitable friction losses in the shallow water range. When slopes become steeper or channel widths are reduced rapidly, reflection effects should be considered, however no adequate theory exists at present to take account of this problem. At the other extreme, of abrupt transitions in either depth or width the classical theory is applied, based on small amplitude assumptions, conservation of energy and continuity. This approach must necessarily be subject to question in the intermediate range when

2

gradual transitions in width and depth are encountered. In addition, variations in wave steepness may modify the reflection and transmission characteristics in a transition.

The review of the available literature in the preceding section has shown that a general treatment of the problem is still missing due to the difficulties in comprehensive theoretical formulation. Such a formulation should comprise consideration of transitions for the entire spectrum of waves in the approach range from "deep water" waves through intermediate water waves to shallow water waves. To determine the general characteristics of this wave reflection and transmission problem only the experimental approach seems feasible at this time. While providing valuable information necessary for practical purposes, it also delimits the range of applicability of existing approximate theories and defines the physical conditions for future theoretical studies. The present study was therefore planned to explore the phenomena over as wide a range of conditions as could be met with the experimental equipment.

The wave channel in the Hydrodynamics Laboratory was divided for this study into two rectangular sections of different uniform depth connected by a transition of linearly varying depth. Three such transitions were employed with slopes of 1:.58 (60°), 1:2.75 (20°), and 1:16 (3.57°). The arrangement of these transitions is illustrated in Figures 1 and 2 and the detailed description is given in the following sections.

The wave conditions in the approach channel were varied from the "deep water" type to the "shallow water" type by means of a flap-type and of a piston type wave maker respectively. By varying the water depth in the wave channel, different ratios of depth between the deeper upstream section and the shallower downstream section of the channel could be established. The experiments could thus be conducted over a wide range of the governing parameters: ratio of wave length to depth, wave steepness, transition slope and relative length, and relative depth ratio.

II. EXPERIMENTAL EQUIPMENT

2.1 General Description of Wave Tank

The wave channel and associated equipment with which the experiments
were carried out are shown schematically in Figure 1. The wave channel
is of rectangular cross section and is 100 feet long, 2.5 feet wide, and
3 feet deep. The walls over the entire length and 40 feet of the bottom
of the channel are plate glass and the remainder of the bottom is of steel.
At one end of the channel there are: a piston type wave maker with continuously
variable stroke and frequency and a flap type wave maker; at the other end
energy absorbers are placed to reduce the effect of reflection from this
end to a minimum. Near the wave maker, an expanded aluminum filter is located
to smooth out minor wave disturbances.

a. The first test program was conducted with linearly sloping transitions of
1:0.58 (60°) and 1:2.75 (20°). The toe of each of these transitions was
40 feet from the wave maker, the transition and the section of low depth were
20.17 feet in length, terminating with an abrupt increase to the initial
depth in the channel as shown schematically in Figure 1. At the end of the
wave channel after a section of uniform depth 13.50 feet in length the
energy was dissipated by a beach of 1:16 and an aluminum wool wave absorber.
However small reflections were still experienced and had to be considered in
the data reduction process. In these tests a flap-type wave maker was used
predominantly.

b. The second more detailed test program was carried out with a transition
of slope 1:16 (3.57°) in the same position, however the beach at the end was
eliminated and the section of reduced depth was extended nearer to the end of
the wave channel. A tubular wave dissipator followed by an aluminum wool ab-
sorber were placed in the short end section of larger depth. Both the
piston-type and the flap-type wave makers were employed in this part of the
program. For the measurement of wave amplitudes two resistance type wave
gauges were employed, which were mounted on two self-propelled carriages
travelling slowly along the channel, one upstream and the other downstream of
the transition. The carriages moved along carefully levelled rails on top
of the channel sides, so that the gauges measured the time averaged envelopes
of the wave amplitudes, which were recorded by a Sanborn oscillograph
(Model 150). Each of the carriages is equipped with an electrical circuit to
locate the position along the channel at any time. The circuit is actuated
every 0.25 feet by a small brass strip making contact with one of the rails
on which the carriage is moving.

2.2 Wave Makers

1. The piston type wave maker shown in Figure 5a consists of an
aluminum plate with its plane oriented perpendicular to the axis of the wave
channel and oscillating in a direction parallel to the axis of the wave channel
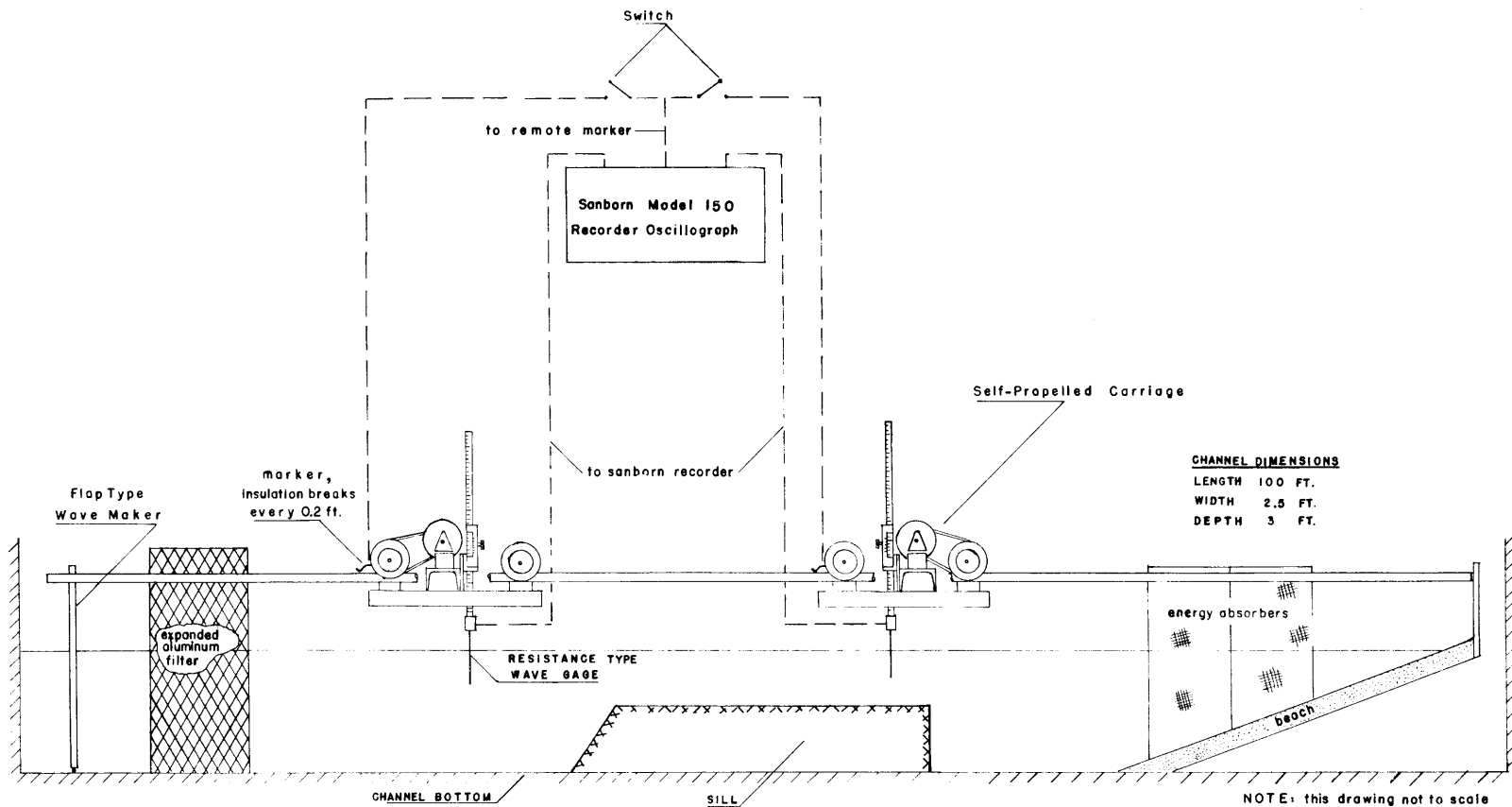
Fig. 1 — Functional sketch of experimental equipment.
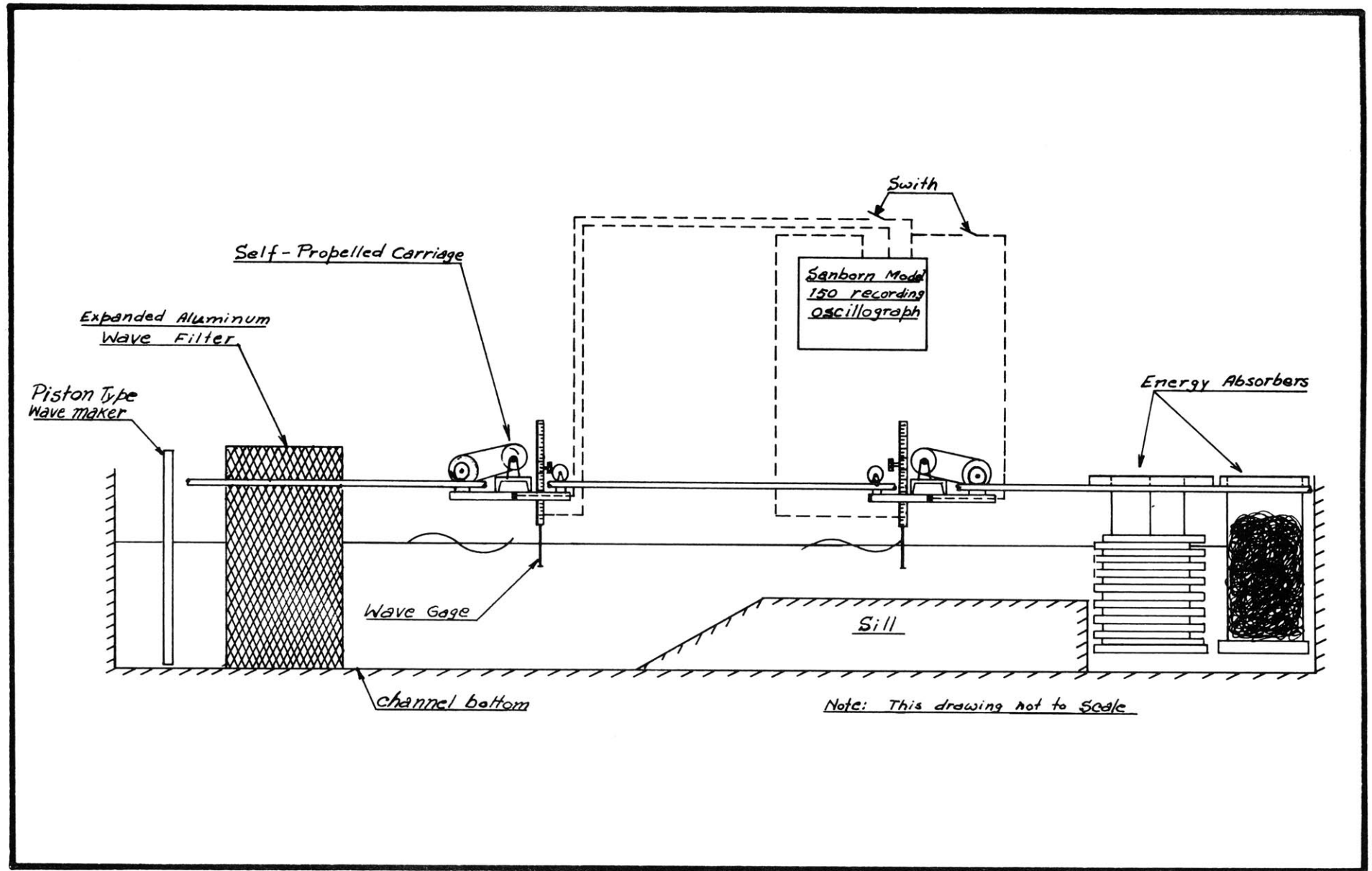
Fig·2 Schematic Diagram of Experimental Equipment

(Figure 3). This wave maker plate is fastened to a carriage, moving on
rails on the sides of the channel. The carriage is driven back and forth
horizontally by a reciprocating piston which is hydraulically driven. There
is a small clearance of approximately 1/4 inch between the edges of the wave
maker plate and the side walls and the bottom of the channel; the clearance
was closed by an adjustable sponge rubber seal, thereby minimizing any effects
due to leakage around the edges of the wave maker.

The motion of the piston is controlled by a hydraulic servo-mechanism
system. The shaft of the double-acting cylinder is connected directly to the
carriage from which the wave maker plate is suspended. Flow of oil under
pressure into and out of the two chambers of the double-acting cylinder drives
the wave maker and is metered by a valve, the output of which is prescribed
by a rotating cam acting through a mechanical leverage system, magnifying
the input from the cam. The linear displacement of the wave maker with time is
designed to be the same (except for a scale factor) as the angular variation
of the distance from the surface of the cam to the rotational axis of the cam
(Figure 4). By use of different cams, each with a different control surface,
the motion of the wave maker can, in principle, be given any desired periodic
form. In practice, with a simple harmonic cam, the motion of the wave maker
is not quite harmonic but tends to some irregularities due to frictional
forces (particularly at lower frequencies). This irregularity in the motion
had previously been traced to frictional forces in the end seals of the double-
acting cylinder and is particularly pronounced at the ends of the stroke,
where the frictional forces are static rather than sliding. To eliminate
the effect of static friction, a motor and reducer were used to continuously
rotate the shaft of the piston, within the end seals, thereby reducing the
frictional forces to their sliding value at all time.

These precautions were effective in eliminating much of the effect of the
higher harmonics; however, some irregularity in the wave motion remained.

2. The flap-type wave maker consists of an aluminum plate, 32 inches
in height and occupying the whole width of the channel; on each side of the
plate, the clearance between this plate and the glass walls is small, so that
the leakage has negligible effects, even at high speeds. The small transverse
waves generated by this leakage are rapidly dissipated by friction on the
sides of the channel but mostly by the subsequent filter, so that no effect
was felt after the filter. The aluminum plate is hinged at the bottom of the
channel perpendicularly to its axis. The pendulum motion of the plate is
provided by an arm, which has one end fixed to the center of the top of the
plate, and the other end fixed to a block rotating eccentrically on a small
wheel. The shaft of this wheel is acted upon by a variable speed motor to
which it is connected by a V-type belt. A diagram in figure 6 illustrates
the functioning of this wave maker schematically. The eccentric block on
the rotating wheel slides through a fillet rod, to which a revolution
counter is attached. The eccentricity of the block can be set at predetermined
values and repeated very accurately. The motor is an A.C. variable speed

Schematic Diagram of Wave Generator

Cylinder (g)

(p)

Clevis

Feedback Arm (m)

Bushings

Pivot (n)

Valve

Pivot

(f) Control Valve

Cam Follower (l)

Valve stem (o)

Cam (i)

(j) (k) Gear box

Cam drive motor

Cool Water in

Relief Valve

(e)

High Pressure Filter

(d)

Check Valve

Heat Exchanger (h)

Hot Water Out

Reservoir

Strainer

(c)

(b)

Motor (a)

Pump

Carria

Solid lines repr

mechanical link

Dashed lines re

hydraulic system

From : Hydrod

Laboratory TF

MIT.

Fig· 3

NEUTRAL CIRCLE

CENTER OF ROTATION

FOLLOWER ARM

r_{min}

r_{max}

t_1

t_2

T

t

SKETCH OF CONTROL CAM

SINUSOIDAL CURVES

S(STROKE)

$r_{max.}$

NEUTRAL POSITION

$S/2$

$r_{min.}$

t

t_1

t_2

T(TOTAL CYCLE TIME AND WAVE PERIOD)

MOTION IMPARTED TO PLUNGER

From Hydro· Lab· T.R. No.24. MIT.

Fig. 4   Wave Generator Cam Schematic

9

"Speed Ranger", combined with a reducer; the output speed can be varied continuously from 19 rpm to a maximum of 250 rpm. The output speed is held fairly constant, provided that the reduction system and the oil bath in which it is rotating, have attained a constant temperature, which is reached after about 1/2 hour. This could be verified by the special equipment used to determine the wave period as described below.

This arrangement consists of a thin aluminum circular plate, 26 inches in diameter, affixed to the other end of the shaft on which the eccenter wheel is mounted. This plate is perforated with 400 equally-spaced holes on a circle near its periphery. A light source is focused on this circle.so that with the passage of each hole a light signal hits a photoelectric cell on the other side. The corresponding electric impulse is relayed to a Hewlett-Packard electronic counter. The total number of counts is registered during an interval of 1/10, 1 or 10 seconds. The desired period can be obtained with an accuracy of $\pm$ 0.2 $^\circ$/o, which includes the variation in the number of electric impulses recorded and the error inherent in the counter itself. Figure 6 shows, in a schematic way, the arrangement of the whole set up.

2.3 Wave Filters and Energy Dissipators

The waves generated by the wave maker tend to be somewhat disturbed due to the presence of higher harmonics of the fundamental wave motion, and also by the presence of small transverse waves at higher speeds of the piston or flap. To eliminate these effects a wave filter, illustrated in Figure 7b, is placed about 8 feet from the piston wave maker. The filter is made of thin expanded aluminum sheets hung from a wooden frame resting on the side walls of the wave tank. This filter eliminates the higher harmonics and irregularities to a great extent by damping.

The length of the wave tank being finite, the wave component transmitted over the gradual transition would be reflected back from the far end of the tank. To eliminate this reflection as much as possible, energy dissipators were employed. Two energy dissipators placed in series were used for this purpose. For the type of steeper transitions illustrated in Figure 1 with the abrupt downstream end the purpose of energy dissipation was served by a beach of slope 1:16 and by two wire mesh baskets in series filled with aluminum wool. The amplitude of the reflected wave from the beach was found in a range 0.005 - 0.018 feet. For the more gradual transition represented in Figure 2 the first of the dissipators consisted of an array of open tubes aligned with the direction of wave motion and occupying approximately 30-40 per cent of the section through which the waves pass. The characteristic of this dissipator is that it dissipates the major portion of the wave energy by currents induced in the tubes and generating turbulence at the tube exits by surface resistance and by interference with energy transmission through the array of tubes.

The second of the energy dissipators consisted of a basket, 4-1/2 feet long, placed along the length of the channel, behind the first dissipator.

10
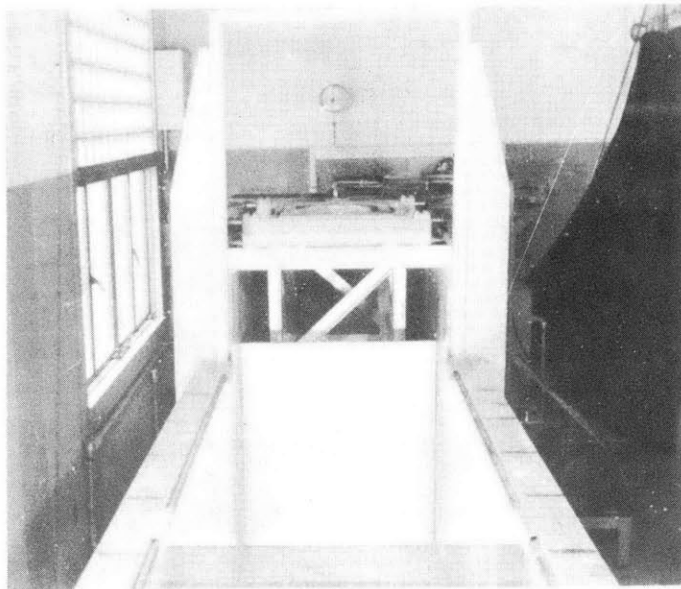
Figure 5a Wave Generator
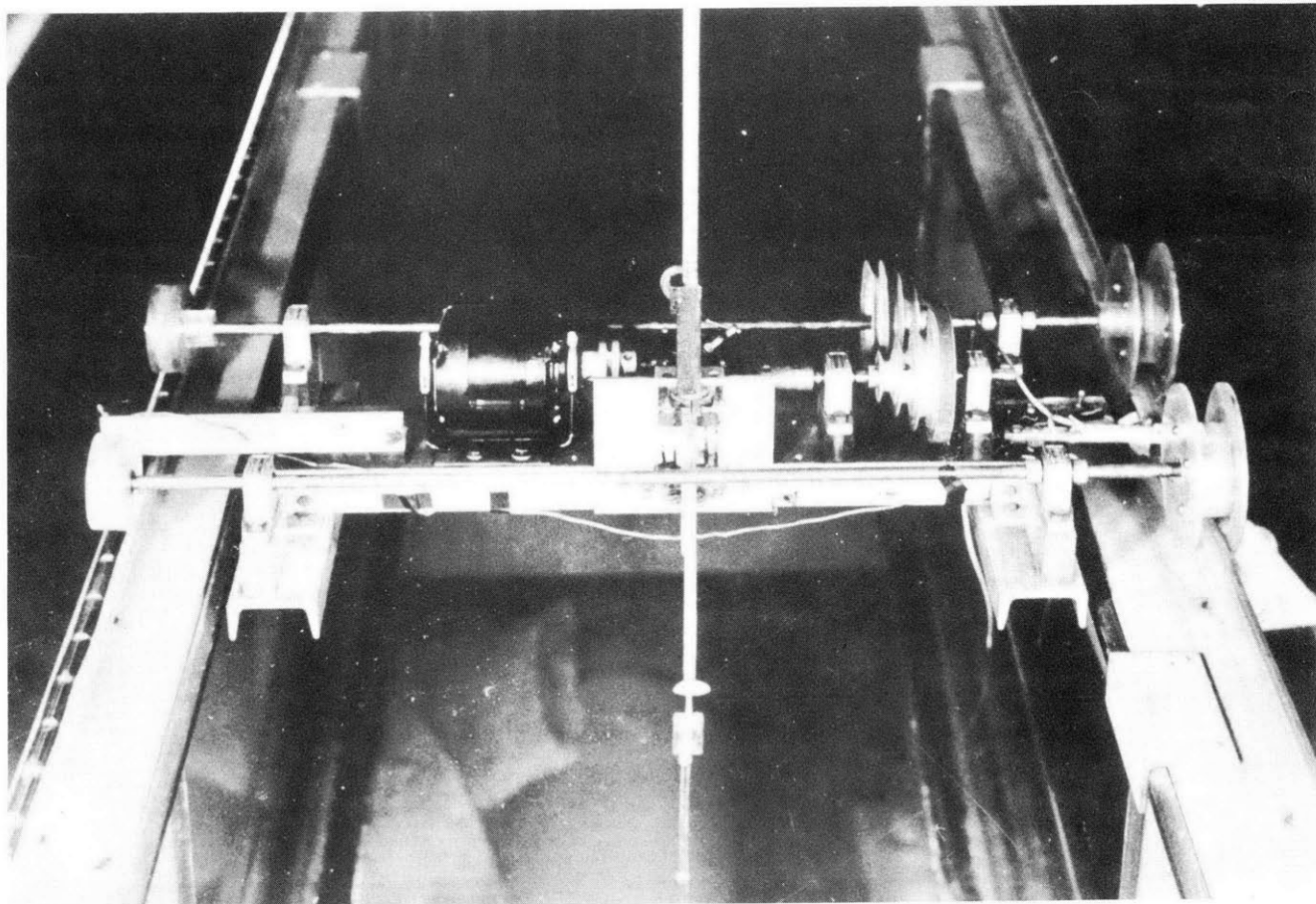
Figure 5b Wave Gage Carriage

Bar

Eccenter Wheel

Plate

V-belt Transmission

Hinge

Channel Bottom

Motor

Floor

Elevation

Photoelectric Cell

Light Source

Disc

Eccenter Wheel

Shaft

V-belt Transmission

Hewlett-Packard
Electronic Counter
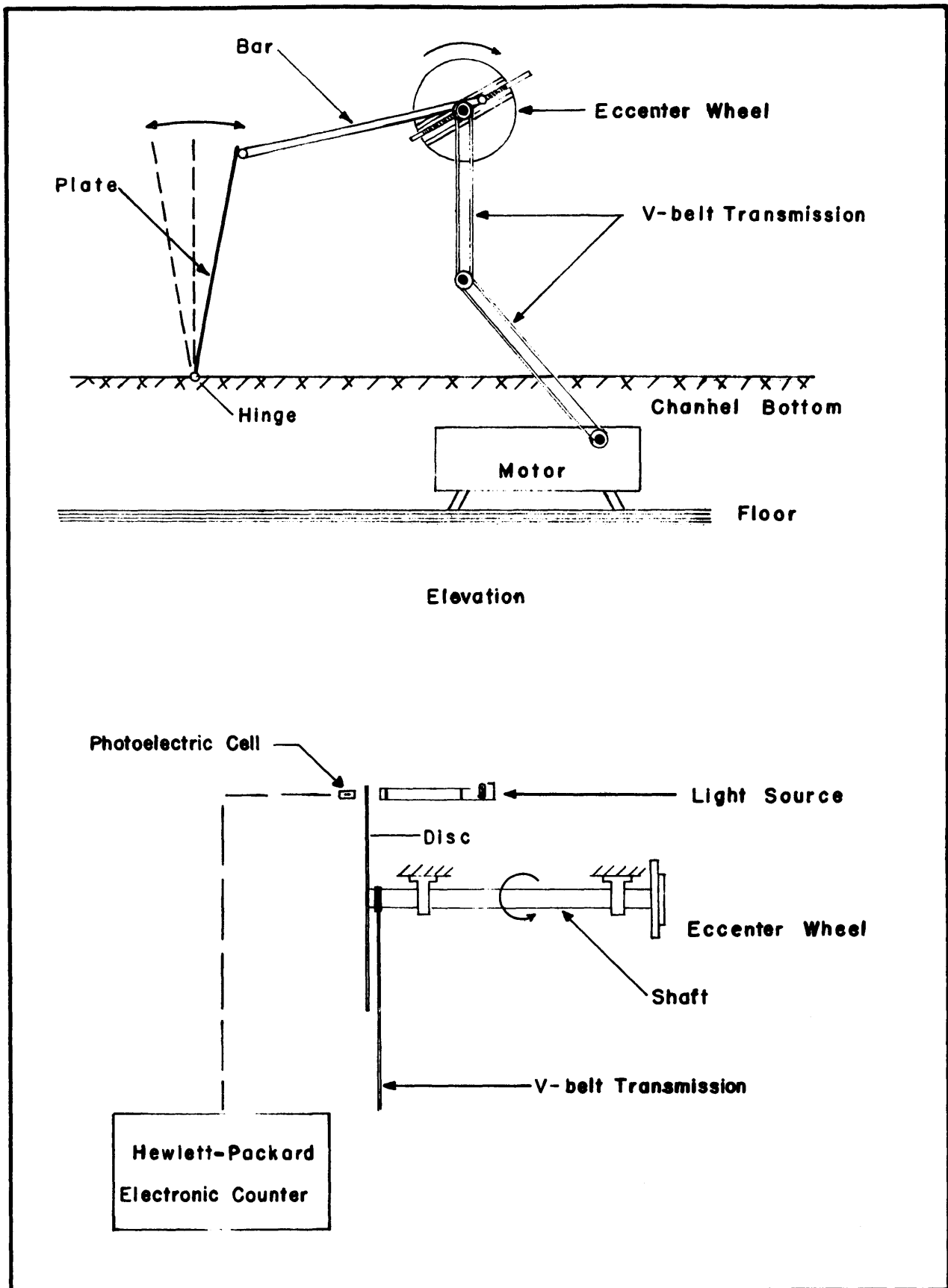
Fig. 6   Schematic Drawing of Wave Maker

12
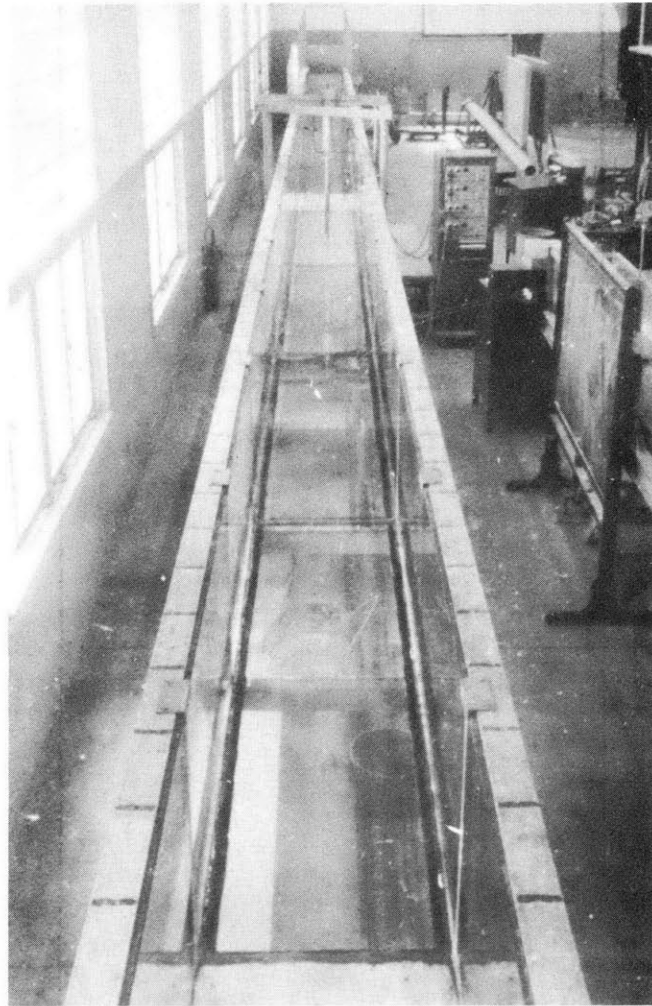
Figure 7a Wave Tank
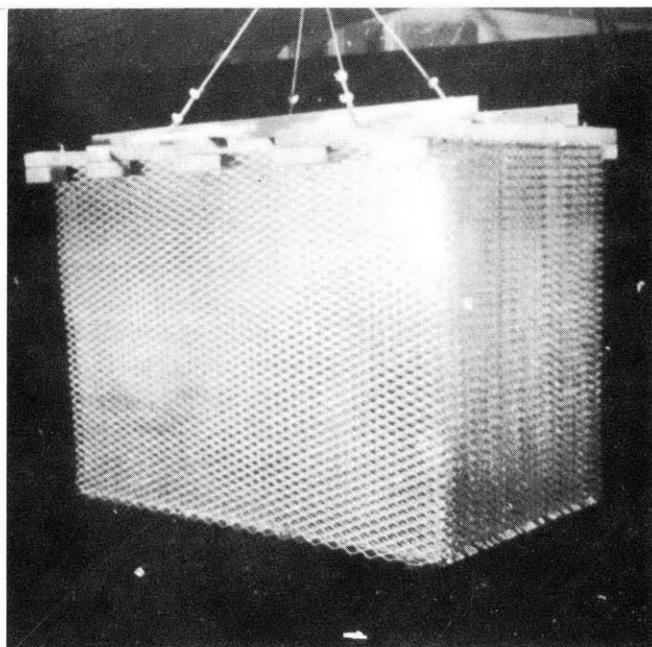
Figure 7b Wave Filter

13

It is made out of aluminum wire mesh, and is divided into three equal sections. These sections are filled with aluminum wool with increasing density away from the first dissipator. The purpose of this arrangement is to dissipate more and more energy of the transmitted wave as it proceeds. In combination these two energy dissipators were found to be very effective for short and intermediate waves. For long waves, however, these dissipators become somewhat less effective. The amplitude of the reflection from this tubular dissipator was found a little less than that of the beach reflection.

2.4 Wave Gages and Carriages

Accurate measurements of wave height and length were required in this study. Resistance type wave gages have been used for this purpose. The active elements of the resistance wave gage are two platinum wires, 8 inches long, 0.036 inches in diameter, oriented vertically, insulated from each other and spaced at a distance of 1/4 inch from each other, as illustrated in Figure 8 reproduced from ref. (11). An alternating current voltage is impressed across these two wires and when they are partially immersed in water a flow of current occurs which is essentially proportional to the depth of immersion. This current is then amplified and recorded by one of the 4 channels of the Sanborn Recorder.

The most convenient way to calibrate a gage such as the one described is to calibrate it statically by lowering (and raising) the gage in steps, a known distance into water and then correlating the successive positions with the corresponding output of the recorder. It is usual to assume that this calibration is valid when the gage is measuring a water surface elevation which fluctuates fairly rapidly. Actually in such a case there is the possibility that the water draining off the wires does not follow the water surface, in which case the indicated wave height will differ from the actual wave height. Thus, the actual wave height must be obtained by correction for these influences.

For this purpose a calibration is used approaching the actual dynamic condition. Instead of letting the surface of the water attain complete equilibrium after each displacement of the point gage staff, to which the wave gage is connected (Figure 8b), these displacements are made as fast as possible, and the point gage staff is brought back to its neutral position after each of them. A dynamic calibration of this type corresponds more exactly to the response of the gages under actual test conditions. A sample of the calibration data and the resulting calibration curve is shown in Figure 9.

The wave channel is equipped with two self-propelled wave gage carriages to measure the wave envelope profiles in the channel upstream and downstream of the transition, over distances of 40 feet and of 24 feet respectively. The wave gage carriages consist of a self-propelled aluminum frame, mounted on plastic wheels which travels on two rails, fixed to the two sides of the channel as shown in Figure 5. The propulsion is provided by a small motor connected to a reducer and pulley. Through a belt system the speed of travel may be regulated in discrete steps. The function of the wave gage carriage

14
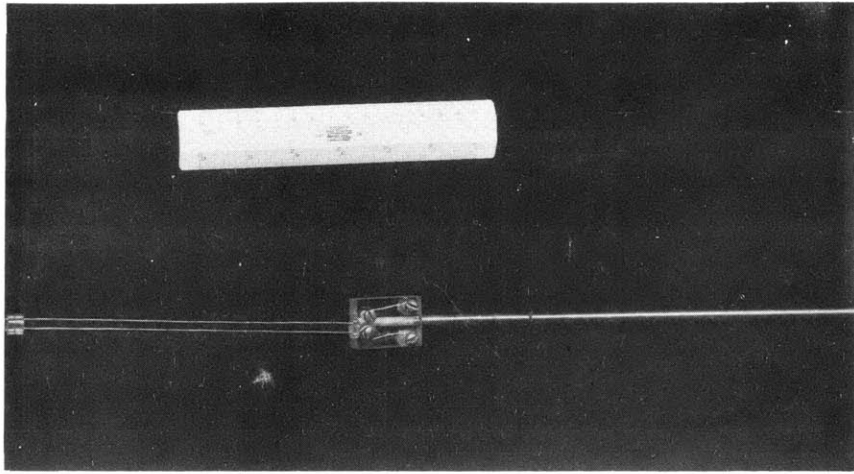
a - Photograph of wave gage.
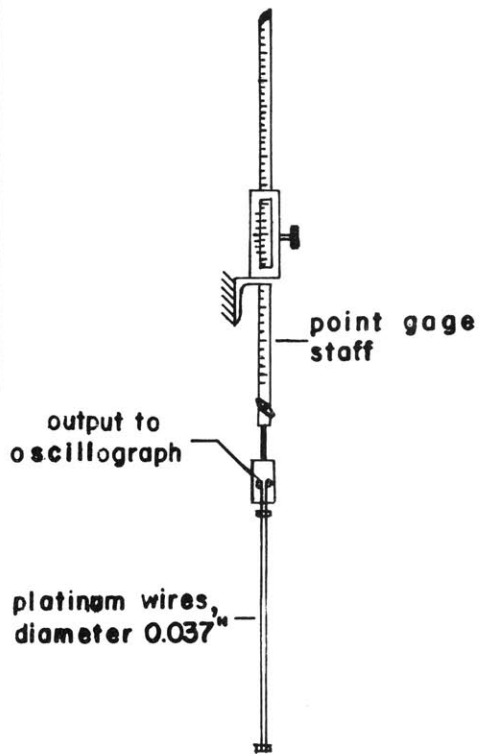
b - Wave gage set-up.   c - Electrical circuit.
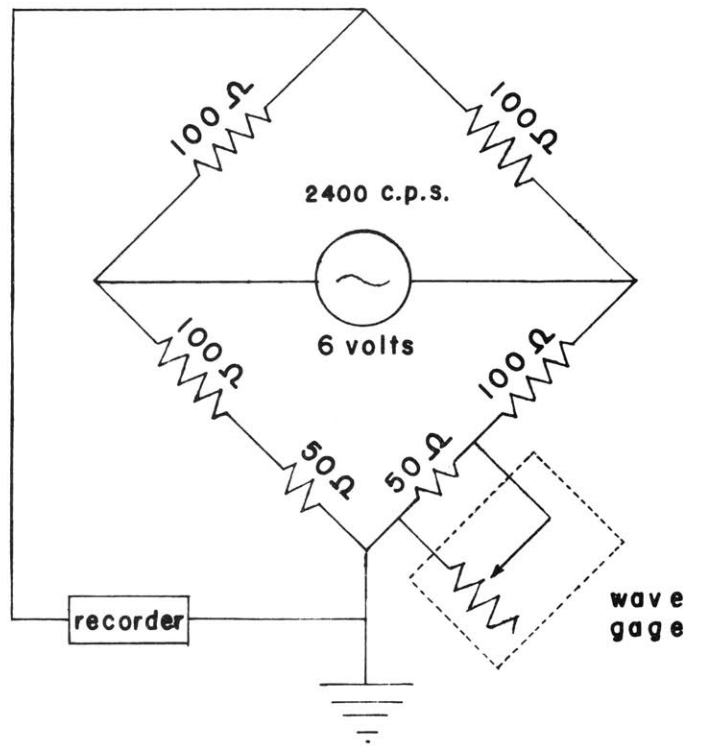
Fig. 8 - Photograph and Electrical circuit of wave gage.
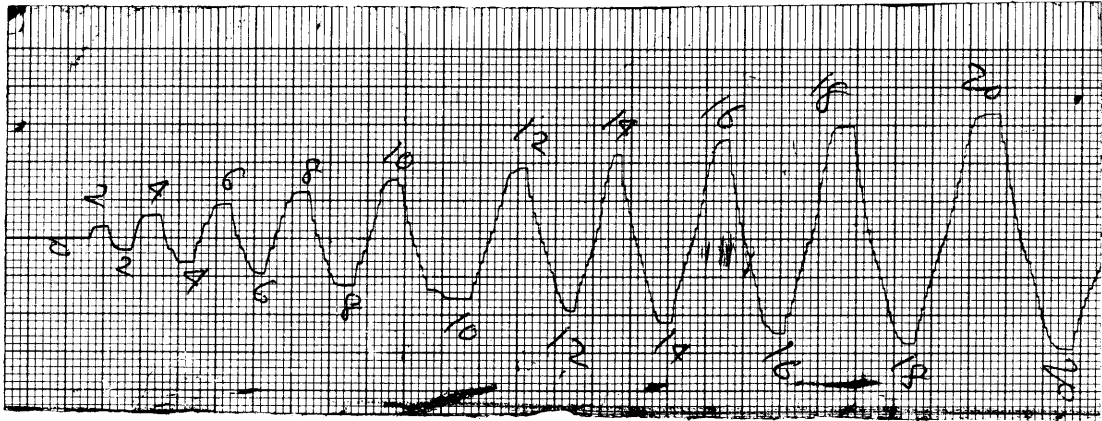
Sample of Calibration Record
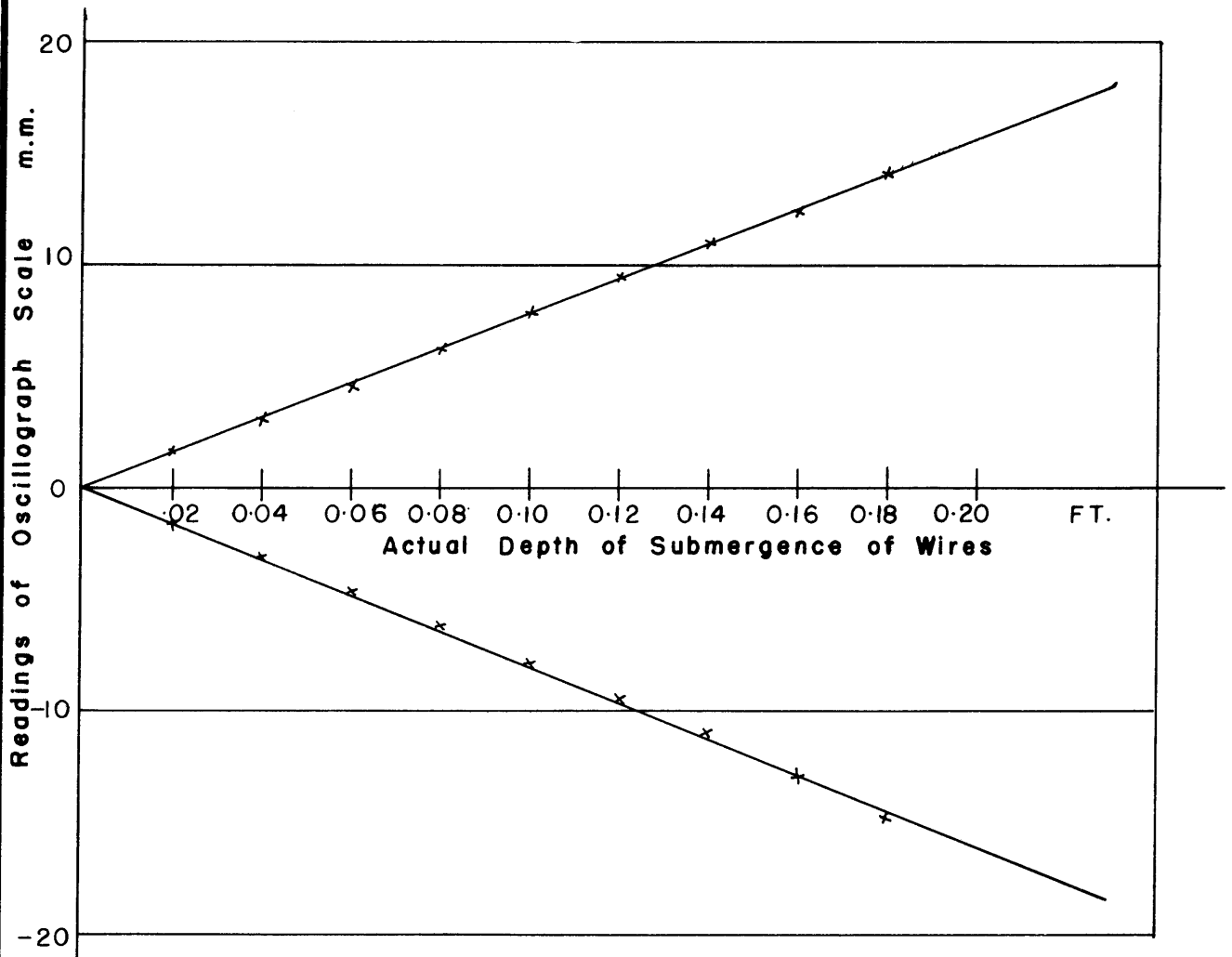
Fig·9 Sample Data and Calibration Curve of Wave Gages

16

is two-fold: 1) It serves to move the wave gage slowly along the wave channel, thereby measuring the water surface elevation along the axis of the channel, recording its minimum and maximum position. 2) It also actuates a circuit at 0.25 feet intervals along the channel which marks on the recorder the location of each measurement of water surface elevation. Since there was only one provision on the recorder for one location marker operating at a time, the two wave gages and carriages are operated alternately. The carriages can be run in both directions, simply by reversing a switch which alters the winding connections and makes the motor rotate in the opposite direction.

2.5 Sills — Sections of Reduced Depth

The depth of water in the downstream portion of the channel is changed from the upstream portion by the insertion of a "sill" consisting of a length of linearly varying depth and a section of uniform reduced depth, as illustrated in Figures 10b and 11.

These sills were constructed with three different slopes :1:0.58 (60°), 1:2.75 (20°), and 1:16 (3.57°) of aluminum plates (3/16" thick) and angles 2" x 1-1/2" x 1/4"). The transitions with steeper slopes had a section of uniform depth of 20.17 feet in length terminated by a vertical face. The height of the sill was 18.44 inches. The portion of the wave channel downstream extended 13.6 feet to the toe of the beach, on which the wave absorbers were placed.

The transition of slope 1:16 was followed by a uniform depth section 24 feet in length and 1 foot above the bottom of the wave tank. Due to the total length of this sill of 40 feet the downstream beach was replaced by the tubular dissipator followed by an aluminum wool wave absorber directly after the vertical downstream face.

In order to prevent flow between the free-surface portion of the channel and the water below the sill-bottom, the joints between channel sides and sill-bottom were sealed with strong adhesive tape commerically known as Permacel.

2.6 Sanborn Recorder

A Sanborn Model 150 four-channel direct writing recorder equipped with 2400 cps - 6 volt output preamplifiers was used to record the wave profiles and profile envelopes. This Sanborn unit is equipped with heated styli and records 4 traces simultaneously on plastic coated heat sensitive paper. A fifth stylus is provided which records one second pulses along one margin. A wide choice of paper speeds is available, from 0.25 to 100 mm/sec by use of a clutch and gear shift lever arrangement. Provision is also made for the determination and setting of the gage factor of the transducer for obtaining maximum sensitivity of the amplifier.

17

UNIFORM WIDTH

Region 1   Transitional Region   Region 3

ELEVATION
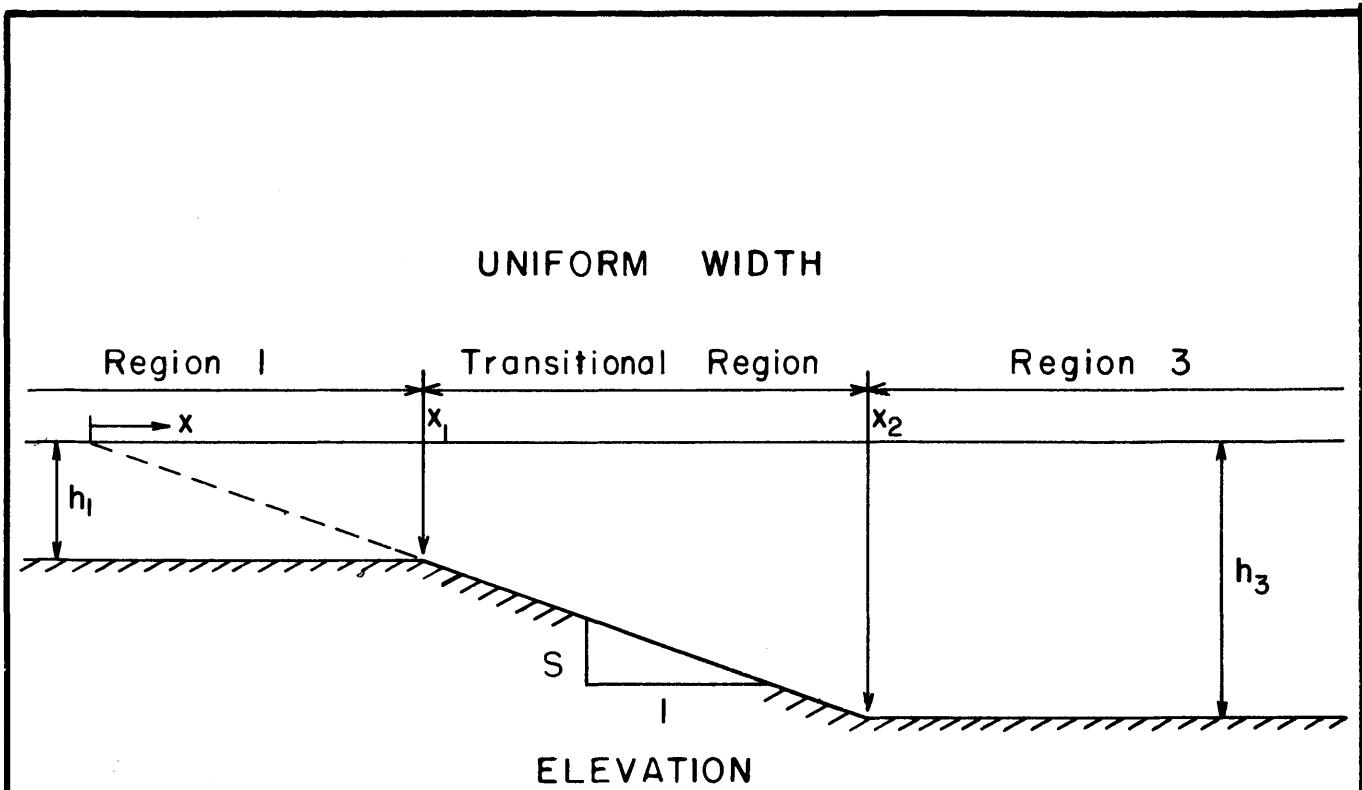
(a) Definition Sketch of Dean's Analysis

Region 1   Transitional Region   Region 3

+x ←

Channel Bottom
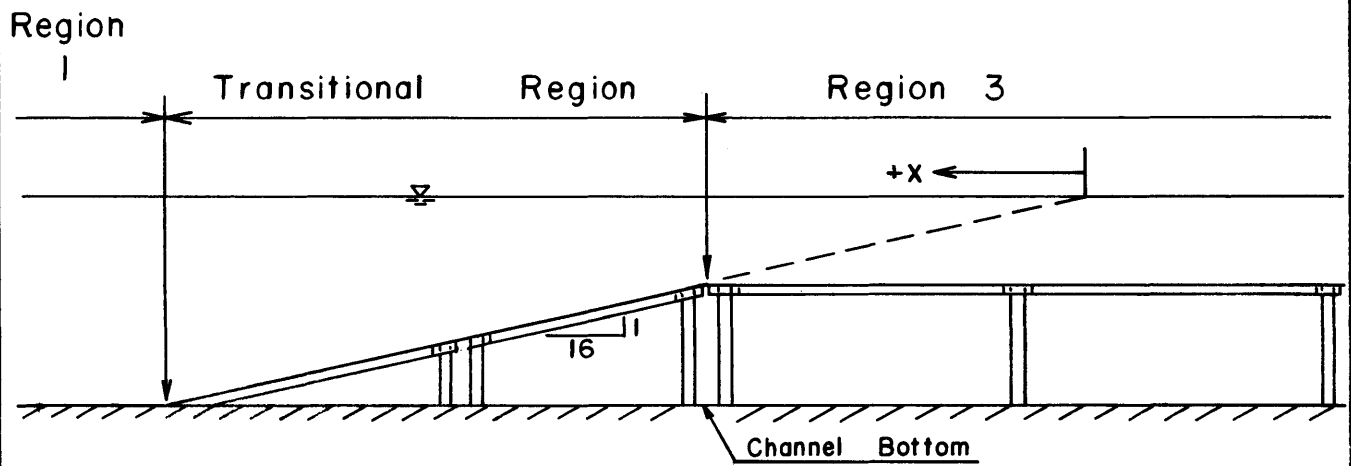
Note: This Drawing Not To Scale

(b) Schematic Diagram of Sill

Fig. 10

18

SILL MADE OF ALUMINUM PLATES,
AND SEALED WITH AN ADHESIVE TAPE.

SECTION 1   SECTION 2   SECTION 3

X'   X   STILL WATER SURFACE.

20'

18"

GLASS BOTTOM OF CHANNEL.

SUPPORTING FRAME MADE OF
$1\frac{1}{2}" \times 2" \times \frac{1}{4}"$ ALUMINUM ANGLES.
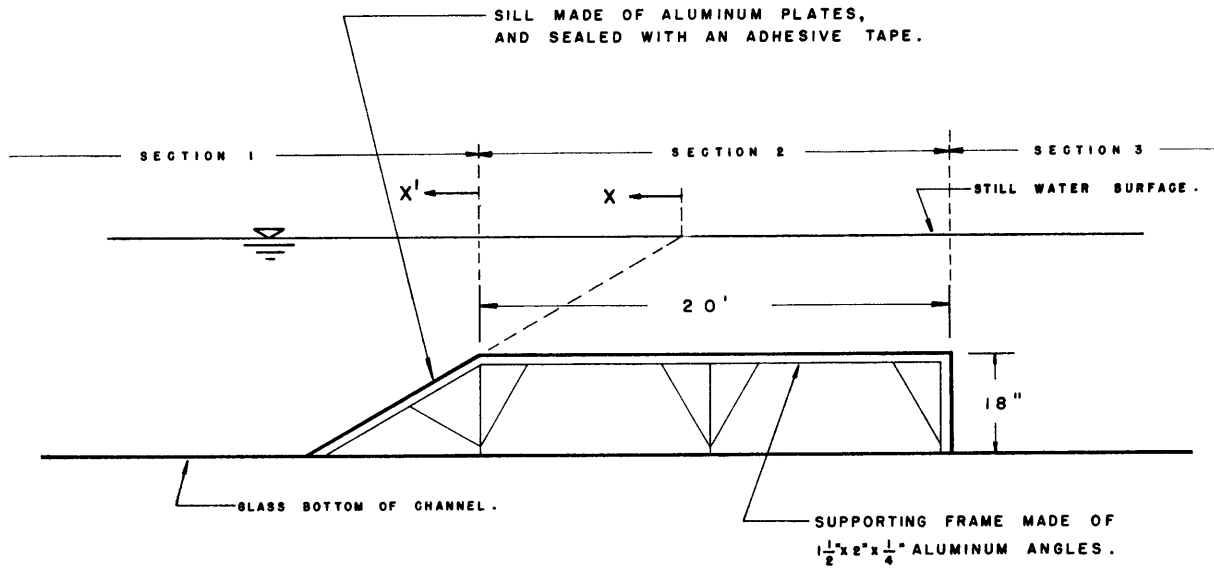
Sketch of aluminum sill.

NOTE : Both drawings are not to scale.

Sketch of energy dissipators.

4.5'   4.5'

STILL WATER SURFACE.

16   1

TWO BASKETS, FILLED WITH ALUMINUM
WOOL OF INCREASING DENSITY IN
THE DIRECTION OF THE ARROW.

$\frac{3}{4}"$ THICK PLYWOOD BEACH.
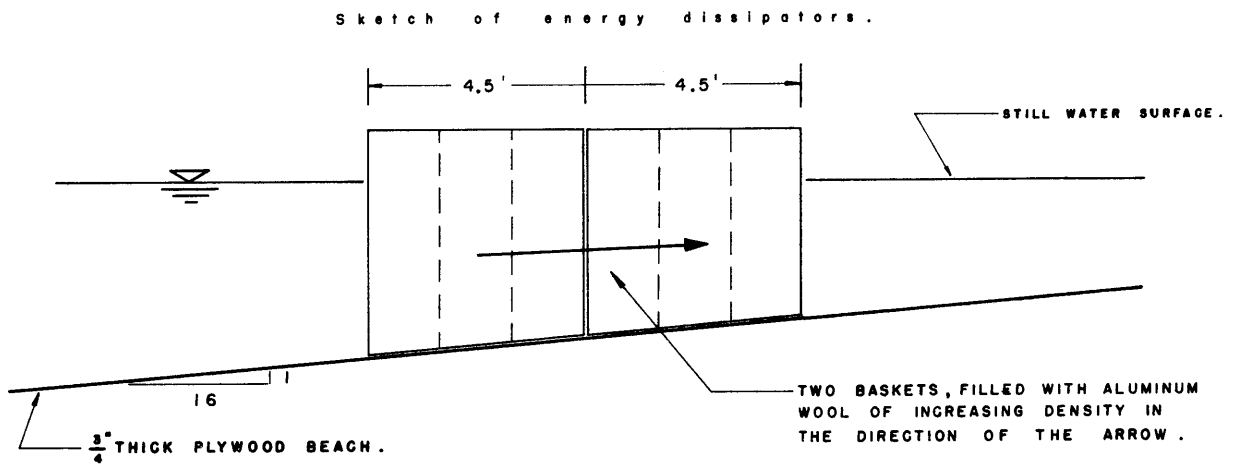
Fig. 11 — Schematic drawing of sill and energy dissipators.

III. EXPERIMENTAL PROGRAM AND PROCEDURE

3.1 Test Programs

The phenomenon of wave reflection and transmission in channels of gradually varying section is one of the many problems in fluid mechanics which cannot be solved mathematically without making certain far-reaching approximations.

The existing theory is summarized in Section IV to the extent essential for this experimental study and amplified in the Appendix. Since the theory fails to consider anything but "small amplitude" waves, it cannot account for differences as a result of variations in amplitude. Also, for gradually varying depth, the reflection process must extend over the length of the sloping bottom in a non-linear fashion. The assumptions valid for abrupt changes in channel section must break down for this case and have not been adequately replaced in the theories reviewed (7) (10). The experimental program of the present study was therefore designed to establish:

1. The reflection and transmission characteristics of waves for a gradual depth change in relation to abrupt depth changes,

2. The effect of wave amplitude and steepness on the reflection and transmission coefficients.

It is natural that these characteristics should further be differentiated by the property of the incoming waves, by which they are classified either as "long or shallow water" waves or "short or deep water" waves, with intermediate waves between these extremes. Consequently the program was planned to cover the widest spectrum of wave characteristics within the possibilities of the experimental channel and wave generator. The wide range of wave properties applied in this experimental program is given in Tables I and II.

For the first test program (11) with the steeper transitions the flap-type wave maker was used throughout and therefore the type of waves in the approach section was predominantly in the "short" and "intermediate" range. Relatively low amplitudes were employed throughout this series, of the order of one half inch. Wave steepness was not considered as an important parameter, an assumption confirmed during the tests for the transition of smaller slope for short and intermediate waves. The experiments in this series covered the ratios of upstream to downstream depth as follows: h_1/h_3 = 2.5, 3.0, 4.0, 5.0 and 7.0.

A complete summary of the pertinent test conditions and of the results derived is given in Table I. In this series transmission and reflection coefficients were derived for the upstream sloping transitions as well as for the vertical face downstream.

20

The second test program (14) for the transition with slope 1:16 was conducted utilizing the piston type wave maker throughout. Thus the range of waves could be extended well into the shallow-water wave type. Wave steepness was considered as one of the important parameters in this experimental series. The water depth in the channel upstream was varied from 18 inches to 24 inches in steps of 2 inches. Variation of upstream water depth from 18 to 24 inches resulted in a variation of downstream water depth from 6 inches to 12 inches. Thus the resulting upstream to downstream depth ratios were: $h_1/h_3 = 2.0, 2.2, 2.5, 3.0$.

For shallow water waves the wave periods T were varied from 3.84 sec to 7.25 sec and the resulting wavelengths L varied from 30.0 ft to 50.0 ft respectively for the upstream portion and from 21.7 ft to 29.0 ft for the downstream portion. Wave periods for short and intermediate waves were varied in the range of $T = 0.672$ sec to 3.49 sec and the resulting upstream wavelengths covered the range of $L = 2.31$ ft to 24.85 ft respectively, whereas the downstream wavelengths were 2.092 ft to 16.0 ft.

Wave steepnesses (H/L) were varied from 0.00072 to 0.00606 in the upstream portion for shallow water waves, whereas the corresponding wave steepnesses for the downstream portion were 0.00122 and 0.01093 respectively. Short and intermediate wave steepnesses were in the range of 0.00514 to 0.0586 in region 1 as defined in Figure 10b and the corresponding values in region 3 were 0.0088 to 0.0600. Table II summarizes all test conditions and results.

3.2 Test Procedure

In general the same experimental procedures with the techniques adopted were followed for all tests reported herein with only minor variations.

Initially the wave gages were calibrated before and after each day of testing. Experience subsequently showed the instrumentation to be sufficiently stable to permit a single daily calibration. Following the calibration of instruments the specific wave to be used was set. Setting a wave in the flume necessitated trial adjustments of plunger speed and stroke for the wave machine. Two different methods have been used to set a wave of particular wavelength. In the first method, two wave gages were placed in the flume the desired wavelength apart and the wave generator speed was adjusted until the two wave gage tracers were in phase indicating that the wavelength was correct. Once the wave was set, a record was made of the passage of 10-20 waves, the length again checked, and the height verified using the previously prepared calibration curves.

The second method of setting the wavelength was to record a number of waves passing the gage by keeping one of the gages stationary, at a fixed paper speed. Then if ℓ is the recorded length on the Sanborn oscillograph paper, N the number of wave periods in the length ℓ, and u the paper speed in in/sec, the wave period T is given by the relation.

$$T = \frac{\ell}{uN} \text{ sec} \qquad (3.1)$$

Once the wave period is known, the incident and transmitted wavelengths can be determined from the knowledge of water depths before and after the transition. The deep water wavelength L_o can be computed from the relation

$$L_o = \frac{g}{2\pi} T^2 \qquad (3.2)$$

Knowing L_o, the ratios of upstream and downstream water depths to the deep water wavelength, i.e. h_1/L_o and h_3/L_o, are then calculated. The basic relationship of

$$(h/L)\tanh \frac{2\pi h}{L} = h/L_o \qquad (3.3)$$

is then used to determine the values h_1/L_1 and h_3/L_3 respectively, from which upstream and downstream wavelengths are calculated easily. In order to save time a wave table (12) is used to determine the values of h_1/L_1 and h_3/L_3 for corresponding values of h_1/L_o and h_3/L_o respectively.

Once the desired waves are established in the channel, the wave gages are moved along the channel to record the wave envelope. In order to avoid confusion each of the wave gage carriages is started from the same position everytime. As the wave carriage moves along the channel, the wave gage records the envelope of wave profile. In order to record the position of the gage in the channel at any time the Sanborn position marker was used. Due to the availability of only one position marker in the Sanborn Recorder each wave gage had to be moved separately. The simultaneous recording of the wave envelope and of the location of the wave gage along the channel facilitates the determination of the position of maximum and minimum wave envelopes needed for the evaluation of the recorded data. The recorded upstream and downstream wave envelopes are then analyzed and the reflection and transmission coefficients evaluated by the procedure described in detail in section IV.

IV. ANALYSIS AND DATA REDUCTION

The analysis of the reflection and transmission characteristics of waves is greatly simplified if a channel extending to infinity is assumed. Since in practice it is impossible to have a channel of infinite length, the experimental investigation must obviously be conducted in a channel of finite length. Because the theory is based on a channel of infinite length, the experimental results are not compatible with the theory unless the measured wave system is transformed. It has been concluded by Dean and Ursell that the presence of the wave maker only modifies the amplitude and phase of the incident wave (6). Therefore the experimental results can be compared with the theory for the infinite channel if the reflection from the far end of the wave tank alone is eliminated. Dean and Ursell have developed a mathematical procedure for eliminating the reflection from the downstream end of the wave tank. This method is modified to be applicable in the present study and is presented in this section. Also presented in this section is the method of analysis of the recorded experimental data. At the end of the section a sample calculation for one of the tests is given to illustrate the method of data reduction.

The measured wave system has been designated as S_1 and the transformed wave system after elimination of the reflection from the far end as S_3, following Dean and Ursell (6). The general scheme of the waves assumed in the S_1 and in the S_3 system respectively is indicated in Figure 12.

4.1 Description of the S_1 System

In order to determine the characteristics of the S_1 system, the wave system in the region 1 before the transition is considered. The two waves defined by the surface variations η_1 (incoming wave) and η_2 (reflected wave) may be superimposed as follows,

$$\eta_1 + \eta_2 = a_1 \sin(k_1 x + \sigma t + \delta_1) + a_2 \sin(k_1 x - \sigma t + \delta_2)$$

$$= [a_1 \sin(k_1 x + \delta_1) + a_2 \sin(k_1 x + \delta_2)] \cos \sigma t \qquad (4.1)$$

$$+ [a_1 \cos(k_1 x + \delta_1) - a_2 \cos(k_1 x + \delta_2)] \sin \sigma t$$

with a, k, σ, and δ representing amplitudes, wave numbers, frequencies and phase angles respectively. The times at which the maxima or minima of this combined wave system occur can be found by:

$$\frac{\partial}{\partial t} (\eta_1 + \eta_2) = 0$$

which gives the time t_{max} at which the maxima occur for any location in section 1,

$\eta_{1,1} = a_1 \sin(k_1 x + \sigma t + \delta_1)$

$\eta_{2,1} = a_2 \sin(k_1 x - \sigma t + \delta_2)$

$\eta_{3,1} = a_3 \sin(k_3 x + \sigma t + \delta_3)$ $\eta_{4,1} = a_4 \sin(k_3 x - \sigma t + \delta_4)$

+ x

h_3

h_1

$\frac{1}{16}$

$S_1(x,t)$, Measured Wave System.

$\eta_{1,3} = a_1' \sin(k_1 x + \sigma t + \delta_1')$

$\eta_{2,3} = a_2' \sin(k_1 x - \sigma t + \delta_2')$

$\eta_{3,3} = a_3' \sin(k_3 x + \sigma t + \delta_3')$ $\eta_{4,3} = 0$

+ x

h_3

h_1

$\frac{1}{16}$

$S_3(x,t)$, Transformed Wave System.

REF: AFTER DEAN & URSELL TR. 37·
REF· NO· 6·
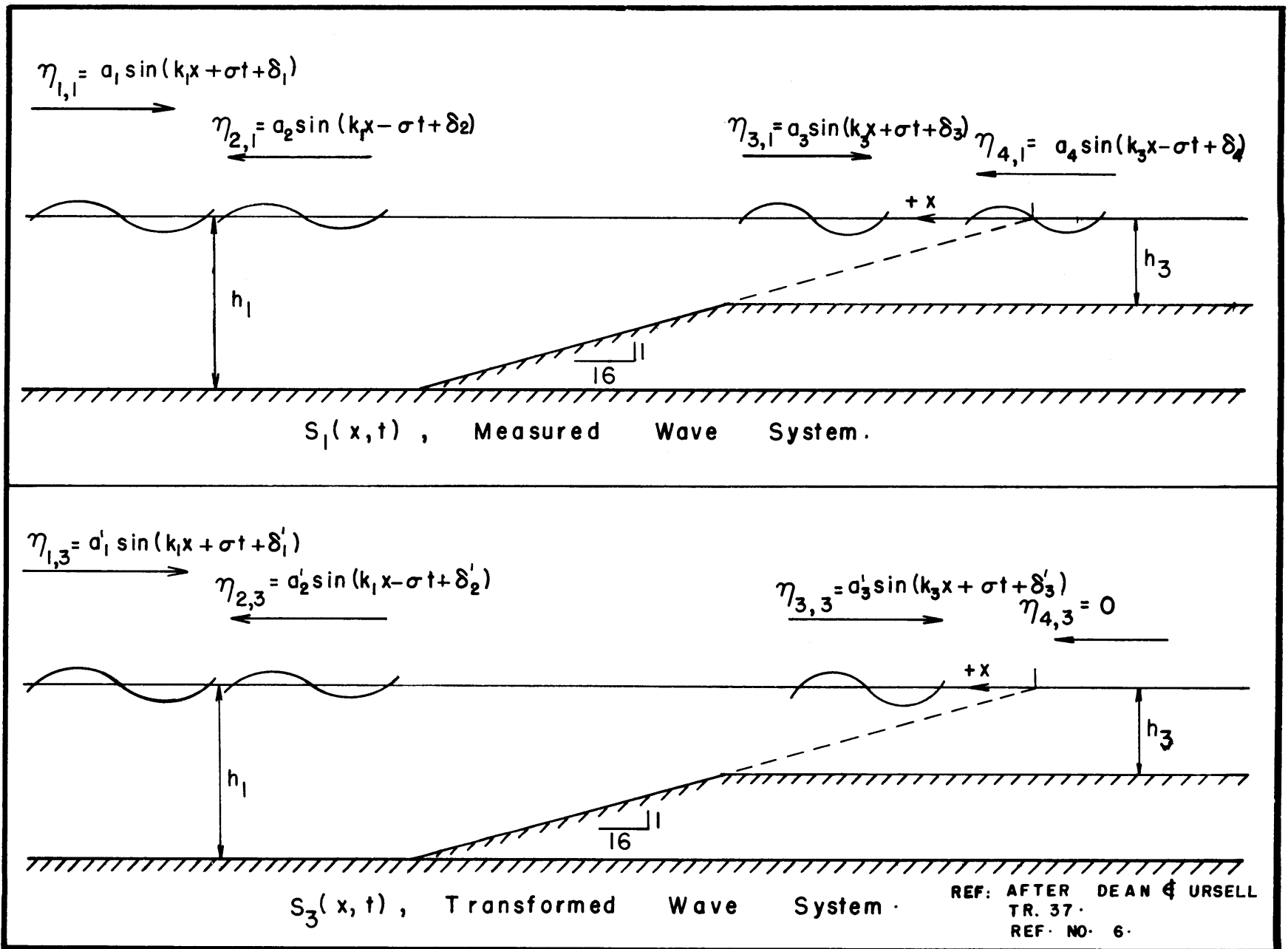
Fig. 12 Measured and Transformed Wave System.

$$\tan \sigma\, t_{max} = \frac{+a_1 \cos(k_1 x + \delta_1) - a_2 \cos(k_1 x + \delta_2)}{a_1 \sin(k_1 x + \delta_1) + a_2 \sin(k_1 x + \delta_2)} \qquad (4.2)$$

The values $\sin \sigma\, t_{max}$ and $\cos \sigma\, t_{max}$, implied by equation (4.2) may be substituted into equation (4.1). Then the variation of the maximum amplitude of the combined waves with distance or the "wave envelope" is given by:

$$\left| \eta_1 + \eta_2 \right|_{\substack{max \\ or\ min}} = \sqrt{a_1^2 + a_2^2 - 2a_1 a_2 \cos(2k_1 x + \delta_1 + \delta_2)} \qquad (4.3)$$

Hence the maximum and minimum values of $\left| \eta_1 + \eta_2 \right|$ and their locations are obtained as follows:

$$\left| \eta_1 + \eta_2 \right|_{max} \begin{cases} \text{for } \cos(2k_1 x_{max} + \delta_1 + \delta_2) = -1 \\[2mm] \text{or } 2k_1 x_{max} + \delta_1 + \delta_2 = (2n+1)\pi \\[2mm] \text{and} \end{cases} \qquad (4.4)$$

$$\left| \eta_1 + \eta_2 \right|_{max} = (a_1 + a_2) \qquad (4.5)$$

$$\left| \eta_1 + \eta_2 \right|_{min} \begin{cases} \text{for } \cos(2k_1 x_{min} + \delta_1 + \delta_2) = +1 \\[2mm] \text{or } 2k_1 x_{min} + \delta_1 + \delta_2 = 2n\pi \\[2mm] \text{and} \end{cases} \qquad (4.6)$$

$$\left| \eta_1 + \eta_2 \right|_{min} = (a_1 - a_2) \qquad (4.7)$$

Equations (4.5) and (4.7) give:

$$a_1 = \frac{\left| \eta_1 + \eta_2 \right|_{max} + \left| \eta_1 + \eta_2 \right|_{min}}{2} \qquad (4.8)$$

$$a_2 = \frac{\left| \eta_1 + \eta_2 \right|_{max} - \left| \eta_1 + \eta_2 \right|_{min}}{2} \qquad (4.9)$$

Also, from equation (4.4), the value of $(\delta_1 + \delta_2)$ is

$$(\delta_1 + \delta_2) = (2n+1)\pi - 2k_1 x_{max} \qquad n = 0,1,2 \qquad (4.10)$$

Combining the wave components η_3 and η_4 in region 3 after the transition in the same manner as η_1 and η_2, the t_{max} at which the maximum water surface elevation occurs at any location in region 3 after the transition is obtained similarly as:

$$\tan \sigma t_{max} = \frac{+a_3 \cos k_3 x - a_4 \cos (k_3 x + \delta_4)}{a_3 \sin k_3 x + a_4 \sin (k_3 x + \delta_4)} \qquad (4.11)$$

The variation of wave amplitude with distance is then:

$$\left| \eta_3 + \eta_4 \right| = \sqrt{a_3^2 + a_4^2 - 2a_3 a_4 \cos (2k_3 x + \delta_4)}$$

Maximum and minimum values of $\left| \eta_3 + \eta_4 \right|$ and their locations are then defined by:

$$\left| \eta_3 + \eta_4 \right|_{max} \begin{cases} \text{for } 2k_3 x_{max} + \delta_4 = (2n+1)\pi & (4.12) \\ \text{and} & \\ \left| \eta_3 + \eta_4 \right|_{max} = a_3 + a_4 & (4.13) \end{cases}$$

$$\left| \eta_3 + \eta_4 \right|_{min} \begin{cases} \text{for } 2k_3 x_{min} + \delta_4 = 2n\pi & (4.14) \\ \text{and} & \\ \left| \eta_3 + \eta_4 \right|_{min} = (a_3 - a_4) & (4.15) \end{cases}$$

Equations (4.13) and (4.15), give:

$$a_3 = \frac{\left| \eta_3 + \eta_4 \right|_{max} + \left| \eta_3 + \eta_4 \right|_{min}}{2} \qquad (4.16)$$

$$a_4 = \frac{\left| \eta_3 + \eta_4 \right|_{max} - \left| \eta_3 + \eta_4 \right|_{min}}{2} \qquad (4.17)$$

Equation (4.12) results in:

$$\delta_4 = (2n+1)\pi - 2k_3 x_{max}, \qquad n = 0,1,2,\text{etc.}$$

26

Five of the original unknowns involving the wave amplitudes and phases in the S_1 system are now defined. The remaining unknowns are δ_1 and δ_2 and their sum is known. In order to determine δ_1 and δ_2 equations (4.2) and (4.11) may be examined which express the times at which the maximum water surface elevation occurs in regions 1 and 3 at any two stations x_a and x_b, respectively, where

x_a = distance before transition

x_b = distance after transition

Equating equations (4.2) and (4.11) will define two stations in regions 1 and 3 at which the maxima occur simultaneously. This is accomplished experimentally by moving the wave gages along the wave channel until the phases of the outputs coincide on the oscillograph. Assuming that the gauges are then at stations, x_a and x_b, the condition of the above equality gives:

$$\frac{+a_1\cos(k_1x_a+\delta_1)-a_2\cos(k_1x_a+\delta_2)}{a_1\sin(k_1x_a+\delta_1)+a_2\sin(k_1x_a+\delta_2)} = \frac{+a_3\cos k_3x_b-a_4\cos(k_3x_b+\delta_4)}{a_3\sin k_3x_b+a_4\sin(k_3x_b+\delta_4)}$$

After considerable reduction:

$$\tan\delta_2 = \frac{\cos(k_1x_a+\delta_1+\delta_2)+R\sin(k_1x_a+\delta_1+\delta_2)-\frac{a_2}{a_1}(\cos k_1x_a-R\sin k_1x_3)}{-\sin(k_1x_a+\delta_1+\delta_2)+R\cos(k_1x_a+\delta_1+\delta_2)-\frac{a_2}{a_1}(\sin k_1x_a+R\cos k_1x_3)} \quad (4.18)$$

wherein:

$$R = \frac{-\cos k_3x_b + \frac{a_4}{a_3}\cos(k_3x_b+\delta_4)}{\sin k_3x_b + \frac{a_4}{a_3}\sin(k_3x_b+\delta_4)}$$

Since δ_4 is given by the condition (4.12) and since the sum $(\delta_1+\delta_2)$ is known, δ_1 can be determined by equation (4.10). Thus the amplitudes and phases of the wave components are now known for the $S_1(x,t)$ system.

4.2 Elimination of Far End Reflection From Measured Wave System

The measured wave system $S_1(x,t)$ has been considered to be composed of four components of progressive waves. The second subscript on the water surface elevations η indicates the system $S_1(x,t)$. Denote next a second system $S_2(x,t)$ which is formed according to the following transformation:

$$S_2(x,t) = S_1\left[x, -(t+\frac{\delta_4}{\sigma})\right] \quad (4.19)$$

27

A third wave system $S_3 (x,t)$ may finally be defined by the transformation:

$$S_3 (x,t) = S_1 (x,t) - \frac{a_4}{a_3} S_2 (x,t) \qquad (4.20)$$

carrying out the transformations (4.19) and (4.20), the wave components in the $S_3 (x,t)$ system are shown in Figure 12, where:

$$\eta_{1,3} = a_1 \sqrt{1+\left(\frac{a_2}{a_1}\right)^2 \left(\frac{a_4}{a_3}\right)^2 - 2\left(\frac{a_2}{a_1}\right)\left(\frac{a_4}{a_3}\right) \cos (\delta_1 - \delta_2 + \delta_4)} \sin(k_1 x + \sigma t + \delta_1')$$

$$\eta_{2,3} = a_2 \sqrt{1+\left(\frac{a_1}{a_2}\right)^2 \left(\frac{a_4}{a_3}\right)^2 - 2\left(\frac{a_1}{a_2}\right)\left(\frac{a_4}{a_3}\right) \cos (\delta_1 - \delta_2 + \delta_4)} \sin(k_1 x - \sigma t + \delta_2')$$

$$\eta_{3,3} = a_3 \left[1 - \left(\frac{a_4}{a_3}\right)^2 \right] \sin(k_3 x + \sigma t + \delta_3')$$

$$\eta_{4,3} = 0$$

The S_3 system is defined so that the amplitude of the wave reflected from the far end is zero; the wave components of the S_3 system are therefore directly comparable to wave components in a channel of infinite length, and the preceding development permits transformation of the amplitudes in the channel of finite length into the corresponding amplitudes for the channel of infinite length. These amplitudes may be denoted as follows:

$$a'_1 = a_1 \sqrt{1+\left(\frac{a_2}{a_1}\right)^2 \left(\frac{a_4}{a_3}\right)^2 - 2\left(\frac{a_2}{a_1}\right)\left(\frac{a_4}{a_3}\right)\cos(\delta_1 - \delta_2 + \delta_4)} \qquad (4.21)$$

$$a'_2 = a_2 \sqrt{1+\left(\frac{a_1}{a_2}\right)^2 \left(\frac{a_4}{a_3}\right)^2 - 2\left(\frac{a_1}{a_2}\right)\left(\frac{a_4}{a_3}\right)\cos(\delta_1 - \delta_2 + \delta_4)} \qquad (4.22)$$

$$a'_3 = a_3 \left[1 - \left(\frac{a_4}{a_3}\right)^2 \right] \ldots \ldots \qquad (4.23)$$

The desired reflection and transmission coefficients are now given by:

$$K_r = \frac{a'_2}{a'_1} \qquad (4.24)$$

$$K_t = \frac{a'_3}{a'_1} \qquad (4.25)$$

28

4.3 Analysis of Data

In the preceding sections the different wave components of the S_1 system have been described and the methods for eliminating the far-end reflection from the measured wave system have been developed. In this section a sample calculation is presented to illustrate the above procedure. Test No. 48 has been selected for this purpose.

The first step is to identify and locate clearly the maxima and minima on the wave envelopes on the recording paper, both upstream and downstream of the transition, relative to the coordinate origin (x=0) (see Figure 10). Once they are thus defined the maxima and minima amplitudes are evaluated with the help of the previously prepared calibration curves of the respective gages. The values obtained for Test No. 48 in the series given in Table II for the transition 1:16 are given below:

Upstream envelope

$$\left| \eta_1 + \eta_2 \right|_{max} = 0.049 \text{ ft.}$$

$$\left| \eta_1 + \eta_2 \right|_{min} = 0.019 \text{ ft.}$$

$$X_{max} = 55.83 \text{ ft.}$$

$$L_1 = 50 \text{ ft.}$$

Downstream envelope

$$\left| \eta_3 + \eta_4 \right|_{max} = 0.048 \text{ ft.}$$

$$\left| \eta_3 + \eta_4 \right|_{min} = 0.030 \text{ ft.}$$

$$X_{max} = 0.67 \text{ ft.}$$

$$L_2 = 33.9 \text{ ft.}$$

The second step is to locate the position of the two gages such that both the gages record the maximum envelope simultaneously in the upstream and

downstream part of the channel respectively. This is done from the record of the longitudinal position of the gage on the recording paper. The record of the tape from which the location is transferred to the paper by electrical contacts is adjusted to read $x = 0$ at the origin shown on Figure 12. From the recording paper this is

$$X_a = +40.58 \text{ ft.}$$

$$X_b = +4.53 \text{ ft.}$$

In order to determine the phase angles the wave numbers are required. These are

$$k_1 = 2\pi/L_1 = 0.1256$$

$$k_3 = 2\pi/L_2 = 0.1853$$

From equations (4.8), (4.9), and (4.10):

$$a_1 = \frac{0.049+0.019}{2} = 0.034 \text{ ft.}$$

$$a_2 = \frac{0.049-0.019}{2} = 0.015 \text{ ft.}$$

$$\delta_1 + \delta_2 = (2n+1)\pi - 2(0.1256)\ (5583)$$

$$= -263.69^\circ$$

Similarly, from equations (4.16), (4.17), and (4.18),

$$a_3 = \frac{0.048+0.030}{2} = 0.039 \text{ ft.}$$

$$a_4 = \frac{0.048-0.030}{2} = 0.009 \text{ ft.}$$

$$\delta_4 = (2n+1)\pi - 2(0.2073)\ (-0.67)$$

$$= +193.17^\circ$$

From the values obtained above:

$$\frac{a_2}{a_1} = 0.4411 \qquad\qquad \frac{a_1}{a_2} = 2.2667 \qquad\qquad \frac{a_4}{a_3} = 0.2308$$

Also:

$$k_1 x_a = +219.9°$$ $$k_2 x_b = +48.07°$$

$$\cos k_1 x_a = 0.3730$$ $$\cos k_2 x_b = 0.6683$$

$$\sin k_1 x_a = -0.9278$$ $$\sin k_2 x_b = 0.7439$$

$$\cos(k_1 x_a + \delta_1 + \delta_2) = 0.8812$$ $$\cos(k_3 x_b + \delta_4) = -0.4774$$

$$\sin(k_1 x_a + \delta_1 + \delta_2) = 0.4728$$ $$\sin(k_3 x_b + \delta_4) = -0.8787$$

Therefore,

$$R = \frac{-0.6683 + (0.2308)\ (-0.4774)}{0.7439 + (0.2308)\ (-0.8787)}$$

$$= -1.4386$$

Once R is known, $\tan \delta_2$ can be calculated from equation (4.18),

$$\therefore \tan \delta_2 = \frac{(0.8812)+(-1.4386)\ (0.4728) - (0.4411)\left[0.3730-(-1.4386)\ (-0.9278)\right]}{(-0.4728)+(-1.4386)\ (0.8812) - (0.4411)\left[-0.9278 +(-1.4386)\ (0.3730)\right]}$$

$$\tan \delta_2 = -0.5712$$

hence, $\delta_2 = -29.72°$

$$\therefore \delta_1 = -233.96°$$

$$(\delta_1 - \delta_2 + \delta_4) = -11.06°$$

Therefore,

$$\cos (\delta_1 - \delta_2 + \delta_4) = 0.9814$$

The transformed wave amplitudes can be calculated now by using equations (4.21), (4.22), and (4.23). Therefore,

$$a_1' = 0.034\ [1+(0.4411)^2\ (0.2308)^2 -2(0.4411)\ (0.2308)\ (0.9814)]^{1/2}$$
$$= 0.0306\ ft.$$

$$a_2' = 0.015\ [1+(2.2667)^2\ (0.2308)^2 -2(2.2667)\ (0.2308)\ (0.9814)]^{1/2}$$
$$= 0.00745\ ft.$$

31

$$a_3' = 0.039 \ [1 - (0.2308)^2]$$

$$= 0.0362 \ \text{ft.}$$

From the transformed wave amplitudes the reflection and transmission coefficients can be calculated from equations (4.24) and (4.25),

∴ Reflection coefficient

$$K_r = \frac{a_2'}{a_1'} = \frac{0.00745}{0.0306} = 0.243$$

Also,

Transmission coefficient

$$K_t = \frac{a_3'}{a_1'} = \frac{0.0362}{0.0306} = 1.183$$

4.4 Summary of Results in Tabular Form

A complete summary of all experimental results reduced by the procedures discussed above is represented by Tables I and II. Table I contains the results of the first test series for the transitions of slope 1:.58 and 1:2.75 as well as results obtained simultaneously for the abrupt transition existing downstream of the section of lower depth. These results were obtained for short and intermediate waves only.

Table II summarizes the results for the more gradual transition with a slope of 1:16 for the entire range of waves from the deep-water to the shallow-water wave type in the approach section. As an additional parameter variations in the wave steepness H/L were considered in this second, more extensive test program.

TABLE I TEST SERIES WITH TRANSITION OF SLOPES:

a) $1:0.58$ ($\alpha = 60^\circ$), b) $1:2.75$ ($\alpha = 20^\circ$)
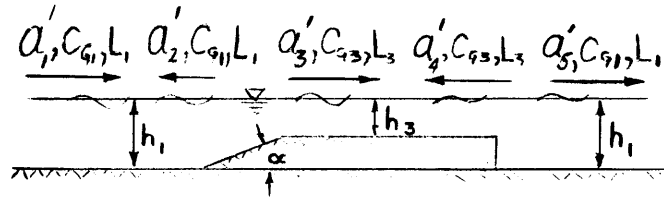
Table Ia Transition Slope $1:0.58$ ($\alpha = 60^\circ$)

Test No.	h_1	h_3	h_1/h_3	C_{G_1}	C_{G_3}	C_{G_3}/C_{G_1}	L_1	L_3	$K_t = a_3'/a_1'$	$K_r = a_2'/a_1'$	$K_t = a_5'/a_3'$	$K_r = a_4'/a_3'$
1	1.7956	0.2565	7.0	5.291	2.751	0.5199	12.780	5.314	1.043	0.547	0.572	0.641
2	1.7956	0.2565	7.0	3.339	2.532	0.7583	6.383	3.171	1.021	0.177	0.706	0.231
3	1.7956	0.2565	7.0	2.436	2.380	0.9770	4.261	2.469	0.732	0.498	0.785	0.410
4	1.7956	0.2565	7.0	2.026	2.207	1.0893	3.159	2.066	0.574	0.295	0.819	0.117
5	1.7956	0.2565	7.0	1.799	2.076	1.1539	2.525	1.801	0.838	0.184	0.924	0.188
6	1.7956	0.2565	7.0	1.658	1.956	1.1797	2.145	1.626	0.850	0.077	0.905	0.105
7	1.7956	0.2565	7.0	1.513	1.813	1.1943	1.799	1.451	0.752	0.106	1.001	0.078
8	1.9240	0.3850	5.0	5.706	3.318	0.5815	13.760	6.720	1.437	0.205	0.622	0.460
9	1.9240	0.3850	5.0	3.473	2.979	0.8577	6.857	3.960	0.955	0.289	0.873	0.135
10	1.9240	0.3850	5.0	2.495	2.674	1.0717	4.478	3.022	0.933	0.103	0.924	0.128
11	1.9240	0.3850	5.0	2.103	2.455	1.1673	3.407	2.545	0.828	0.116	0.961	0.125
12	1.9240	0.3850	5.0	1.896	2.256	1.1898	2.805	2.232	0.866	0.052	1.002	0.091
13	2.0520	0.5130	4.0	5.934	3.773	0.6358	13.585	7.740	1.153	0.220	0.799	0.293
14	2.0520	0.5130	4.0	3.572	3.282	0.9188	7.280	4.640	0.981	0.250	0.905	0.175
15	2.0520	0.5130	4.0	2.604	2.905	1.1156	4.860	3.540	0.917	0.207	0.967	0.125
16	2.0520	0.5130	4.0	2.173	2.579	1.1868	3.640	2.920	0.844	0.058	0.999	0.119
17	2.0520	0.5130	4.0	1.932	2.315	1.1982	2.913	2.500	0.834	0.021	1.007	0.101
18	2.3086	0.7695	3.0	6.283	4.467	0.7109	16.609	10.324	1.106	0.215	0.879	0.126

Table Ia (continued)

Test No.	h_1	h_3	h_1/h_3	c_{G_1}	c_{G_3}	c_{G_3}/c_{G_1}	L_1	L_3	$K_t=a'_3/a'_1$	$K_r=a'_2/a'_1$	$K_t=a'_5/a'_3$	$K_r=a'_4/a'_3$
19	2.3086	0.7695	3.0	3.814	3.754	0.9842	8.260	5.910	0.976	0.129	0.932	0.149
20	2.3086	0.7695	3.0	2.766	3.182	1.1504	5.490	4.420	0.855	0.103	1.021	0.140
21	2.3086	0.7695	3.0	2.055	2.388	1.1620	3.300	3.040	0.905	0.008	0.955	0.075
22	2.5651	1.0260	2.5	6.596	5.039	0.7639	18.340	12.420	1.009	0.337	0.847	0.246
23	2.5651	1.0260	2.5	4.027	4.098	1.0176	9.210	7.070	1.085	0.037	0.948	0.147
24	2.5651	1.0260	2.5	2.907	3.361	1.1561	6.090	5.200	0.900	0.165	1.008	0.028
25	2.5651	1.0260	2.5	2.423	2.808	1.1588	4.520	4.150	0.861	0.028	1.012	0.035
26	2.5651	1.0260	2.5	2.145	2.394	1.1160	3.590	3.420	0.857	0.043	0.988	0.016

Table Ib   Transition Slope   1:2.75   ($\alpha = 20^\circ$)
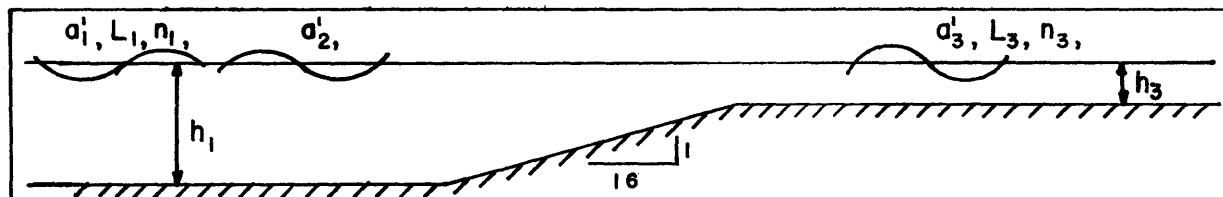
Test No.	h_1	h_3	h_1/h_3	c_{G_1}	c_{G_3}	c_{G_3}/c_{G_1}	L_1	L_3	$K_t=a'_3/a'_1$	$K_r=a'_2/a'_1$	$K_t=a'_5/a'_3$	$K_r=a'_4/a'_3$
27	1.7895	0.2556	7.0	6.574	2.791	0.4245	20.317	8.000	1.275	0.382	0.829	0.254
28	1.7895	0.2556	7.0	5.957	2.761	0.4635	15.271	6.189	1.795	0.138	0.728	0.141
29	1.7895	0.2556	7.0	5.371	2.723	0.5069	12.179	5.103	1.516	0.161	0.849	0.148
30	1.7895	0.2556	7.0	4.805	2.684	0.5586	10.172	4.413	1.550	0.244	0.519	0.483
31	1.7895	0.2556	7.0	4.353	2.638	0.6060	8.811	3.961	1.312	0.152	0.599	0.377
32	1.7895	0.2556	7.0	3.386	2.548	0.7525	6.472	3.196	0.657	0.212	1.418	0.311
33	1.7895	0.2556	7.0	1.978	2.183	1.1036	3.029	1.997	1.055	0.032	0.924	0.188
34	1.9173	0.3835	5.0	6.824	3.412	0.5000	21.887	10.164	1.301	0.283	0.815	0.354
35	1.9173	0.3835	5.0	6.220	3.394	0.5456	16.389	7.819	1.345	0.100	0.854	0.221
36	1.9173	0.3835	5.0	5.596	3.286	0.5872	13.179	6.479	1.516	0.149	0.778	0.271
37	1.9173	0.3835	5.0	4.905	3.177	0.6477	10.700	5.470	1.060	0.111	0.699	0.213
38	1.9173	0.3835	5.0	4.480	3.132	0.6991	9.388	4.949	0.821	0.237	0.836	0.255

Table Ib (continued)

Test No.	h_1	h_3	h_1/h_3	C_{G_1}	C_{G_3}	C_{G_3}/C_{G_1}	L_1	L_3	$K_t = a_3'/a_1'$	$K_r = a_2'/a_1'$	$K_t = a_5'/a_3'$	$K_r = a_4'/a_3'$
39	1.9173	0.3835	5.0	3.332	2.952	0.8859	6.544	3.833	0.916	0.354	0.882	0.193
40	1.9173	0.3835	5.0	2.050	2.402	0.5546	3.255	2.456	0.802	0.039	1.071	0.105
41	2.0451	0.5113	4.0	7.070	3.921	0.5940	23.313	12.081	0.956	0.532	0.674	0.275
42	2.0451	0.5113	4.0	6.441	3.826	0.5940	17.533	9.316	1.141	0.139	0.766	0.231
43	2.0451	0.5113	4.0	5.759	3.700	0.6424	13.996	7.657	1.094	0.149	0.737	0.432
44	2.0451	0.5113	4.0	5.145	3.602	0.7001	11.626	6.570	1.143	0.034	0.787	0.177
45	2.0451	0.5113	4.0	4.577	3.477	0.7596	9.834	5.763	1.074	0.163	0.819	0.278
46	2.0451	0.5113	4.0	3.427	3.232	0.9431	6.939	4.483	0.694	0.096	0.867	0.247
47	2.0451	0.5113	4.0	2.125	2.536	1.1934	3.489	2.836	0.865	0.142	0.992	0.136
48	2.3008	0.7669	3.0	7.428	4.720	0.6354	25.289	15.106	1.158	0.334	0.726	0.465
49	2.3008	0.7669	3.0	6.775	4.580	0.6760	20.590	11.920	1.578	0.200	0.800	0.277
50	2.3008	0.7669	3.0	6.102	4.414	0.7233	14.780	9.800	0.977	0.180	0.846	0.195
51	2.3008	0.7669	3.0	5.437	4.280	0.7871	13.010	8.380	1.216	0.062	---	---
52	2.3008	0.7669	3.0	4.887	4.120	0.8430	11.180	7.420	0.989	0.114	0.884	0.204
53	2.3008	0.7669	3.0	3.634	3.673	1.0107	7.801	5.665	0.807	0.296	---	---
54	2.3008	0.7669	3.0	2.256	2.670	1.1835	3.933	3.475	0.868	0.117	1.025	0.052
55	2.5564	1.0226	2.5	7.147	5.177	0.7243	21.741	14.423	0.900	0.458	0.735	0.244
56	2.5564	1.0226	2.5	6.434	4.996	0.7764	17.358	11.808	1.076	0.287	0.760	0.394
57	2.5564	1.0226	2.5	5.743	4.800	0.8358	14.495	10.124	0.989	0.138	0.886	0.260
58	2.5564	1.0226	2.5	5.133	4.559	0.8881	12.346	8.867	0.727	0.512	0.810	0.289
59	2.5564	1.0226	2.5	3.819	3.989	1.0445	8.672	6.745	0.880	0.039	0.867	0.233
60	2.5564	1.0226	2.5	2.370	2.743	1.1574	4.361	4.021	0.873	0.052	0.957	0.080

TABLE II   TEST SERIES WITH TRANSITION OF SLOPE 1:16

UNIFORM WIDTH $b_1 = b_3$

PARAMETERS $H_1 = 2a'_1$, $H_3 = 2a'_3$

$Z_1 = \dfrac{4\pi h_1}{L_1 S}$, $S = 1/16$

TEST NO.	T sec.	h_1 FT.	h_3 FT.	L_1 FT.	L_3 FT.	h_1/h_3	a'_1 FT.	a'_2 FT.	a'_3 FT.	H_1/L_1	H_3/L_3	$\dfrac{n_3 L_3 b_3}{n_1 L_1 b_1}$	Z_1	$K_r = \dfrac{a'_2}{a'_1}$	$K_t = \dfrac{a'_3}{a'_1}$
1	3.84	2.0	1.0	30.0'	21.7'	2.0	0.039	0.00785	0.0445	2.6×10^{-3}	4.1×10^{-3}	0.72	13.4	0.2011	1.1420
2	"	"	"	"	"	"	0.051	0.0085	0.0586	3.4×10^{-3}	5.4 "	"	"	0.1667	1.1492
3	"	"	"	"	"	"	0.0555	0.00826	0.0645	3.7 "	5.94 "	"	"	0.1489	1.1610
4	"	"	"	"	"	"	0.0670	0.00869	0.0787	4.47 "	7.25 "	"	"	0.1297	1.174
5	"	"	"	"	"	"	0.078	0.00912	0.0927	5.20 "	8.54 "	"	"	0.1169	1.189
6	4.175	"	"	32.5'	23.3'	"	0.0255	0.00647	0.02874	1.57 "	2.47 "	0.714	12.4	0.2537	1.126
7	"	"	"	"	"	"	0.0272	0.00677	0.03076	1.67 "	2.64 "	"	"	0.2488	1.130
8	"	"	"	"	"	"	0.0345	0.00777	0.0390	2.12 "	3.35 "	"	"	0.2251	1.1299
9	"	"	"	"	"	"	0.0630	0.01161	0.0727	3.88 "	6.24 "	"	"	0.1851	1.1530
10	"	"	"	"	"	"	0.060	0.00937	0.0697	3.69 "	5.98 "	"	"	0.1561	1.1610
11	"	"	"	"	"	"	0.0645	0.00984	0.0749	3.97 "	6.43 "	"	"	0.1525	1.162
12	4.46	"	"	35.0'	25.1'	"	0.032	0.00753	0.0363	1.93 "	2.89 "	"	11.5	0.2351	1.133
13	"	"	"	"	"	"	0.037	0.00833	0.0417	2.12 "	3.32 "	"	"	0.2248	1.126
14	"	"	"	"	"	"	0.0445	0.00903	0.0507	2.54 "	4.04 "	"	"	0.2026	1.138
15	"	"	"	"	"	"	0.0565	0.00980	0.0647	3.23 "	5.16 "	"	"	0.1749	1.145
16	"	"	"	"	"	"	0.0685	0.0112	0.0801	3.92 "	6.38 "	"	"	0.1622	1.168
17	4.76	"	"	37.5'	26.8'	"	0.042	0.00925	0.04475	2.24 "	3.34 "	"	10.7	0.2221	1.136
18	"	"	"	"	"	"	0.0475	0.00957	0.0543	2.53 "	4.05 "	"	"	0.2078	1.142
19	"	"	"	"	"	"	0.059	0.01118	0.0675	3.15 "	5.04 "	"	"	0.1895	1.144
20	"	"	"	"	"	"	0.0655	0.01135	0.0756	3.5 "	5.64 "	"	"	0.1732	1.154
21	"	"	"	"	"	"	0.079	0.01126	0.0922	4.21 "	6.88 "	"	"	0.1425	1.167
22	5.055	"	"	40.0	28.5	"	0.0345	0.00867	0.0391	1.72 "	2.74 "	"	10.1	0.2510	1.132

36

TABLE II CONTINUED

TEST NO.	T Sec.	h_1 FT.	h_3 FT.	L_1 FT.	L_3 FT.	h_1/h_3	a'_1 FT.	a'_2 FT.	a'_3 FT.	H_1/L_1	H_3/L_3	$\frac{n_3 L_3 b_3}{n_1 L_1 b_1}$	Z_1	$K_r = \frac{a'_2}{a'_1}$	$K_t = \frac{a'_3}{a'_1}$
23	"	"	"	"	"	"	0.0440	0.00945	0.0498	2.20×10^{-3}	3.49×10^{-3}	"	"	0.2169	1.131
24	"	"	"	"	"	"	0.0635	0.01111	0.0729	3.18 "	5.12 "	"	"	0.1750	1.148
25	5.38	"	"	42.5'	30.3'	"	0.0325	0.00853	0.0366	1.53 "	2.42 "	"	9.5	0.2622	1.126
26	"	"	"	"	"	"	0.038	0.00932	0.0431	1.79 "	2.84 "	"	"	0.2451	1.132
27	"	"	"	"	"	"	0.0545	0.0115	0.0615	2.57 "	4.06 "	"	"	0.2109	1.127
28	6.075	2.0	1.0	47.5'	33.7'	2.0	0.026	0.00809	0.02917	1.1×10^{-3}	1.73×10^{-3}	0.714	8.5	0.3111	1.121
29	"	"	"	"	"	"	0.038	0.00946	0.0427	1.6 "	2.53 "	"	"	0.2489	1.123
30	"	"	"	"	"	"	0.072	0.0209	0.0821	3.03 "	4.89 "	"	"	0.2828	1.140
31	6.30	"	"	50.0'	35.6'	"	0.026	0.00819	0.0294	1.04 "	1.65 "	"	8.1	0.3152	1.130
32	"	"	"	"	"	"	0.0385	0.00997	0.0434	1.54 "	2.44 "	"	"	0.2588	1.127
33	"	"	"	"	"	"	0.0735	0.01267	0.0847	2.95 "	4.76 "	"	"	0.1723	1.152
34	4.00	1.833	0.833	30.0'	20.7'	2.2	0.0465	0.00815	0.0546	3.10 "	5.28 "	0.694	12.3	0.1752	1.174
35	"	"	"	"	"	"	0.0670	0.00954	0.0805	4.47 "	7.78 "	"	"	0.1423	1.201
36	"	"	"	"	"	"	0.0910	0.0110	0.1131	6.06 "	10.93 "	"	"	0.1208	1.242
37	4.65	"	"	35.0'	23.8'	"	0.0345	0.00789	0.04025	1.97 "	3.38 "	"	10.6	0.2289	1.166
38	"	"	"	"	"	"	0.0450	0.00899	0.0526	2.57 "	4.42 "	"	"	0.1997	1.168
39	"	"	"	"	"	"	0.0640	0.01024	0.0761	3.66 "	6.39 "	"	"	0.1599	1.188
40	5.275	"	"	40.0'	27.2'	"	0.0245	0.00667	0.02486	1.23 "	1.83 "	"	9.24	0.2721	1.160
41	"	"	"	"	"	"	0.0305	0.00766	0.0355	1.53 "	2.61 "	"	"	0.2511	1.164
42	"	"	"	"	"	"	0.0465	0.01018	0.0546	2.33 "	4.01 "	"	"	0.2188	1.174
43	5.93	"	"	45.0'	30.8'	"	0.026	0.00651	0.0303	1.16 "	1.97 "	"	8.2	0.2502	1.164
44	"	"	"	"	"	"	0.0365	0.00886	0.0424	1.62 "	2.75 "	"	"	0.2427	1.162
45	"	"	"	"	"	"	0.0515	0.01076	0.0603	2.28 "	3.92 "	"	"	0.2089	1.171
46	6.56	"	"	50.0'	33.9'	"	0.018	0.00651	0.02066	0.72 "	1.22 "	"	7.4	0.3619	1.148
47	"	"	"	"	"	"	0.0235	0.00722	0.0272	0.94 "	1.60 "	"	"	0.3068	1.157

37

TABLE II CONTINUED

TEST NO.	T sec	h_1 FT.	h_3 FT.	L_1 FT.	L_3 FT	h_1/h_3	a'_1 FT.	a'_2 FT.	a'_3 FT.	H_1/L_1 ×10⁻³	H_3/L_3 ×10⁻³	$\dfrac{n_3 L_3 b_3}{n_1 L_1 b_1}$	Z_1	$K_r = \dfrac{a'_2}{a'_1}$	$K_t = \dfrac{a'_3}{a'_1}$
48	6.56	1.833	0.833	50.0'	33.9'	2.2	0.0306	0.00745	0.0362	1.36	2.35	0.694	7.4	0.243	1.183
49	4.185	1.667	0.667	30.0'	19.2'	2.5	0.0365	0.00717	0.0436	2.43	4.54	0.653	11.2	0.1962	1.194
50	"	"	"	"	"	"	0.0565	0.00947	0.0678	3.7	7.06	"	"	0.1675	1.200
51	"	"	"	"	"	"	0.076	0.01046	0.0928	5.03	9.67	"	"	0.1377	1.221
52	4.74	"	"	35.0'	22.3'	"	0.0225	0.00591	0.0268	1.29	2.40	"	9.64	0.2622	1.190
53	"	"	"	"	"	"	0.0345	0.00786	0.041	1.97	3.68	"	"	0.2276	1.188
54	"	"	"	"	"	"	0.050	0.00984	0.0598	2.86	5.36	"	"	0.1967	1.196
55	5.52	1.667	0.667	40.0	25.4	2.5	0.0165	0.00581	0.0192	0.825	1.51	0.653	8.4	0.3522	1.156
56	"	"	"	"	"	"	0.023	0.00633	0.0273	1.15	2.15	"	"	0.2751	1.186
57	"	"	"	"	"	"	0.0315	0.00797	0.0375	1.57	2.95	"	"	0.2528	1.190
58	6.201	"	"	45.0	28.4	"	0.0190	0.00662	0.0223	0.85	1.57	"	7.46	0.3481	1.174
59	"	"	"	"	"	"	0.029	0.00763	0.03444	1.29	2.43	"	"	0.2628	1.188
60	"	"	"	"	"	"	0.044	0.01012	0.0523	1.96	3.68	"	"	0.2299	1.190
61	6.87	"	"	50.0	31.6	"	0.0215	0.00745	0.02525	0.86	1.60	"	6.7	0.3467	1.174
62	"	"	"	"	"	"	0.030	0.00823	0.03559	1.2	2.25	"	"	0.2741	1.184
63	"	"	"	"	"	"	0.043	0.01085	0.0517	1.72	3.27	"	"	0.2425	1.201
64	4.38	1.50	0.50	30.0	17.5	3.0	0.0302	0.00619	0.0367	2.35	4.19	0.599	10.1	0.2051	1.215
65	"	"	"	"	"	"	0.0483	0.00871	0.0591	3.42	6.76	"	"	0.1800	1.221
66	"	"	"	"	"	"	0.0651	0.00757	0.0803	4.89	9.18	"	"	0.1163	1.234
67	5.11	"	"	35.0	20.4	"	0.0187	0.00513	0.02265	1.21	2.22	"	8.7	0.2741	1.211
68	"	"	"	"	"	"	0.0255	0.0058	0.03136	1.86	3.07	"	"	0.2271	1.229
69	"	"	"	"	"	"	0.0372	0.00728	0.0453	2.69	4.44	"	"	0.1959	1.219
70	5.81	"	"	40.0	23.2	"	0.0106	0.00316	0.01268	0.90	1.094	"	7.55	0.2981	1.196
71	"	"	"	"	"	"	0.0155	0.00418	0.01867	1.21	1.61	"	"	0.2700	1.204
72	"	"	"	"	"	"	0.0198	0.00483	0.0240	1.51	2.07	"	"	0.2439	1.212

38

TABLE II CONTINUED

TEST NO.	T sec	h_1 FT.	h_3 FT.	L_1 FT.	L_3 FT.	h_1/h_3	a'_1 ft	a'_2 FT.	a'_3 FT.	H_1/L_1 x10⁻³	H_3/L_3 x10⁻³	$\dfrac{n_3 L_3 b_3}{n_1 L_1 b_1}$	Z_1	$K_r = \dfrac{a'_2}{a'_1}$	$K_t = \dfrac{a'_3}{a'_1}$
73	6.53	1.50	0.50	45.0	26.1	3.0	0.0110	0.00340	0.07322	0.93	1.006	0.599	6.7	0.3009	1.201
74	"	"	"	"	"	"	0.0207	0.00549	0.0252	1.32	1.93	"	"	0.2652	1.210
75	"	"	"	"	"	"	0.0332	0.00721	0.04035	2.07	3.09	"		0.2170	1.217
76	7.25	"	"	50.0	29.0	"	0.0167	0.00467	0.02018	1.11	1.392	"	6.05	0.2793	1.208
77	"	"	"	"	"	"	0.0244	0.00657	0.02946	1.28	2.03	"	"	0.2693	1.207
78	"	"	"	"	"	"	0.0321	0.00763	0.0387	1.75	2.67	"	"	0.2375	1.205
79	0.674	2.0	1.0	2.34	2.3	2.0	0.027	0.00713	0.0254	2.33×10^{-2}	2.19×10^{-2}	1.035		0.264	0.941
80	"	"	"	"	"	"	0.031	0.0080	0.02946	2.68 "	2.54 "	"		0.258	0.951
81	"	"	"	"	"	"	0.040	0.00993	0.03728	3.43 "	3.22 "	"		0.248	0.932
82	0.73	"	"	2.73	2.68	"	0.071	0.01647	0.0690	5.15 "	5.14 "	1.067		0.232	0.972
83	"	"	"	"	"	"	0.077	0.01802	0.0746	5.65 "	5.56 "	"		0.234	0.968
84	"	"	"	"	"	"	0.081	0.01832	0.0805	5.86 "	6.00 "	"		0.226	0.994
85	0.814	"	"	3.39	3.25	"	0.049	0.01215	0.0452	2.84 "	2.78 "	1.11		0.248	0.923
86	"	"	"	"	"	"	0.051	0.01296	0.0471	2.96 "	2.89 "	"		0.254	0.922
87	"	"	"	"	"	"	0.059	0.01464	0.0565	3.42 "	3.47 "	"		0.248	0.958
88	0.931	"	"	4.41	4.06	"	0.047	0.01213	0.0426	2.11 "	2.09 "	1.135		0.258	0.906
89	"	"	"	"	"	"	0.052	0.01316	0.0495	2.38 "	2.44 "	"		0.253	0.952
90	"	"	"	"	"	"	0.058	0.0145	0.0545	2.66 "	2.68 "	"		0.250	0.940
91	1.054	"	"	5.57	4.88	"	0.069	0.01781	0.0650	2.49 "	2.66 "	1.11		0.258	0.942
92	"	"	"	"	"	"	0.076	0.01664	0.0704	2.74 "	2.88 "	"		0.219	0.927
93	"	"	"	"	"	"	0.083	0.02308	0.0803	3.0 "	3.70 "	"		0.278	0.968
94	1.236	"	"	7.36	6.1	"	0.061	0.01611	0.0547	1.65 "	1.79 "	1.036		0.264	0.897
95	"	"	"	"	"	"	0.064	0.01652	0.06058	1.74 "	1.98 "	"		0.258	0.946
96	1.545	"	"	10.28	8.01	"	0.058	0.01532	0.04924	1.14 "	1.22 "	0.922		0.264	0.849
97	"	"	"	"	"	"	0.065	0.01697	0.0596	1.28 "	1.48 "	"		0.261	0.916

TABLE II CONTINUED

TEST NO.	T sec	h_1 FT.	h_3 FT.	L_1 FT.	L_3 FT.	h_1/h_3	a'_1 ft	a'_2 FT.	a'_3 FT.	H_1/L_1 x10⁻³	H_3/L_3 x10⁻³	$\dfrac{n_3 L_3 b_3}{n_1 L_1 b_1}$	Z_1	$K_r = \dfrac{a'_2}{a'_1}$	$K_t = \dfrac{a'_2}{a'_1}$
98	2.128	2.0	1.0	15.52	11.54	2.0	0.077	0.02142	0.0707	1.0	1.22	0.816		0.278	0.918
99	"	"	"	"	"	"	0.082	0.0254	0.0768	1.065	1.33	"		0.306	0.937
100	3.145	"	"	24.23	17.45	"	0.066	0.01010	0.0768	5.4	0.82	0.752		0.153	1.163
101	"	"	"	"	"	"	0.073	0.01176	0.0859	5.96	0.98	"		0.161	1.176
102	0.673	1.833	0.833	2.32	2.27	2.2	0.025	0.00653	0.0239	2.17	2.1	1.07		0.261	0.956
103	"	"	"	"	"	"	0.030	0.00756	0.02738	2.6	2.41	"		0.252	0.917
104	"	"	"	"	"	"	0.039	0.00999	0.0377	3.38	3.32	"		0.256	0.966
105	0.731	"	"	2.74	2.64	"	0.069	0.0156	0.0689	5.0	5.22	1.105		0.226	0.998
106	"	"	"	"	"	"	0.076	0.01696	0.0740	5.5	5.45	"		0.223	0.974
107	"	"	"	"	"	"	0.081	0.01870	0.0783	5.86	5.93	"		0.232	0.967
108	0.826	"	"	3.48	3.23	"	0.047	0.01256	0.0447	2.72	2.76	1.145		0.267	0.951
109	"	"	"	"	"	"	0.050	0.0129	0.0458	2.9	2.83	"		0.258	0.917
110	"	"	"	"	"	"	0.059	0.01487	0.0555	3.42	3.43	"		0.252	0.941
111	0.928	"	"	4.36	3.86	"	0.044	0.01194	0.0408	2.02	2.11	"		0.271	0.929
112	"	"	"	"	"	"	0.050	0.013	0.0454	2.29	2.35	"		0.260	0.909
113	"	"	"	"	"	"	0.057	0.01608	0.0506	2.62	2.62	"		0.282	0.886
114	1.063	"	"	5.61	4.67	"	0.068	0.01844	0.0656	2.46	2.8	1.085		0.271	0.965
115	"	"	"	"	"	"	0.076	0.0203	0.0701	2.75	3.0	"		0.267	0.922
116	"	"	"	"	"	"	0.082	0.02116	0.0770	2.97	3.29	"		0.258	0.939
117	1.259	"	"	7.40	5.8	"	0.06	0.01896	0.0565	1.63	1.95	0.988		0.316	0.942
118	"	"	"	"	"	"	0.064	0.01652	0.0599	1.74	2.06	"		0.258	0.936
119	1.545	"	"	10.03	7.44	"	0.057	0.01505	0.0520	1.12	1.39	0.874		0.264	0.912
120	"	"	"	"	"	"	0.064	0.01677	0.0592	1.26	1.59	"		0.262	0.925
121	2.185	"	"	15.45	10.9	"	0.076	0.02258	0.06680	0.986	1.22	0.773		0.297	0.879
122	"	"	"	"	"	"	0.082	0.02165	0.07610	1.07	1.396	"		0.264	0.928

40

TABLE II CONTINUED

TEST NO.	T (sec)	h_1 (FT.)	h_3 (FT.)	L_1 (FT.)	L_3 (FT.)	h_1/h_3	a'_1 (ft)	a'_2 (FT.)	a'_3 (FT.)	H_1/L_1 $\times10^{-2'}$	H_3/L_3 $\times10^{-2^3}$	$\dfrac{n_3 L_3 b_3}{n_1 L_1 b_1}$	Z_1	$K_r = \dfrac{a'_2}{a'_1}$	$K_t = \dfrac{a'_3}{a'_1}$
123	3.3	1.833	0.833	24.45	16.8	2.2	0.064	0.01004	0.0756	5.28	0.9	0.714		0.1566	1.181
124	"	"	"	"	"	"	0.073	0.01172	0.08730	5.97	1.04	"		0.1603	1.1957
125	0.674	1.667	0.667	2.33	2.222	2.5	0.021	0.0054	0.01951	1.82	1.75	1.12		0.257	0.929
126	"	"	"	"	"	"	0.027	0.00681	0.02480	2.33	2.44	"		0.252	0.918
127	"	"	"	"	"	"	0.035	0.00876	0.03277	3.03	2.94	"		0.250	0.936
128	0.736	"	"	2.77	2.564	"	0.066	0.01584	0.0636	4.77	4.96	1.15		0.240	0.963
129	"	"	"	"	"	"	0.072	0.01693	0.0733	5.21	5.71	"		0.235	1.018
130	"	"	"	"	"	"	0.077	0.01772	0.0794	5.58	6.19	"		0.23	1.031
131	0.826	"	"	3.50	3.085	"	0.045	0.01080	0.0425	2.61	2.75	1.18		0.24	0.943
132	"	"	"	"	"	"	0.0498	0.01316	0.0444	2.88	2.87	"		0.264	0.892
133	"	"	"	"	"	"	0.055	0.01276	0.0522	3.18	3.38	"		0.232	0.948
134	0.929	"	"	4.35	3.79	"	0.042	0.01272	0.03875	1.92	1.78	1.135		0.305	0.922
135	"	"	"	"	"	"	0.047	0.01156	0.0443	2.16	2.33	"		0.246	0.943
136	"	"	"	"	"	"	0.052	0.01092	0.0487	2.38	2.57	"		0.21	0.936
137	1.061	"	"	5.52	4.32	"	0.067	0.01836	0.06450	2.42	2.98	1.05		0.274	0.962
138	"	"	"	"	"	"	0.073	0.01745	0.0689	2.63	3.19	"		0.239	0.944
139	"	"	"	"	"	"	0.079	0.02284	0.0712	2.86	3.29	"		0.289	0.902
140	1.274	"	"	7.41	5.42	"	0.058	0.01496	0.05385	1.57	1.96	0.93		0.258	0.928
141	"	"	"	"	"	"	0.063	0.01588	0.0595	1.71	2.19	"		0.252	0.944
142	1.636	"	"	10.45	7.19	"	0.054	0.01587	0.0517	1.06	1.44	0.806		0.294	0.957
143	"	"	"	"	"	"	0.061	0.01525	0.05425	1.2	1.51	"		0.250	0.889
144	2.263	"	"	15.6	10.25	"	0.075	0.02522	0.0653	0.975	1.27	0.71		0.323	0.872
145	"	"	"	"	"	"	0.082	0.02092	0.0742	1.07	1.44	"		0.255	0.904
146	3.49	"	"	24.85	16.0	"	0.063	0.0090	0.0707	0.514	0.88	0.665		0.1428	1.1217
147	"	"	"	"	"	"	0.071	0.0117	0.08370	0.58	1.04	"		0.1649	1.1791

47

TABLE II CONTINUED

TEST NO.	T sec	h_1 FT.	h_3 FT.	L_1 FT.	L_3 FT.	h_1/h_3	a'_1 ft	a'_2 FT.	a'_3 FT	H_1/L_1 x10⁻²	H_3/L_3 x10⁻²	$\frac{n_3 L_3 b_3}{n_1 L_1 b_1}$	Z_1	$K_r = \frac{a'_2}{a'_1}$	$K_t = \frac{a'_3}{a'_1}$
148	0.672	1.50	0.50	2.31	2.092	3.0	0.036	0.0100	0.0344	3.12	3.28	1.17		0.278	0.946
149	"	"	"	"	"	"	0.029	0.00754	0.02708	2.52	2.59	"		0.260	0.934
150	"	"	"	"	"	"	0.030	0.0072	0.02755	2.6	2.62	"		0.240	0.918
151	"	"	"	"	"	"	0.032	0.0072	0.0308	2.77	2.94	"		0.225	0.962
152	0.734	"	•	2.76	2.392	"	0.061	0.01483	0.0593	4.42	4.95	1.18		0.243	0.972
153	"	"	"	"	"	"	0.0655	0.01463	0.0656	4.75	5.48	"		0.220	0.986
154	"	"	"	"	"	"	0.0685	0.01521	0.0648	4.96	5.42	•		0.222	0.946
155	0.82	"	"	3.45	2.81	"	0.0865	0.02294	0.0848	5.0	6.03	1.155		0.265	0.980
156	"	"	"	3.45	"	"	0.0825	0.01642	0.07726	4.79	5.5	"		0.199	0.937
157	0.922	"	"	4.36	3.305	"	0.0885	0.01930	0.08586	4.06	5.19	1.02		0.218	0.970
158	"	"	"	"	"	"	0.1035	0.0294	0.0996	4.75	6.02	"		0.284	0.962
159	1.04	"	"	5.59	3.928	"	0.0955	0.02484	0.0883	3.45	4.49	0.97		0.260	0.925
160	"	"	"	"	"	"	0.120	0.02905	0.1136	4.33	5.78	"		0.242	0.932
161	1.28	"	"	7.38	4.89	"	0.0825	0.02185	0.07775	2.33	3.17	0.84		0.265	0.943
162	"	"	"	"	"	"	0.104	0.0257	0.0989	2.82	4.04	"		0.247	0.951
163	1.661	"	"	10.2	6.41	"	0.079	0.02306	0.0715	1.55	2.23	0.735		0.292	0.905
164	"	"	"	"	"	"	0.098	0.02568	0.0924	1.92	2.88	"		0.262	0.943
165	2.18	"	"	15.4	11.25	"	0.066	0.02133	0.0563	0.856	1.0	0.646		0.323	0.854
166	"	"	"	"	"	"	0.082	0.02074	0.07180	1.07	1.27	"		0.253	0.876
167	3.54	"	"	24.5	14.4	"	0.045	0.00905	0.0542	0.367	0.75	0.471		0.2011	1.207
168	"	"	"	"	"	"	0.053	0.0102	0.0635	0.433	0.95	"		0.1923	1.1978

V. PRESENTATION AND DISCUSSION OF RESULTS

5.1 General Specifications

Experimental results tabulated in the preceding section IV are presented on individual graphs for ready reference, identified according to the slope of the transition and according to the characteristics of the waves, whether in the short and intermediate wave range or in the shallow water wave range.

Since a satisfactory theory for gradual transitions does not exist, all results are given as derived from the reduced data for amplitudes of incoming, reflected and transmitted waves. Accordingly in the following presentation the reflection and transmission coefficients are given uniformly as defined by the elementary theory (3) for abrupt transitions and for long waves:

$$K_r = \frac{a'_r}{a'_i} \tag{5.1}$$

and

$$K_t = \frac{a'_t}{a'_i} \tag{5.2}$$

wherein the prime indicates the amplitude obtained on the basis of the preceeding analysis for the infinite channel conditions. The elementary theory for abrupt transitions also defines reflection and transmission coefficients in terms of the wave velocity for shallow water waves, which is identical in this latter case with the velocity of energy transmission. Since for short and intermediate waves the velocity of energy transmission, i.e. the group velocity, is different from the wave or phase velocity, the following results are compared to the results of the elementary theory by employing the "group velocity" C_G throughout. Thus the reflection and transmission coefficients for short and intermediate waves obtained by experiment are plotted against the group velocity ratio as the most meaningful parameter obtained from energy balance considerations.

The theoretical lines appearing in the graphs were computed from the elementary theory for abrupt transitions for shallow-water waves and hence must be considered only for reference rather than as representing a significant theory for short and intermediate waves. It must further be recalled that energy dissipation is not considered in the theory, although it must have a significant influence on the measured quantities.

For purposes of unified presentation these theoretical reflection and transmission coefficients are redefined now as:

$$K_r = \frac{1 - C_{G_3}/C_{G_1}}{1 + C_{G_3}/C_{G_1}} = \frac{1 - \dfrac{n_3 L_3 b_3}{n_1 L_1 b_1}}{1 + \dfrac{n_3 L_3 b_3}{n_1 L_1 b_1}} \tag{5.3}$$

and

$$K_t = \cfrac{2}{1 + C_{G_3}/C_{G_1}} = \cfrac{2}{1 + \cfrac{n_3 L_3 b_3}{n_1 L_1 b_1}} \tag{5.4}$$

All results for K_r and K_t were therefore presented in relation to the group velocity ratio. Only in the case of shallow-water waves will these expressions reduce to:

$$K_r = \cfrac{1 - \cfrac{b_3}{b_1}\sqrt{\cfrac{h_3}{h_1}}}{1 + \cfrac{b_3}{b_1}\sqrt{\cfrac{h_3}{h_1}}} \tag{5.5}$$

$$K_t = \cfrac{2}{1 + \cfrac{b_3}{b_1}\sqrt{\cfrac{h_3}{h_1}}} \tag{5.6}$$

Thus it is appropriate to plot in this case the results against depth ratios. For short and intermediate waves the group velocities were determined in accordance with small amplitude theory from:

$$C_G = C \cdot \frac{1}{2}\left[1 + \frac{2kh}{\sinh 2kh}\right] = C \cdot n \tag{5.7}$$

Wave tables (12) were employed for the evaluation of all ratios of the group velocities C_{G_3}/C_{G_1}. For values of C_{G_3}/C_{G_1} larger than unity the absolute value of K_r was assumed since a negative reflection coefficient has no physical meaning. The energy balance results in:

$$(1 - K_r^2) \, C_{G_1} = K_t^2 \, C_{G_3}$$

hence

$$K_r = \sqrt{1 - K_t^2 \, \frac{C_{G_3}}{C_{G_1}}} \tag{5.8}$$

5.2 Results for Short and Intermediate Waves

a. Reflection Coefficients

The reflection coefficients for the first test program for the transitions of slope 1:.58 (60°) and 1:2.75 (20°) are presented in Figures 13 and 14. The reflection coefficients obtained in the second test series

for the transition of slope 1:16 are given in Figure 15. All coefficients have been plotted as a function of the group velocity ratio in accordance with the preceding discussion. In general, there is a trend of increasing values of the reflection coefficients with decreasing steepness of slope, when those of the flatter slope are compared with those of the steeper slopes. For the two steeper slopes this trend is marked by the limitations of apparent experimental scatter. However the range of relative depth ratios is larger for these transitions than for the 1:16 slope and hence their effect is unfortunately not clearly evident. In comparison to the theoretical values for abrupt transitions and shallow water waves reflections are significantly higher for group-velocity ratios near unity, approaching the theoretical line for lower values of this ratio. In general it may be remarked that reflection coefficients for the wave conditions under discussion show relatively little variation with either the depth ratio or the group velocity ratio, a trend particularly evident from the results of the transition of slope 1:16. Figure 16 gives the reflection coefficient for short and intermediate waves as a function of wave steepness for the slope of 1:16. There is practically no effect except for a slight decreasing trend with increasing wave steepness.

Incidental to the above results with sloping transitions data were also secured for the abrupt transition case simultaneously with the tests for the steeper transitions. For identification with the test series in which these data were obtained, these reflection coefficients for the abrupt section change are plotted in Figures 17 and 18 corresponding to the transition existing upstream. It should be noted that the values of the group velocity ratio are given in accordance with the convention adopted for the direction of wave travel and thus are largely falling above unity. For comparison with the preceding results for sloping transitions the inverse values of the group velocities should be used. Generally again the experimental results give higher values for the group velocity ratio near unity, but approaching the theoretical curve for larger values of this ratio.

To be noted generally for abrupt and for the steeply sloping transitions is the fact that for the group velocity ratios of .85 and 1.18 respectively the experimental results agree with minimum scatter with the theoretical value.

b. Transmission Coefficients

The transmission coefficients for the first test program for the transitions of steeper slope are given in Figures 19 and 20, which results correspond to Figures 13 and 14 for the reflection coefficients. The average values of the transmission coefficients are less than predicted from the elementary theory by about the same amount for both transitions. There is considerable scatter of the values primarily for the higher ratios of h_1/h_3, when waves transmitted suffer considerable change in shape. In general again best agreement exists for values where the group velocity ratio is near or in excess of unity. The transmission coefficients for the second test program
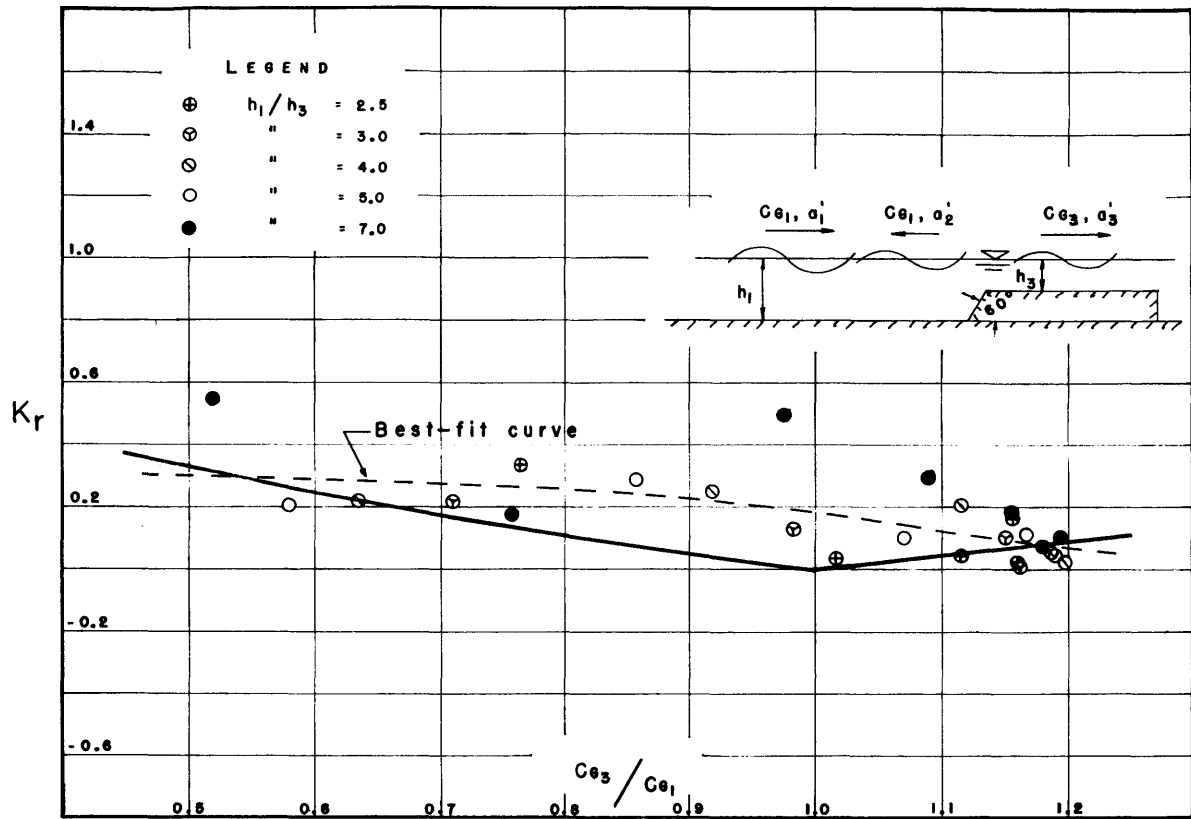
Fig. 13 Reflection Coefficients--Short and Intermediate Waves--
Transition Slope 1:0.58 (α = 60°)

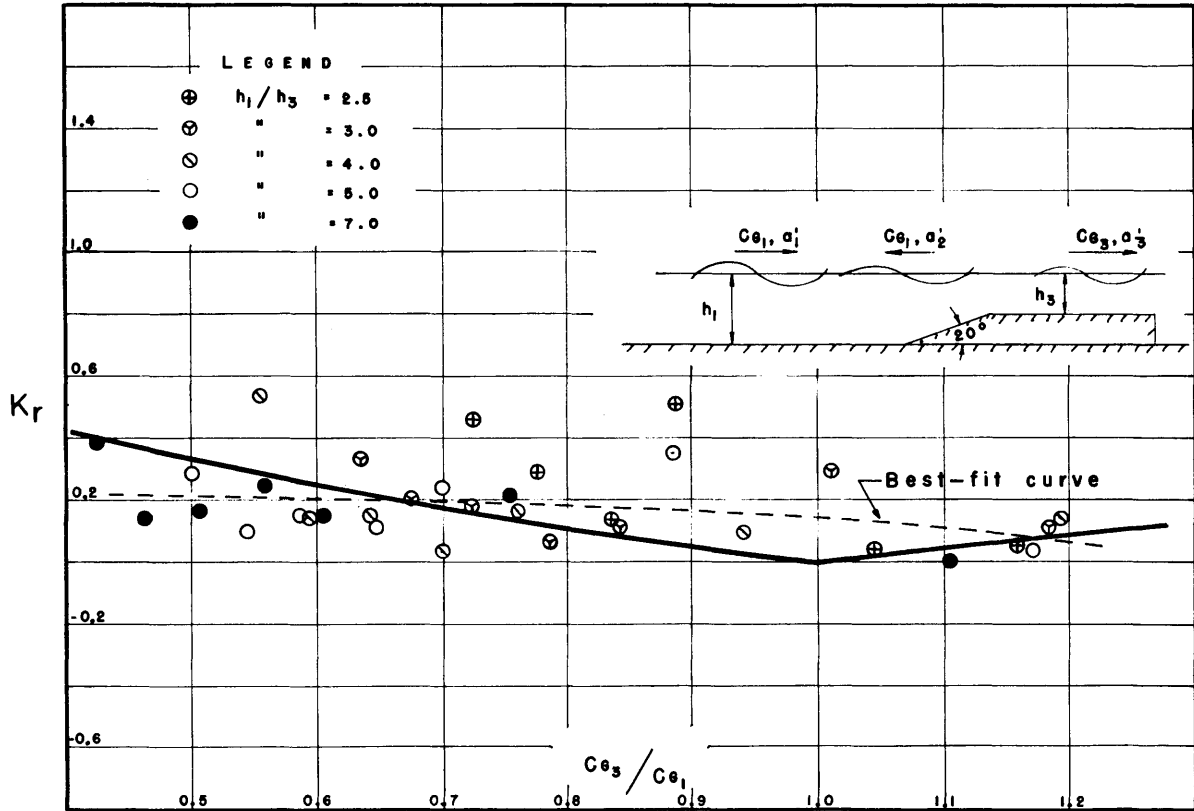Fig. 14 Reflection Coefficients--Short and Intermediate Waves--
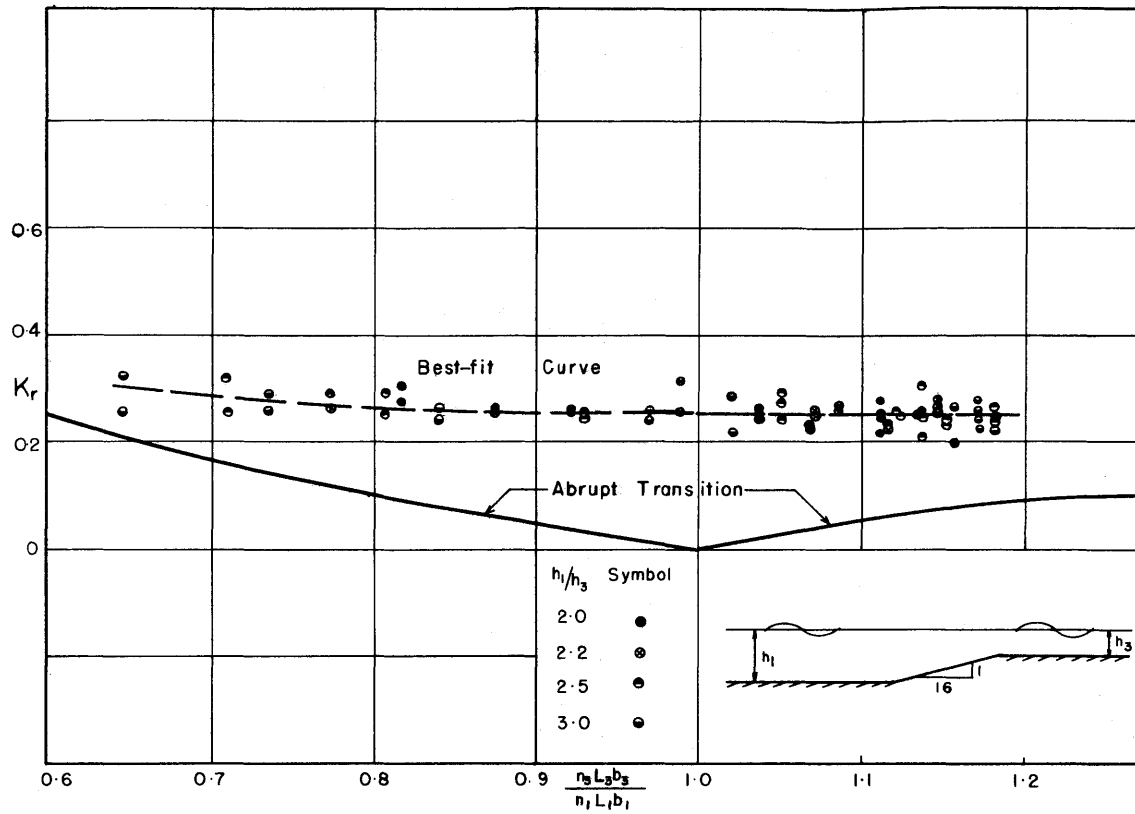Transition Slope 1:2.75 (α = 20°)

46

Fig. 15   Reflection Coefficients--Short and Intermediate Waves--
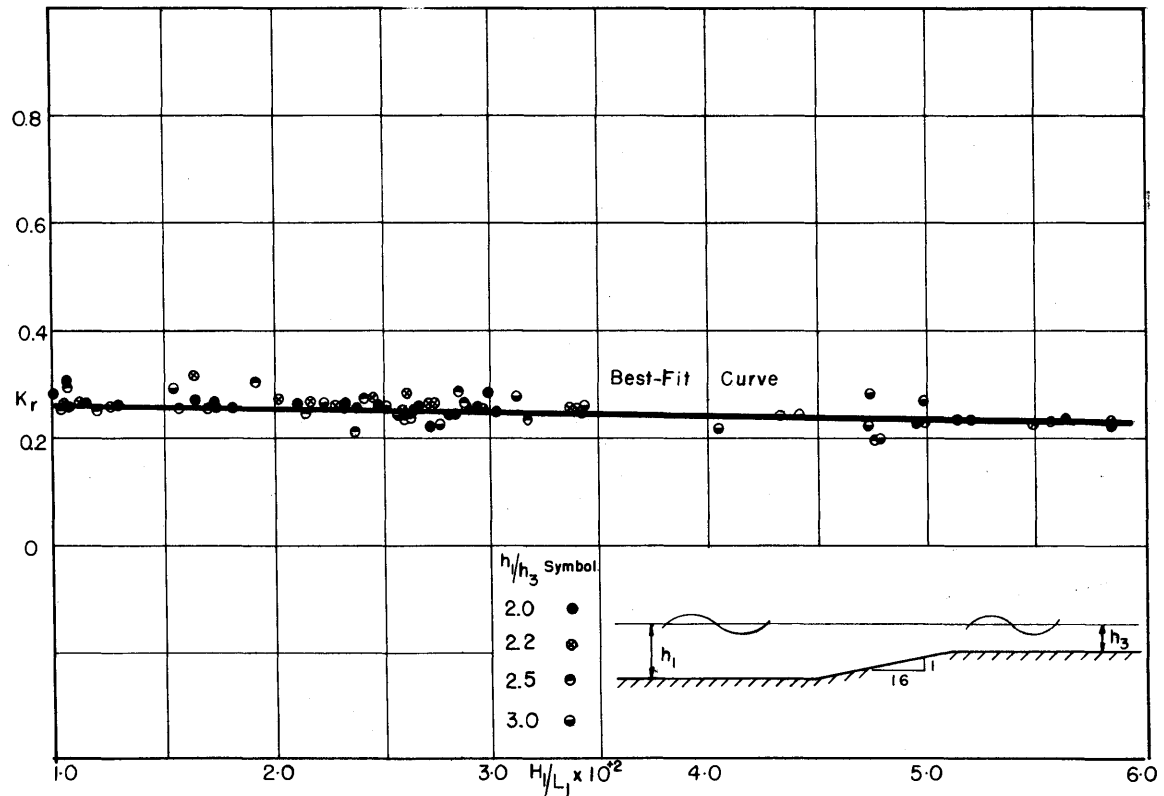Transition Slope 1:16

Fig. 16   Reflection Coefficients Vs. Wave Steepness--Short and Intermediate
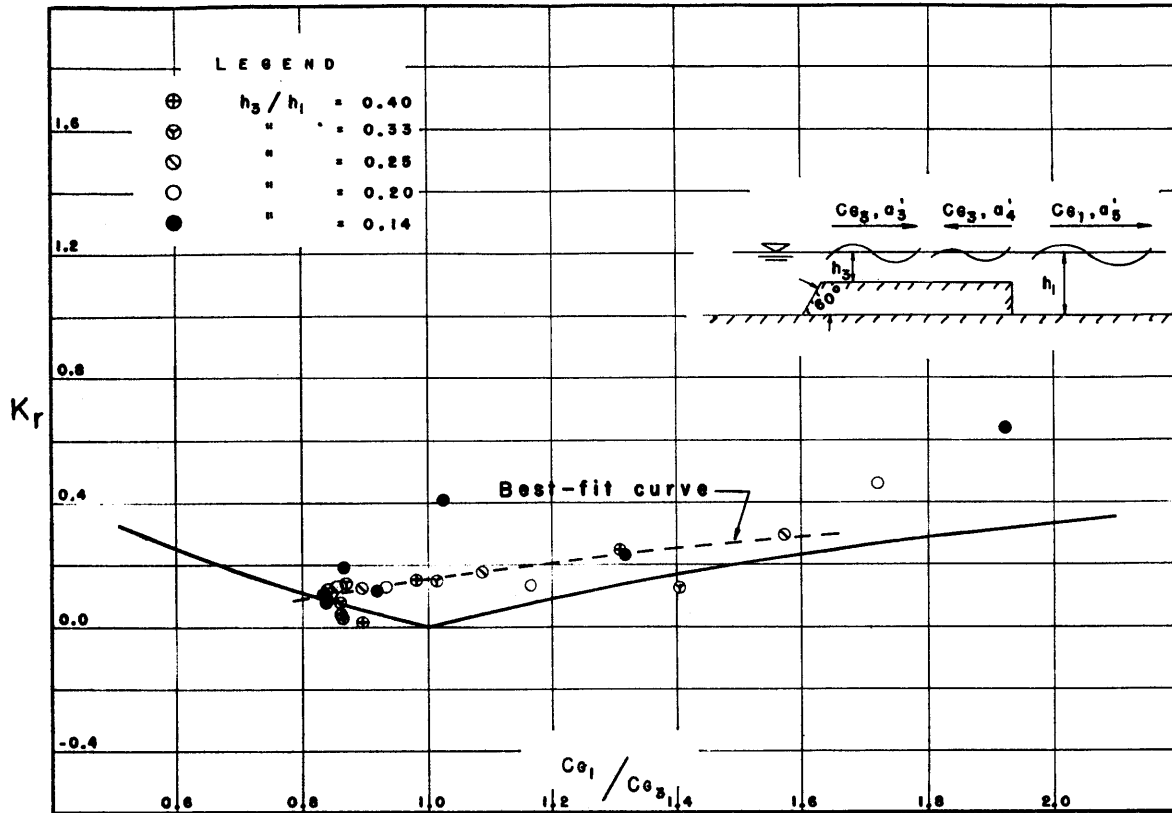Waves--Transition Slope 1:16

47

Fig. 17 Reflection Coefficients--Short and Intermediate Waves--
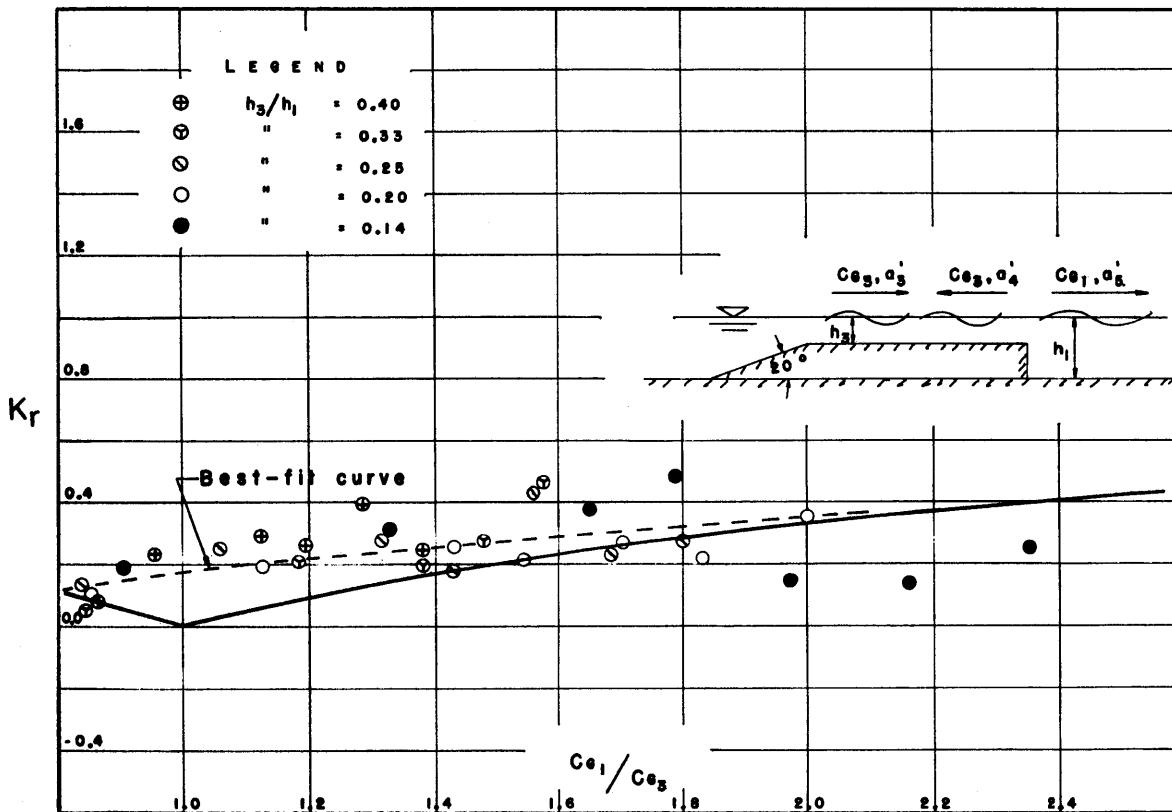Abrupt Transition Downstream

Fig. 18 Reflection Coefficients--Short and Intermediate Waves--
Abrupt Transition Downstream

48

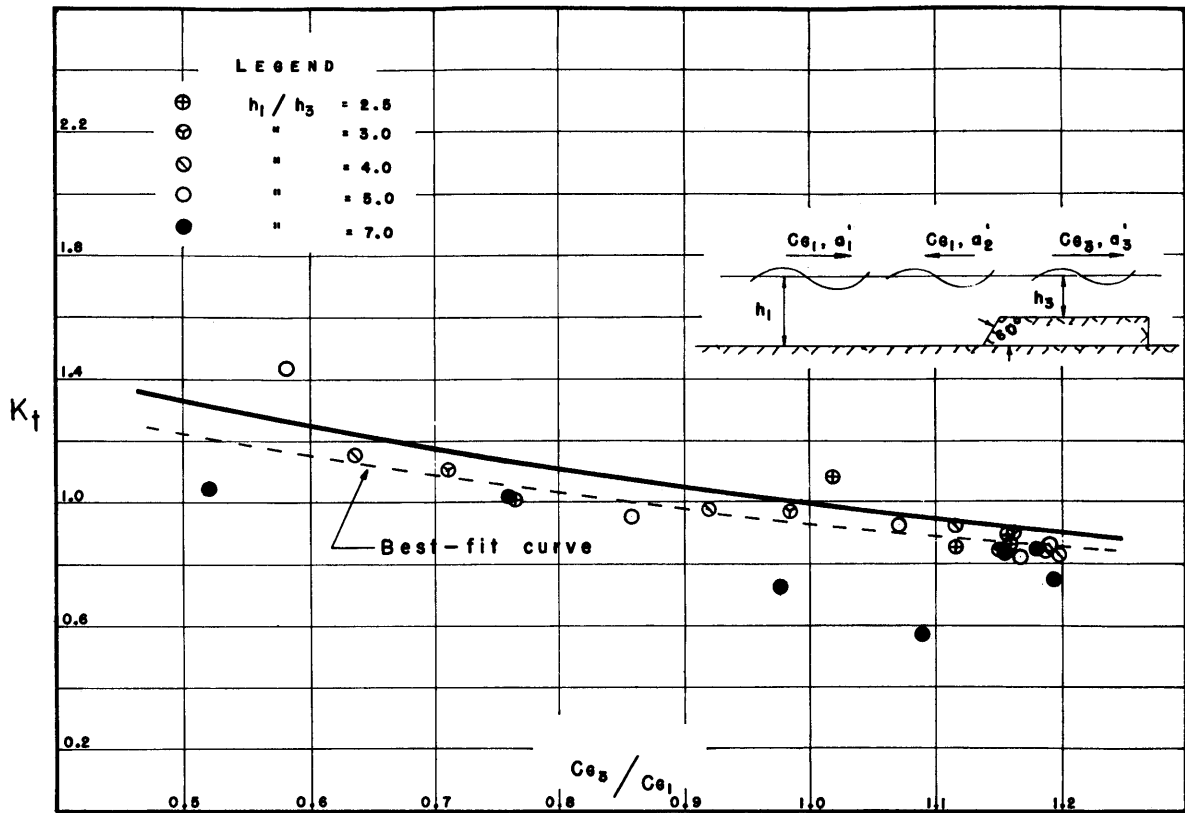Fig. 19   Transmission Coefficients--Short and Intermediate Waves--
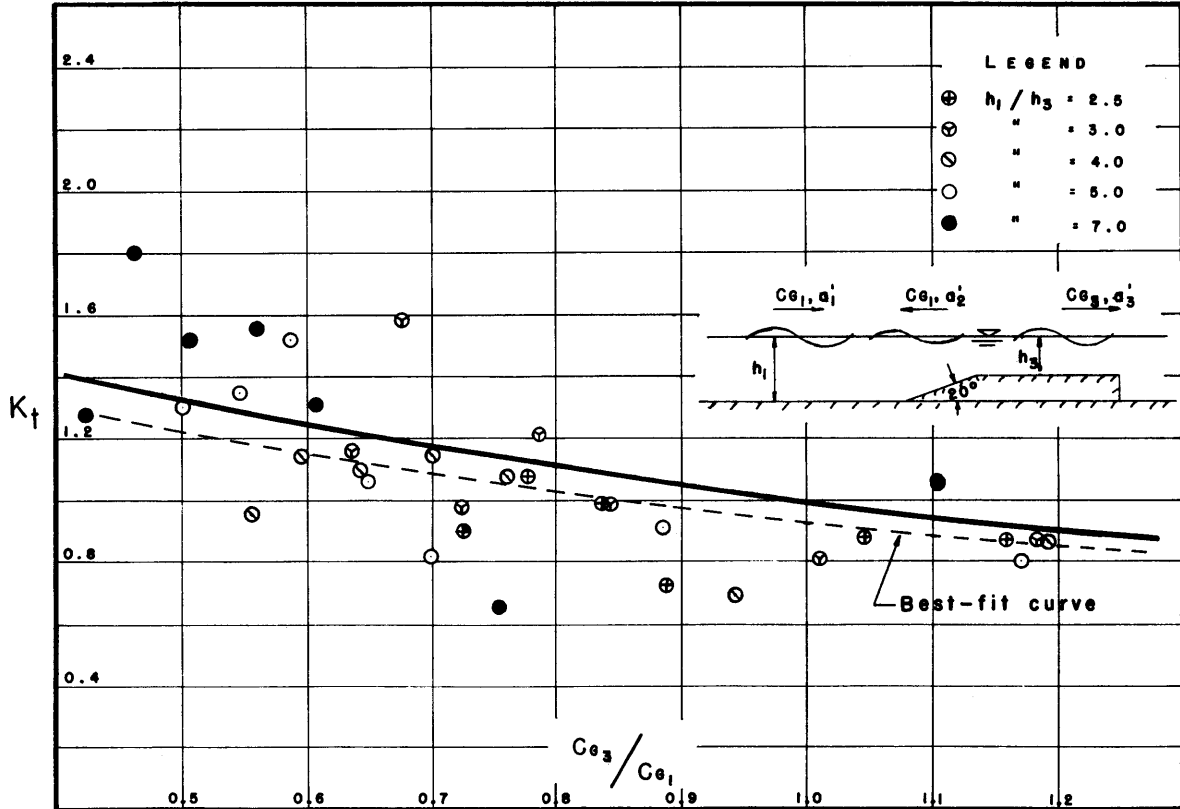   Transition Slope 1:0.58   (α = 60º)

Fig. 20   Transmission Coefficients--Short and Intermediate Waves--
         Transition Slope 1:2.75   (α = 20º)

49

and for the slope 1:16 are given in Figure 21 and show a considerable change in trend over the values for the steeper slopes. Due to the more gradual transition scatter is considerably reduced however the range of h_1/h_3 is much less. Admittedly also, improved technique and experience made for better results. To be noted is the fact that the transmission coefficient is nearly constant at a value of approximately .94 for group velocity ratios above .80. Near values of the latter above unity good agreement exists with the theoretical transmission coefficients. The decrease in transmission effectiveness at lower values of the group velocity ratio must be accounted for largely by increasing transformation of waves with increasing values of h_1/h_3 and by the increased energy dissipation associated therewith.

The results for the 1:16 slope were also analyzed with respect to wave steepness and are given in Figure 22. It is seen that the energy transmission becomes more efficient with increasing wave steepness, especially considering that reflection coefficients varied less over the same range of steepness. Generally it may be added that wave steepness was found not to be a major factor for reflection and transmission coefficients in the range of short and intermediate waves in contrast to the shallow water wave range discussed later.

The transmission coefficients for the abrupt transitions downstream are again plotted separately for the two upstream conditions (slopes 1:.58 and 1:2.75) in Figures 23 and 24 for presentation here. The results are essentially identical as expected. They vary with group velocity as predicted by the elementary theory, but decrease more gradually with the group velocity ratio. Generally the values are less than for the gradual transition of slope 1:16 which must be attributed to the effect on energy dissipation of the abrupt transition.

5.3 Results for Shallow Water Waves

The reflection and transmission phenomena for the experiments in the shallow water wave range are in a somewhat different category from those for short and intermediate waves. On the one hand the group velocity is now uniquely determined for the small amplitude theory by the depth of water and on the other hand, a theory exists for gradual transitions in this range as developed by Dean (10). Consequently the experimental results have been presented graphically with parameters directly related to this theory, i.e. the relative depth ratio h_1/h_3 and the parameter Z_1 defined as:

$$Z_1 = \frac{4\pi h_1}{L_1 S} \tag{5.9}$$

As an additional experimental parameter the wave steepness H_1/L_1 has been introduced, not considered in the above theory. The wave steepness was however found to affect the phenomena of reflection and transmission to a considerable extent for shallow water waves in contrast to the short and intermediate water waves in the approach to the channel transition. Only the transition of slope 1:16 was investigated in detail in this wave range.

50

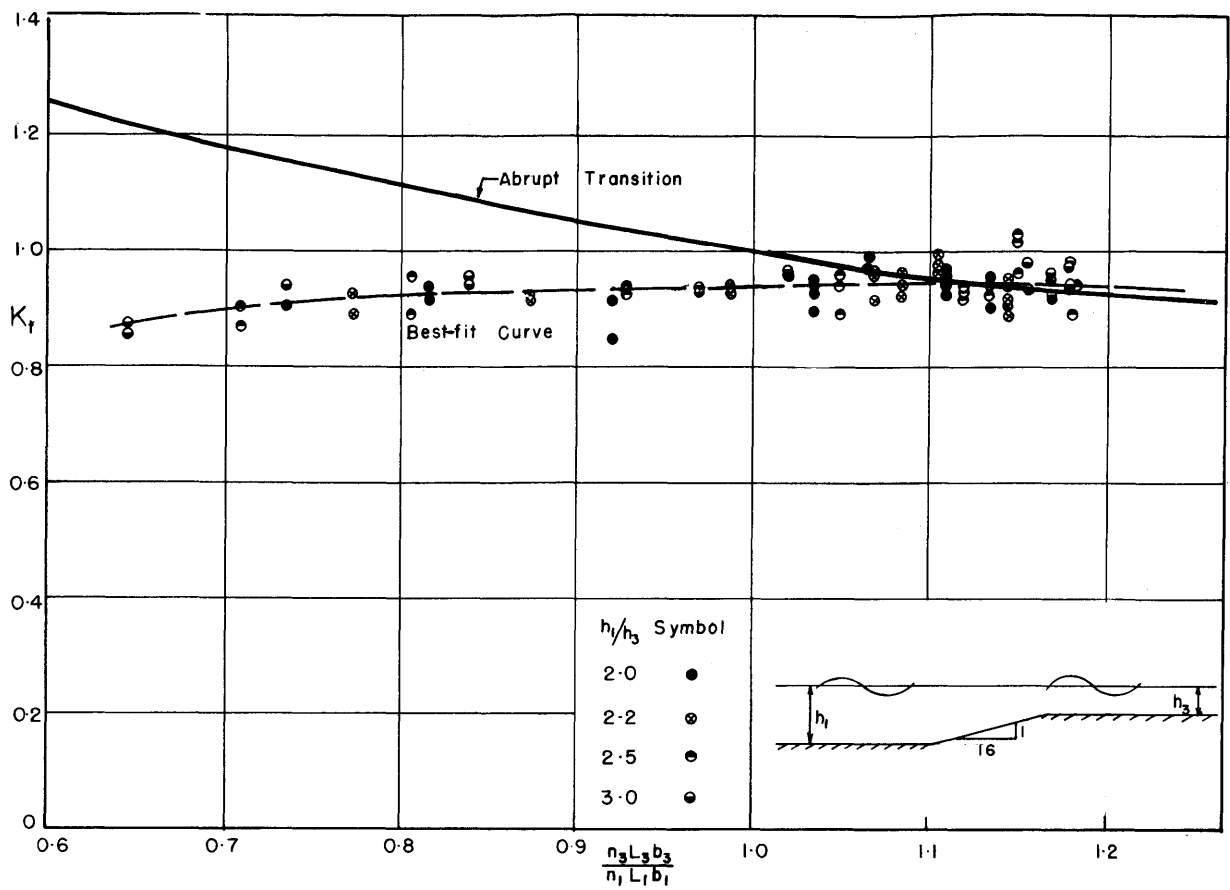Fig. 21 Transmission Coefficients--Short and Intermediate Waves--
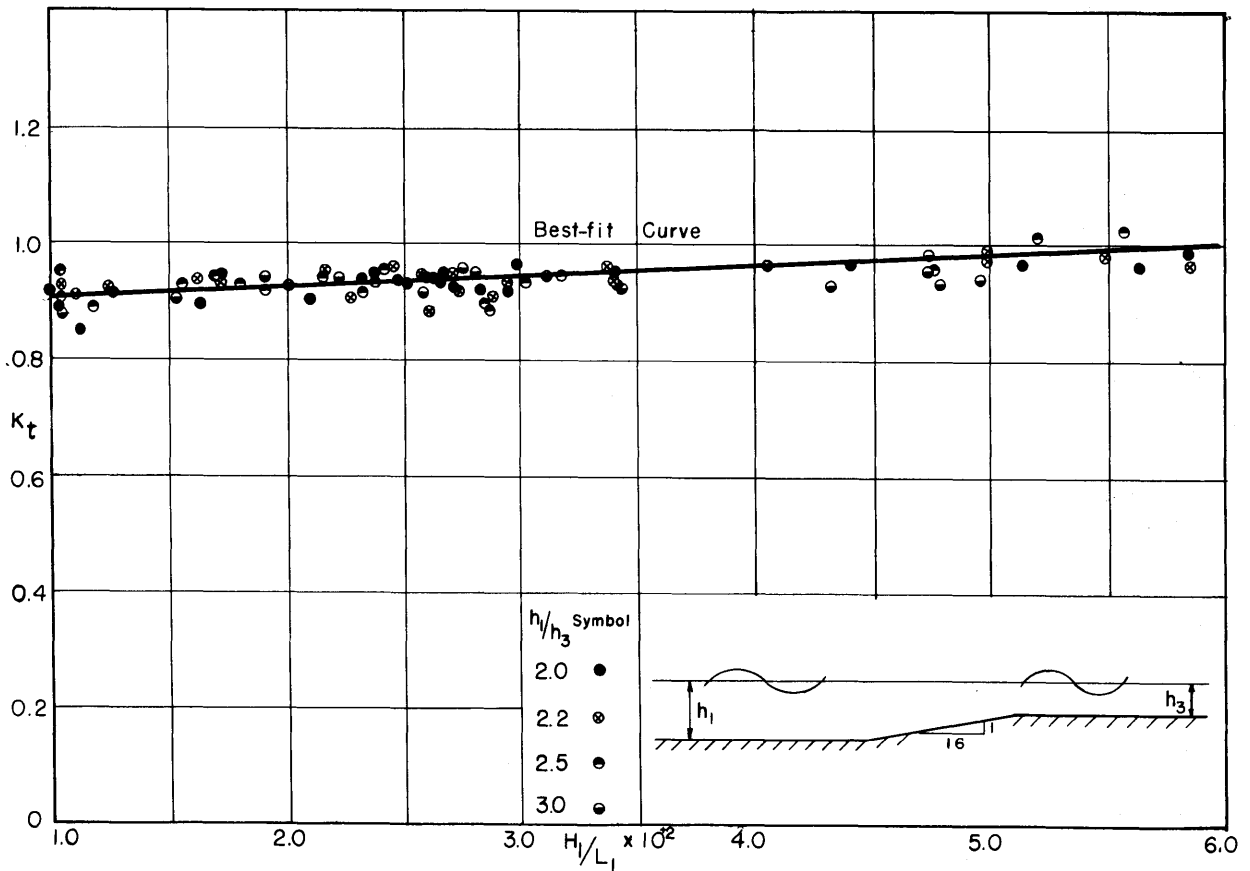Transition Slope 1:16

Fig. 22 Transmission Coefficients Vs. Wave Steepness--Short and Intermediate Waves--
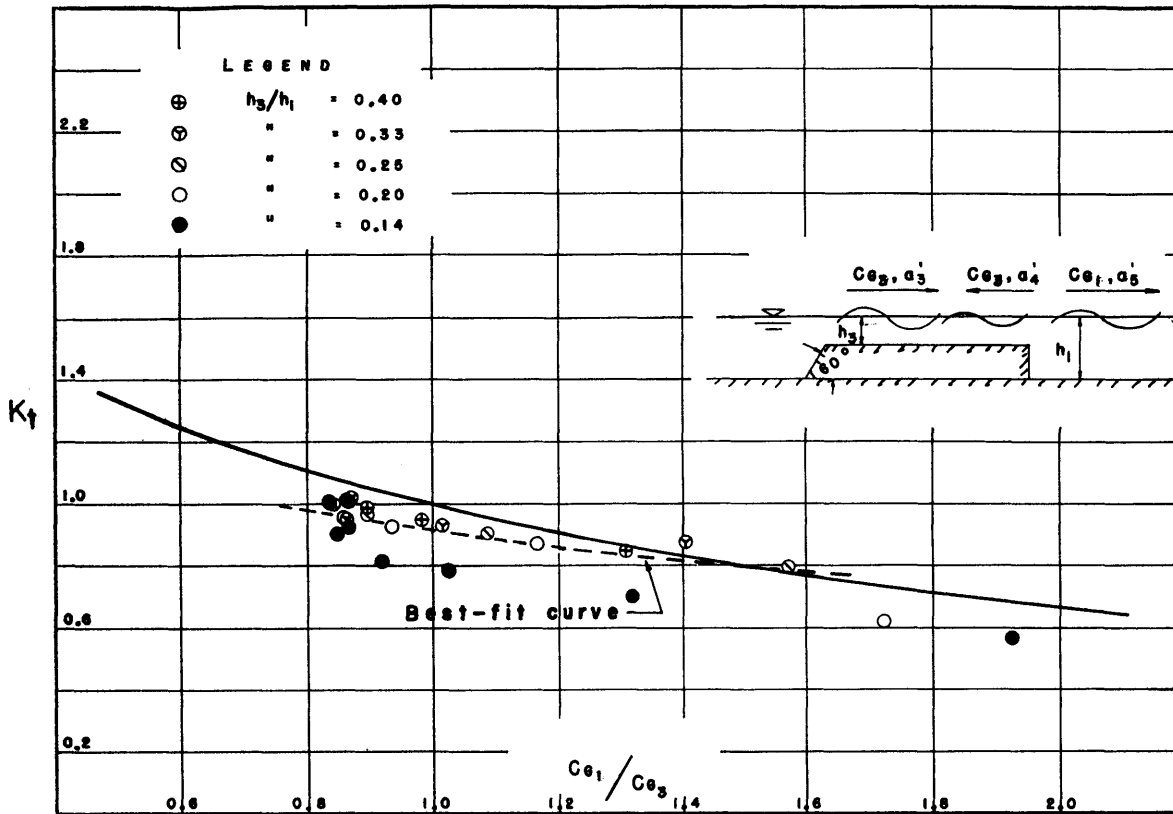Transition Slope 1:16

51

Fig. 23   Transmission Coefficients--Short and Intermediate Waves--
Abrupt Transition Downstream

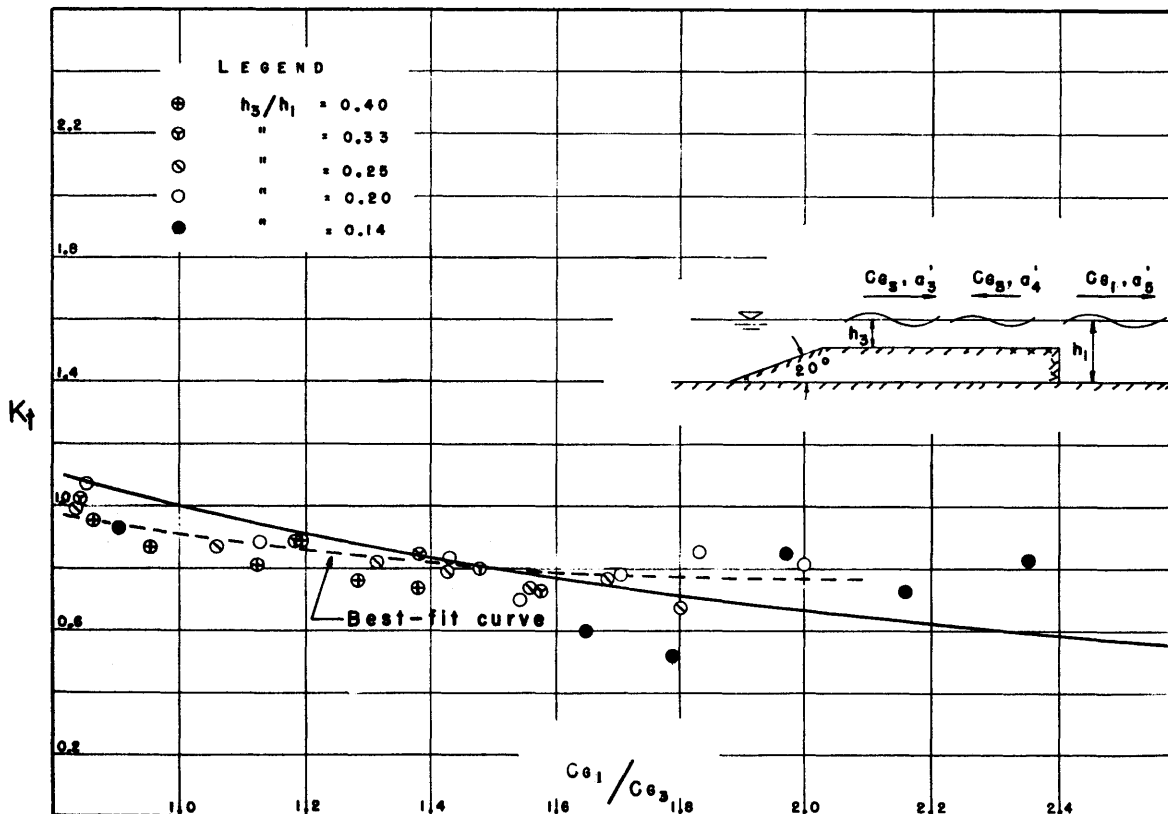Fig. 24   Transmission Coefficients--Short and Intermediate Waves--
Abrupt Transmission Downstream

a. Reflection Coefficients

The reflection coefficients for shallow water waves as listed in Table II are presented in Figure 25 as a function of the ratios of upstream to downstream depth h_1/h_3 for the transition of slope 1:16. Also shown in this figure are the long-wave reflection coefficients predicted by Dean (10) as heavy continuous lines for different values of his parameter defined by equation (5.9). The experimental points are identified by different symbols according to the computed value of Z_1 for each point. Dean's analysis shows a considerable variation of reflection coefficients with increasing values of Z_1 and with the depth ratio h_1/h_3. For zero values of Z_1 the theoretical line is in accordance with that predicted for abrupt transitions, and for infinite values of Z_1 the waves are transmitted without reflection in accordance with Green's law.

The experimental points indicate that in general the reflection coefficients remain more or less constant for different values of the depth ratio covered in the experimental program as long as the steepness of the incoming waves is kept constant. The results differ considerably from the values predicted by Dean for comparable higher values of Z_1. It is found that the reflection coefficients decrease materially however with increasing wave steepness for given values of the depth ratio. This same trend was evident also to a much smaller degree with short and intermediate waves. This relation of the reflection coefficient to wave steepness is best demonstrated in Figure 26. A clearly defined curve is obtained showing the material influence of wave steepness essentially independent of depth ratio for a wider range of wave conditions. This result represents a significant finding of this experimental study.

The deficiencies of the theory must be inherent in the linearized form of the wave equation employed which does not account for the vertical accelerations in the transition. The effect of boundary resistance is also neglected.

b. Transmission Coefficients

The variation of the transmission coefficients identified with regard to Z_1 with relative depth ratio is given in Figure 27. The theoretical transmission coefficients for the range of depth ratio covered in the experimental program are essentially independent of Z_1 including the case of abrupt transition $Z_1 = 0$. As expected from the reflection coefficients in Figure 25 the transmission coefficients show again considerable dependence on the wave steepness and are generally increasing with increasing wave steepness. The trend with the depth ratio h_1/h_3 is rising in accordance with the theory. For smaller values of the depth ratio the agreement with the theory is quite good but all values of K_t are lower; at higher values experimental trends are towards still lower values of the coefficients than given by theory. This would indicate that transmission becomes less efficient due to rising frictional effects as the downstream depth decreases relative to upstream depth.
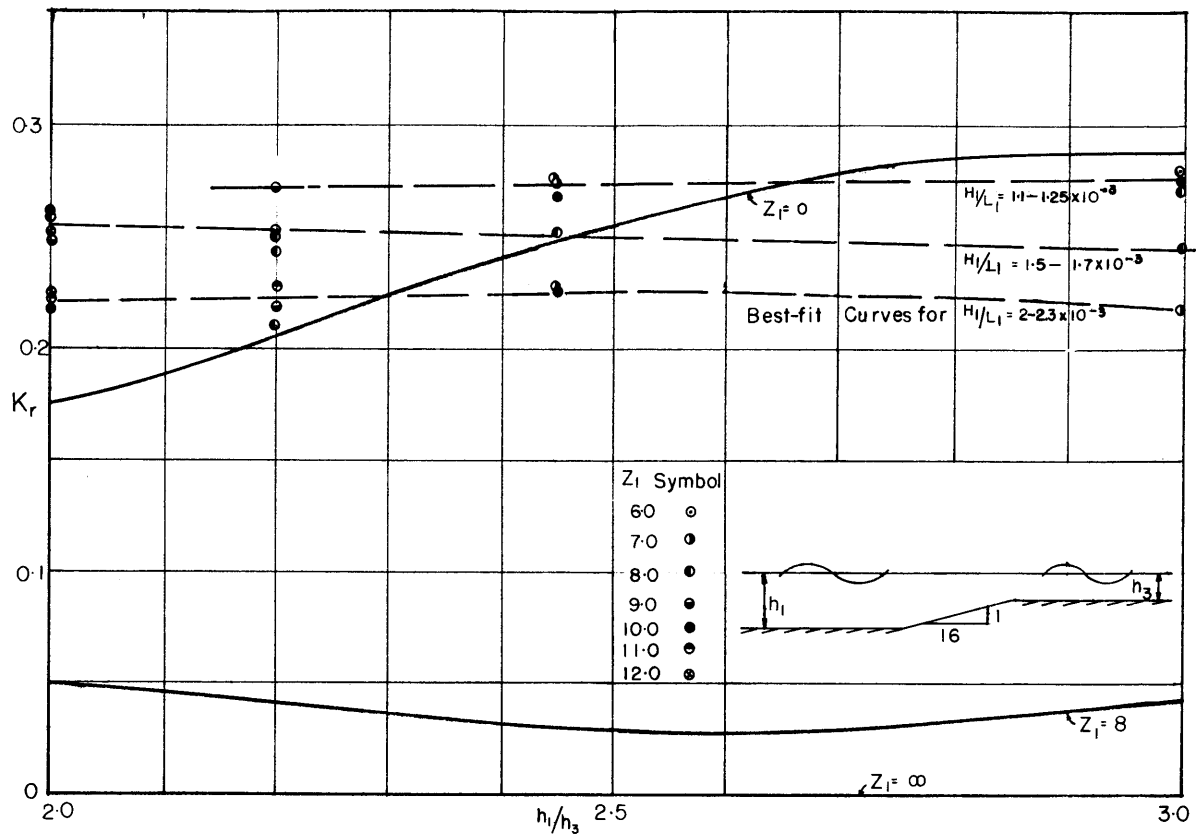
Fig. 25 Reflection Coefficients--Shallow Water Waves-- Transition Slope 1:16
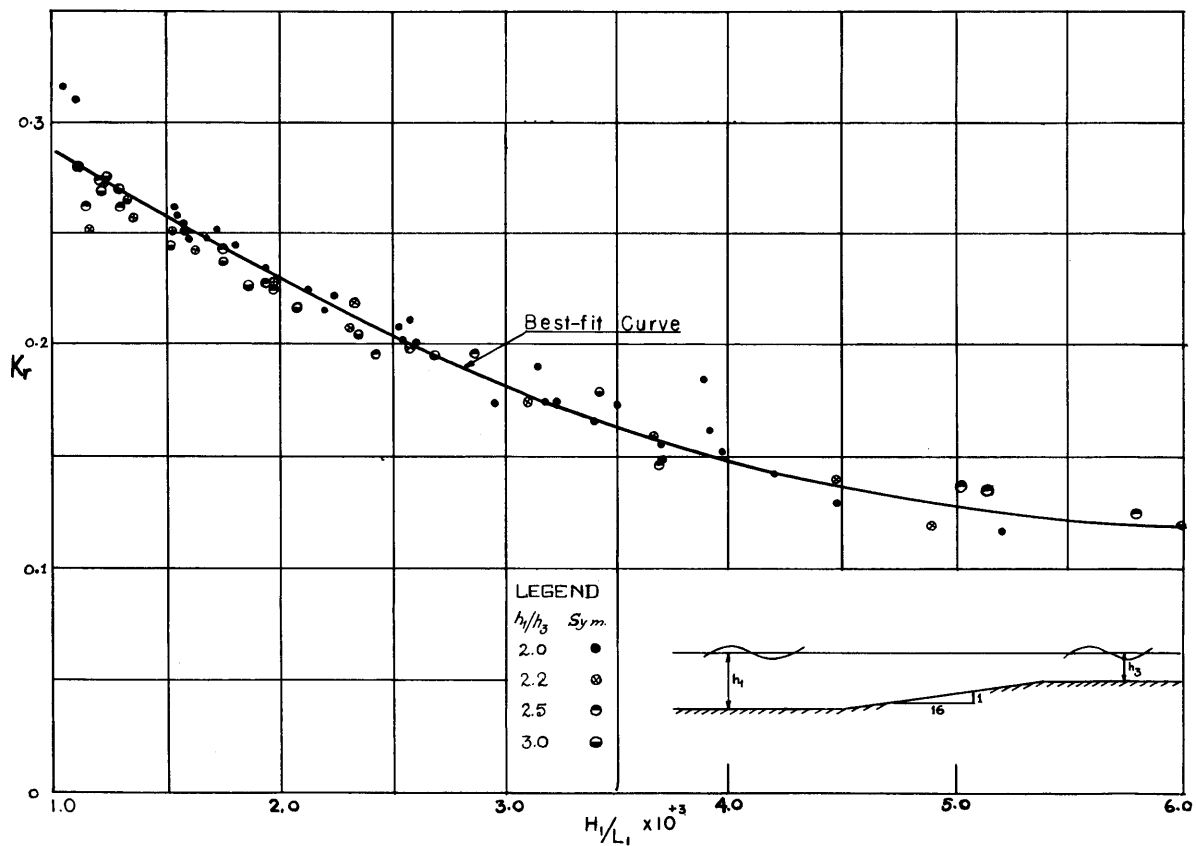

Fig. 26 Reflection Coefficients Vs. Wave Steepness--Shallow Water Waves--
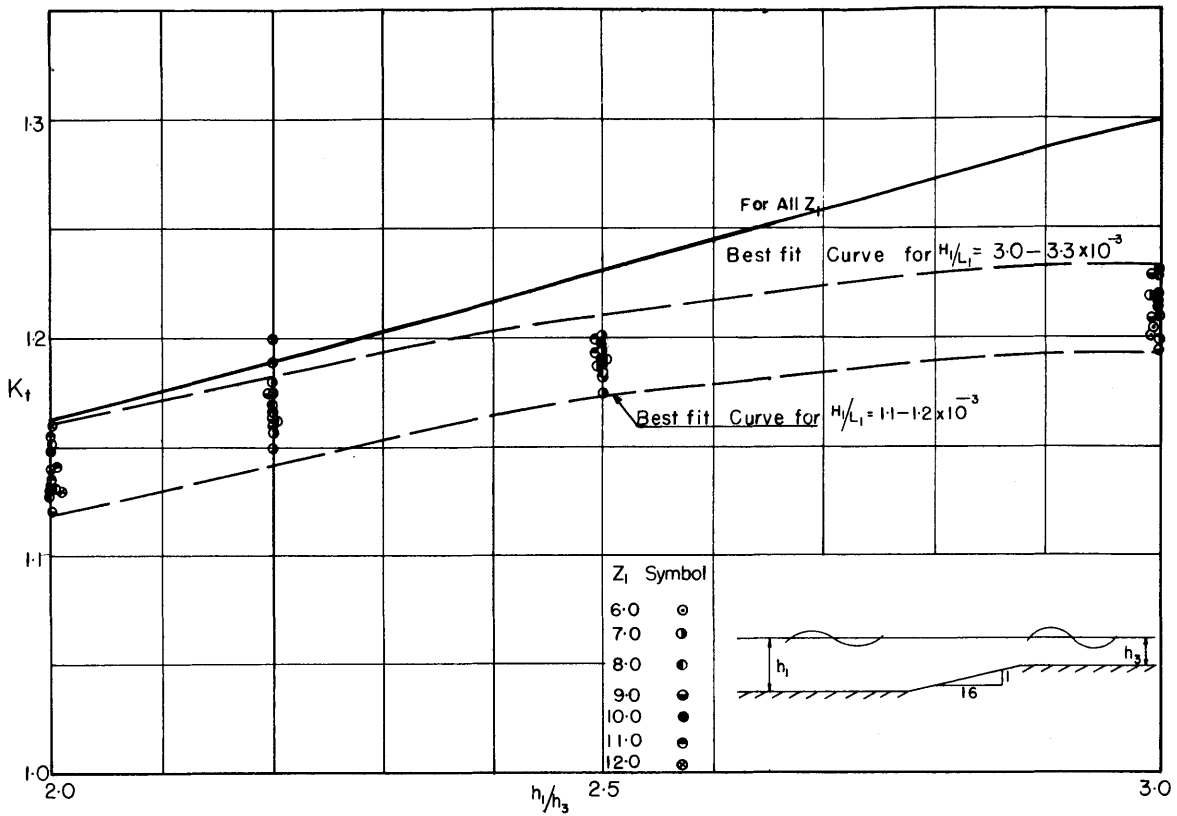Transition Slope 1:16

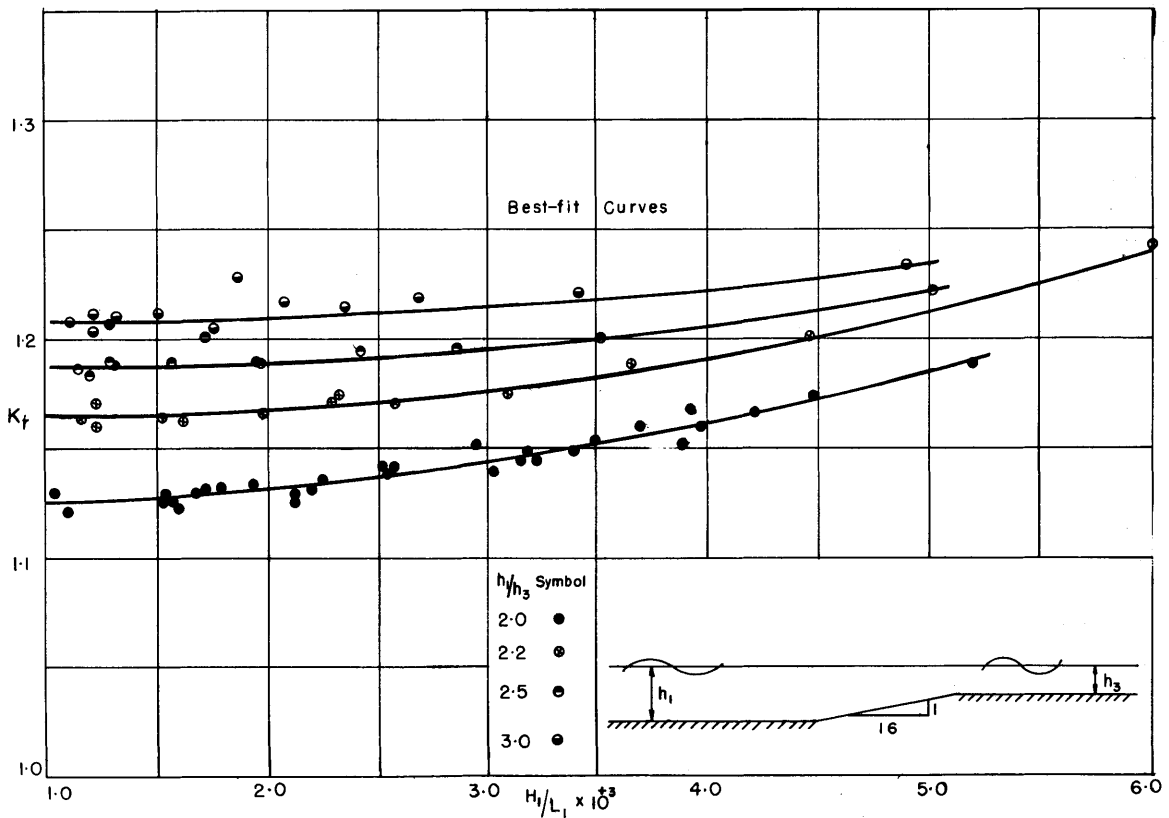Fig. 27 Transmission Coefficients--Shallow Water Waves--Transition Slope 1:16

Fig. 28 Transmission Coefficients Vs. Wave Steepness--Shallow Water Waves--
Transition Slope 1:16

All values of the experimental coefficients lie below the theoretical line as is to be expected, since the latter represents also the case of $Z_1 = \infty$, i.e. it follows Green's law. The dependence of transmission coefficients on wave steepness indicated in Figure 27 is again more clearly demonstrated in Figure 28 analogous to Figure 26 for the reflection coefficient. The values for all relative depths show the rising trend for increasing wave steepness. Noting that the reflection coefficients (Figure 26) showed a considerable decrease with rising wave steepness, it is concluded that for shallow water waves more energy is transmitted for a given depth ratio as the wave steepness increases. Also since reflection coefficients were not dependent on relative depth, at least within experimental accuracy, it would follow that higher transmission coefficients for higher depth ratios reflect lower frictional effects. However this explanation is not logical. The true reason for this phenomena illustrated in Figure 28 must be sought in the fact that the transmitted waves become increasingly non-linear with increasing depth-ratios, hence amplitudes of the transmitted waves assume much higher values than is consistent with the assumed small-amplitude waves of harmonic type. Since only amplitudes were measured upstream and downstream, the experimental results are subject to this inherent distortion. This was noted of course, during the experiments. The results must therefore be accepted as valid with respect to amplitude changes, but not with respect to energy changes. An analysis with respect to the latter consideration could not be followed up within the scope of this investigation. Interesting results however are inherent in the data, which include all the pertinent quantities for the determination of the particular type of the transmitted wave.

5.4 Limitations of the Experimental Program

The experimental equipment had shortcomings primarily with respect to wave gages. In order to reduce reading errors, relatively large amplitudes had to be employed. Although a magnifying glass was used for reading the wave envelopes from the Sanborn recording paper, it was found that the readings could be read with an accuracy of only ± 0.5mm. For waves of smallest amplitude this would lead to an error of about $\pm 6\,^o/o$, in reading the minimum values of the wave envelope. For the maximum values of the wave envelope the error would then be $\pm 2.5\,^o/o$. The combined error in determining reflection coefficients might exceed $10\,^o/o$ in extreme cases. However, the experimental error in transmission coefficients would, for extreme cases, not exceed $\pm 5\,^o/o$.

Although efforts have been made to eliminate the irregularities in the motion of the wave maker, it is found that some of the irregularities remained and particularly so for the longer waves. This introduces errors since the theory assumes only periodic sinusoidal waves; however, their magnitude and actual source are not readily determined. In the preceding section 5.3 the limitations of the data with respect to shallow water waves are pointed out. The form of the latter waves is severely affected in the case of transmission to shallow depth. For this reason the effect of energy dissipation on the reflection and transmission process could not be clarified, since a detailed analysis of the form of the waves could not be attempted within the scope of this study. This remains as an important task for future studies.

During the first part of the study (11) the reduction of the data was accomplished largely by computer program, while in the second part the computations were made by desk calculator for immediate checking. This part of the study proved the most time consuming phase of the program in view of the necessary corrections for end reflections in the wave channel as discussed in section IV.

In view of the above comments the present study was restricted to three cases of linear transitions. The study was confined, as far as the wave steepness is concerned, to the transition of slope 1:16 only. The first part of the study did not include a systematic variation of the wave steepness as a pertinent parameter. Further amplification of the data is therefore desirable for transitions with additional slopes and with variable width.

VI. SUMMARY AND CONCLUSIONS

6.1 Review of Results

An experimental program has been conducted to determine the reflection and transmission characteristics of waves when propagating into channel transitions of gradually varying depth. The results are compared to the theoretical values of the elementary analysis for long waves derived for an abrupt transition. For shallow water waves the results are also compared with the analysis presented by Dean (see Appendix) for gradual transitions. The test program covered transitions of linear slopes 1:0, 1:.58 (60°), 1:2.75 (20°) and 1:16 (3.6°) for short and intermediate waves as well as long waves. The wave lengths ranged from 2.3 to 50 ft. in the approach channel upstream with depths from 1.8 to 2.6 ft. Thus wave lengths shorter and longer than the transition lengths were included in the experiments. The wave steepness was varied from .00072 to .06.

a. Short and Intermediate Wave Range

Generally reflection coefficients are found to be larger than predicted from the theory for long waves and abrupt transitions. As the steepness of the transition slope decreases, reflection coefficients increased for the range of transitions tested. For group velocity ratios C_{G_3}/C_{G_1} near unity the values of the reflection coefficient for short and intermediate waves are significantly higher, while for lower and higher values of this ratio they approach the theoretical values of long wave analysis for abrupt transitions. The reflection coefficient is almost independent of wave steepness for the transition slope 1:16. However a slight decreasing trend with increasing wave steepness can be observed.

In general it can be pointed out that reflection coefficients show relatively little variation with either depth ratio or group velocity ratio, a trend which is particularly evident from the results of the transition slope 1:16.

The transmission coefficients for short and intermediate waves generally agree with theoretical values of long wave analysis for abrupt transitions, for group velocity ratios near or in excess of unity. A trend to lower values for lower group velocity ratios as the slope of transition decreases is observed. The transmission coefficient for the slope 1:16 shows a slightly increasing trend with increasing wave steepness. This trend is significant in relation to the fact that the reflection coefficient decreases by a smaller amount within this range of wave steepness.

b. Shallow Water Wave Range

The reflection coefficients for long or shallow water waves for the transition slope 1:16 are generally closer to the values predicted by the elementary theory for abrupt transitions than those in the short and intermediate wave range. This is expected with wave lengths which are long

relative to the transition length. The values obtained are nearly constant with respect to the group velocity ratio C_{G_3}/C_{G_1} or the depth ratio h_1/h_3 as for the short and intermediate wave range. The predictions made on the basis of the theory for gradual transitions proposed by Dean were not borne out by the experiments.

For shallow water waves the reflection coefficients decrease considerably with increasing wave steepness although the range of the latter was from .001 to .006 only.

The transmission coefficients for long waves for the transition slope 1:16 approach the values anticipated from Green's law (complete transmission). They follow the predicted trend with increasing values of the depth ratio, but tend toward increasingly lower values than predicted with increasing depth ratios. Transmission coefficients exhibit considerably increased values with increasing wave steepness. These trends of changes in transmission coefficients relative to changes in reflection coefficients with depth ratio and wave steepness have been explained on the basis of the increasing influence of non-linear properties of the transmitted waves.

6.2 General Comments

In general the influence of energy dissipation is clearly evident in the experimental results although the theory does not include its effects. The maximum dissipation is obtained for shallow water waves and, as expected, is smaller for short and intermediate waves. For some of the latter waves and for larger wave steepnesses negative dissipation, physically impossible, was deduced. This is explainable by the fact that the wave is transformed in the transition to a shape no longer adequately described by harmonic functions and hence by the results derived from them.

The theory assumes a small amplitude periodic sinusoidal wave. Experiments show that the waves during and after the transformation by the transition are no longer harmonic but approach the shape of cnoidal or solitary waves. The wave energy therefore is only poorly approximated by the expression derived for harmonic waves.

Another reason for the deviation of the experimental results from theory could be the fact that the reflection and transmission coefficients for an abrupt change are derived by assuming that the phase shift for the reflected wave component was assumed to be equal to π, the same as for a completely obstructing vertical wall. Also the transmitted wave is assumed to be in phase with the incident wave. For actual waves in the test channel these assumptions cannot be true. In the case of a finite length of transition these assumptions are not valid. It is difficult to predict at this state of knowledge which one of the above factors is more likely to be responsible for the deviation between theory and the experimental investigation.

From the plots of reflection and transmission coefficients vs. wave steepness it is also believed that without taking account of the wave amplitude and wavelength the reflection and transmission characteristics of waves cannot be described adequately. Therefore, there is reason to believe that wave steepness is an important factor in determining the reflection and transmission characteristics of waves. However, it is difficult to predict these relations from the tests for only one transition, and only additional systematic experiments will yield the solution to the problem concerned.

VII. <u>REFERENCES</u>

1. Rayleigh, Lord, "Theory of Sound", vol. 1, 2nd Ed., MacMillan and Co., Ltd., London, 1926.

2. Stoker, J.J., "Water Waves", Interscience Publishers, New York, 1957.

3. Lamb, H., "Hydrodynamics", Dover Publications, New York, 1945.

4. Eagleson, P.S. and Dean, R.G., "Small Amplitude Wave Theory", Chapter A, Estuary and Coastline Hydrodynamics", Department of Civil Engineering, Massachusetts Institute of Technology, 1963.

5. Ursell, F., Dean, R.G., and Yu, Y.S., "Forced Small-Amplitude Water Waves; A Comparison of Theory and Experiment", MIT Hydrodynamics Laboratory Technical Report No. 29, July, 1958.

6. Dean, R.G. and Ursell, F., "Interaction of a Fixed, Semi-Immersed Circular Cylinder with a Train of Surface Waves", MIT Hydrodynamics Laboratory Technical Report No. 37, September, 1959.

7. Kajiura, K., "On the Partial Reflection of Water Waves Passing Over a Bottom of Variable Depth", Earthquake Research Institute, University of Tokyo, Japan.

8. Perroud, P., "The Propagation of Tidal Waves in Channels of Gradually Varying Section", Beach Erosion Board Technical Memorandum No. 112, Washington, 1959.

9. Evangelisti, G., "On Tidal Waves in a Canal with Variable Cross Section", Paper A-10, 1955, Proceedings of Sixth General Meeting, International Association of Hydraulic Research, The Hague, Netherlands.

10. Dean, R.G., "Long Wave Reflection and Transmission in Channels of Linearly Varying Dimensions", California Research Corporation, LaHabra, California.

11. Gagnon, M.L. and Bocco, V.M., "The Effect of Gradual Change of Depth on a Train of Surface Waves", MIT Thesis, May, 1962.

12. Wiegel, R.L., "Gravity Waves, Tables and Functions", Council on Wave Research, The Engineering Foundation, Berkeley, 1954.

13. Rouse, H. "Engineering Hydraulics", Wiley and Sons, Co., New York.

14. Alam, A.M.Z., "Wave Reflection and Transmission in Channels of Gradually Varying Depth", MIT Thesis, January, 1964.

VIII. APPENDIX A

Reflection and Transmission of Waves Due to an Abrupt Change in Channel

Geometry

(This section summarizes the theoretical treatment of the reflection and transmission phenomena of waves due to an abrupt change in channel geometry presented by P.S. Eagleson and R.G. Dean (4).

Let us consider a progressive wave travelling in the positive x-direction (hereafter referred to as the "incident wave") for $x < 0$ in a channel of depth h_1 and width b_1. Also let it be assumed that at $x = 0$ an abrupt change in channel geometry occurs so that $x > 0$, the depth is h_3 and the width b_3. With waves incident to this transition, a portion of the incident wave will be reflected as a wave in the negative x-direction ("reflected wave") and a portion transmitted in the positive x-direction ("transmitted wave"). An approximate theory for the reflection and transmission properties of any abrupt section change is based on the assumption that at any section x, the water surface is uniform in the z-direction.

From conservation of energy, we may balance the mean energy fluxes in the channels:

$$(EbC_G)_1 = (EbC_G)_3 \qquad \text{(A-1)}$$

which can be written in terms of incident, reflected and transmitted waves with subscripts i, r, and t respectively as

$$n_i E_i C_i b_1 = n_r E_r C_r b_1 + n_t E_t C_t b_3 \qquad \text{(A-2)}$$

where

$$n = \frac{C_G}{C} = \frac{1}{2} \left[1 + \frac{2kh}{\sinh 2kh} \right] \qquad \text{(A-3)}$$

$$E = \frac{\gamma a^2}{2} \qquad \text{(A-4)}$$

$$C = L/T \qquad \text{(A-5)}$$

Noting that

T = constant for all waves

$$\left. \begin{aligned} L_i &= L_r \\[2pt] n_i &= n_r \end{aligned} \right\} \quad \text{Since depth and period are the same} \qquad \text{(A-6)}$$

62

Using the definition of the average total energy per unit surface $E = \gamma a^2/2$, in equation (A-2) we obtain:

$$(a_i^2 - a_r^2) = \frac{n_t L_t b_3}{n_i L_i b_1} \, a_t^2 = \frac{n_3 L_3 b_3}{n_1 L_1 b_1} \, a_t^2 \tag{A-7}$$

The continuity condition at the junction, is

$$\eta_i + \eta_r = \eta_t \quad \text{at } x = 0 \text{ for all time} \tag{A-8}$$

An approximation is introduced here.

Since the true surface configuration at $x = 0$ is not known, the velocity potential ϕ in the vicinity of the junction does <u>not</u> remain the same as was computed for uniform depth and width in the approach region. The wave system developed at the junction is given:

$$\eta_i = a_i \sin(k_1 x - \sigma t + \delta_i)$$

$$\eta_r = a_r \sin(k_1 x + \sigma t + \delta_r) \tag{A-9}$$

$$\eta_t = a_t \sin(k_3 x - \sigma t + \delta_t)$$

Equations (A-9) and (A-8) by assuming $\delta_i = 0$ without loss of generality, give:

$$-a_i \sin \sigma t + a_r \sin(\sigma t + \delta_r) = a_t \sin(\delta_t - \sigma t) \tag{A-10}$$

Equation (A-10) must hold for all time. Then we should expand it and equate coefficients of $\sin \sigma t$ and $\cos \sigma t$.

Thus;

$$-a_i + a_r \cos \delta_r = -a_t \cos \delta_t \tag{A-11}$$

$$a_r \sin \delta_r = a_t \sin \delta_t \tag{A-12}$$

Here additional arbitrary assumptions are made to solve the above equations:

1. $\delta_r = \pi$, which means that the reflected wave has a phase shift $\delta_r = \pi$ with the incoming wave as in the case for reflection from a completely obstructing plane vertical wall,

2. $\delta_t = 0$, the transmitted wave has the same phase angle as the incident wave.

With these additional assumptions, equation (A-11) gives:

$$a_i + a_r = a_t \qquad (A-13)$$

which in combination with equation (A-7) yields:

1. Reflection coefficient

$$K_r = \frac{a_r}{a_i} = \frac{n_1 L_1 b_1 - n_3 L_3 b_3}{n_1 L_1 b_1 + n_3 L_3 b_3} \qquad (A-14)$$

2. Transmission coefficient

$$K_t = \frac{a_t}{a_i} = 1 + K_r = \frac{2 n_1 L_1 b_1}{n_1 L_1 b_1 + n_3 L_3 b_3} \qquad (A-15)$$

Equations (A-14) and (A-15) are plotted in Figures 15 and 21 respectively.

IX. APPENDIX B

Summary of Theory for Gradual Channel Transitions

by R.G. Dean (10)

In this section a summary is given of the theory for the reflection and transmission coefficients for shallow water waves in a channel of linearly varying depth. These theoretical solutions have been obtained by R.G. Dean (10).

In the limit of no reflection the solution reduces to the solution for a very gradual transition usually referred to as Green's Law.

B.1 Governing Equations for Shallow Water Waves

a. Continuity Equation

The equation of continuity states that the net influx into the control volume in time Δt must result in a corresponding rise in water surface, i.e.

$$[Q(x) - Q(x+\Delta x)] \quad \Delta t = b \quad \Delta x \quad [\eta(t+\Delta t) - \eta(t)] \tag{B-1}$$

where $Q(x)$ is the volume rate of flow inward across section x, $Q(x+\Delta x)$ is the volume rate of flow outward across section $x+\Delta x$, and b is the average breadth of the section.

By substituting $Q = Au$, where A is a cross-sectional area of flow and u is the horizontal velocity, and expanding $A(x+\Delta x)\,u(x+\Delta x)$ and $\eta(t+\Delta t)$ in Taylor series expressions and neglecting higher order terms, equation (B-1) gives

$$-\frac{\partial}{\partial x}(Au) = b\,\frac{\partial \eta}{\partial t} \tag{B-2}$$

b. Equation of Motion

The equation of motion for small amplitude, long waves is given by combining the hydrostatic equation with the linearized form of Euler's equation of motion, in the form:

$$-\frac{1}{\rho}\frac{\partial p}{\partial x} = \frac{\partial u}{\partial t} \tag{B-3}$$

For long waves assumption of hydrostatic conditions, the pressure is given by

$$p(x,z,t) = \rho g\,[\eta(x,t) - Z] \tag{B-4}$$

Thus (B-3) and (B-4), combination gives the equation of motion of long waves

$$-g\,\frac{\partial \eta}{\partial x} = \frac{\partial u}{\partial t} \tag{B-5}$$

65

Combining continuity and motion equations (B-2) and (B-5) we obtain:

$$g \frac{\partial}{\partial x} [A \frac{\partial \eta}{\partial x}] = b \frac{\partial^2 \eta}{\partial t^2} \qquad \text{(B-6)}$$

Equation (B-6) expresses η as a function of x and t and is valid for any small amplitude long wave form. We only consider here harmonic motion such that

$$\eta (x,t) = \eta_1 (x) \, e^{i(\sigma t + \delta)}$$

where σ is the angular frequency $(2\pi/T)$, T is the wave period, and δ is a phase angle.

With this assumption, equation (B-6) transforms to:

$$\frac{g}{b} \frac{\partial}{\partial x} [A \frac{\partial \eta}{\partial x}] + \sigma^2 \eta = 0 \qquad \text{(B-7)}$$

B.2 Solution for Uniform Breadth and Linearly Varying Depth

Equation (B-7) can be solved for η for the particular channel form. Here it is solved for a channel consisting of two semi-infinite rectangular sections joined by a transition of linearly varying depth and uniform breadth. For this case, the depth, h, is given by

$$h = h_1 \qquad\qquad x < x_1 \qquad\qquad \text{Region 1}$$

$$h = h_3 \frac{x}{x_2} \qquad\qquad x_1 < x < x_2 \qquad\qquad \text{Transitional Region}$$

$$h = h_3 \qquad\qquad x > x_2 \qquad\qquad \text{Region 3}$$

In the transitional region, we have

$$A = bh = \frac{bh_3}{x_2} x$$

Substituting this into equation (B-7) we get

$$x \frac{\partial^2 \eta}{\partial x^2} + \frac{\partial \eta}{\partial x} + \beta \eta = 0 \qquad \text{(B-8)}$$

where

$$\beta = \frac{\sigma^2 x_2}{gh_3}$$

Equation (B-8) is Bessel's equation of zero order and has a solution for $\eta(x)$

66

$$\eta(x) = \begin{cases} J_o(2\beta^{1/2}x^{1/2}) \\ \\ Y_o(2\beta^{1/2}x^{1/2}) \end{cases}$$

where J_o is a Bessel function of zero order, first kind, and Y_o is a Bessel function of zero order, second kind.

The most general solution of $\eta(x,t)$ in the transitional region is given

$$\eta(x,t) = a_3 J_o(2\beta^{1/2}x^{1/2})\cos(\sigma t + \delta_3)$$
$$+ a_3 Y_o(2\beta^{1/2}x^{1/2})\sin(\sigma t + \delta_3)$$
$$+ a_4 J_o(2\beta^{1/2}x^{1/2})\cos(\sigma t + \delta_4) \tag{B-9}$$
$$- a_4 Y_o(2\beta^{1/2}x^{1/2})\sin(\sigma t + \delta_4)$$

This expression represents a wave system composed of two waves progressing in opposite directions; each wave is of arbitrary amplitude and phase. Continuous amplitude transformation and reflection due to the depth variation takes place in incoming and reflecting wave.

The most general expression of $\eta(x,t)$ in the two rectangular channel segments in Region 1 is given by

$$\eta_1(x,t) = a_1[\cos(k_1 x + \delta_1)\cos\sigma t + \sin(k_1 x + \delta_1)\sin\sigma t]$$
$$+ a_2[\cos(k_1 x + \delta_2)\cos\sigma t - \sin(k_1 x + \delta_2)\sin\sigma t] \tag{B-10}$$

and in region 3 by:

$$\eta_3(x,t) = a_5\cos(k_3 x - \sigma t + \tilde{\delta}_5) \tag{B-11}$$

Without loss of generality we can assume the amplitude of the transmitted wave to be unity and the phase angle $\delta_5 = 0$.

The wave systems in the three regions is expressed in terms of the eight unknowns (i.e., a_1, a_2, a_3, a_4, δ_1, δ_2, δ_3, and δ_4). The unknowns can now be determined by considering the value and the gradient of water surface, η, at the two junctions of the regions, i.e.

$$\eta_1 = \eta_2 \qquad \qquad \text{(B-12a)}$$

$$x = x_1$$

$$\frac{\partial \eta_1}{\partial x} = \frac{\partial \eta_2}{\partial x} \qquad \qquad \text{(B-12b)}$$

$$\eta_2 = \eta_3 \qquad \qquad \text{(B-13a)}$$

$$x = x_2$$

$$\frac{\partial \eta_2}{\partial x} = \frac{\partial \eta_3}{\partial x} \qquad \qquad \text{(B-13b)}$$

Equations (B-12a), (B-12b), (B-13a), (B-13b) each yields two equations by first setting $\sigma t = 0$ and then $\sigma t = \pi/2$. The obtaining eight simultaneous equations can then be solved for the eight unknowns. We are mainly interested in the unknowns a_1 and a_2, thus solving the simultaneous equations, the magnitudes of a_1 and a_2 are obtained for the case of linearly varying depth with constant breadth:

$$\left| a_1 \right| = \frac{\pi}{4} (2\beta^{1/2} x_1^{1/2}) \sqrt{ \Delta_1 \mu_2 - 2 \nu_1 \nu_2 + \Delta_2 \mu_1 + \frac{8}{\pi^2} \frac{1}{(2\beta^{1/2} x_1^{1/2})^2} } \left(\frac{h_1}{h_3} \right)^{1/2} \quad \text{(B-14a)}$$

$$\left| a_2 \right| = \frac{\pi}{4} (2\beta^{1/2} x_1^{1/2}) \sqrt{ \Delta_1 \mu_2 - 2 \nu_1 \nu_2 + \Delta_2 \mu_1 - \frac{8}{\pi^2} \frac{1}{(2\beta^{1/2} x_1^{1/2})^2} } \left(\frac{h_1}{h_3} \right)^{1/2} \quad \text{(B-14b)}$$

where

$$\beta \equiv \frac{\sigma^2 x_2}{g h_3}$$

$$\Delta \equiv J_0^2(2\beta^{1/2} x^{1/2}) + J_1^2(2\beta^{1/2} x^{1/2})$$

$$\mu \equiv Y_0^2(2\beta^{1/2} x^{1/2}) + Y_1^2(2\beta^{1/2} x^{1/2}) \qquad \qquad \text{(B-15)}$$

$$\nu \equiv Y_0(2\beta^{1/2} x^{1/2}) J_0(2\beta^{1/2} x^{1/2}) + Y_1(2\beta^{1/2} x^{1/2}) J_1(2\beta^{1/2} x^{1/2})$$

and the subscripts (1 or 2) on the Δ, μ, or ν refer to the x (i.e. x_1 or x_2) at which these quantities are evaluated. Analogous expressions can be taken in other cases (1) of linearly varying breadth and uniform depth, and (2) of linearly varying depth and breadth.

68

B.3 Approximate Solutions for Gradual Transition (Green's Law)

For cases in which the variations in cross section are regarded as very gradual, the assumption is usually made that no energy reflection occurs due to the transition region, i.e.

$$\gamma \ \frac{a_i^2}{2} \ b_1 \ C_{G_1} \quad = \quad \gamma \ \frac{a_t^2}{2} \ b_3 \ C_{G_3} \qquad (B\text{-}16)$$

$$\underbrace{\gamma \ \frac{a_i^2}{2} \ b_1 \ C_{G_1}}_{\substack{\text{average rate of} \\ \text{energy flux into} \\ \text{transition}}} \qquad\qquad \underbrace{\gamma \ \frac{a_t^2}{2} \ b_3 \ C_{G_3}}_{\substack{\text{average rate of} \\ \text{energy flux from} \\ \text{transition}}}$$

Defining the reflection coefficient for $K_r = a_r/a_i$ and the transmission coefficient for $K_t = a_t/a_i$, then we have in a very gradual transition,

$$K_r = 0$$

$$K_t = \left(\frac{b_1}{b_3}\right)^{1/2} \left(\frac{C_{G_1}}{C_{G_3}}\right)^{1/2} \qquad\qquad (B\text{-}17)$$

For shallow water waves these equations become,

$$K_r = 0$$

$$K_t = \left(\frac{b_1}{b_3}\right)^{1/2} \left(\frac{h_1}{h_3}\right)^{1/4}$$

These equations are referred to as Green's Law.

Chief of Naval Research
Department of the Navy
Washington 25, D.C.
Att: Codes 438   (3)
          416   (2)
          466   (1)
          414   (1)
          463   (1)

Commanding Officer
Office of Naval Research
Branch Office
495 Summer Street
Boston 10, Massachusetts   (1)

Commanding Officer
Office of Naval Research
Branch Office
230 N. Michigan Avenue
Chicago 1, Illinois   (1)

Commanding Officer
Office of Naval Research
Branch Office
207 West 24th Street
New York 11, New York   (1)

Commanding Officer
Office of Naval Research
Branch Office
Navy 100, Box 39
Fleet Post Office
New York, New York   (25)

Commanding Officer
Office of Naval Research
Branch Office
1030 East Green Street
Pasadena 1, California   (1)

Commanding Officer
Office of Naval Research
Branch Office
1000 Geary Street
San Francisco 9, California   (1)

Director
Naval Research Laboratory
Washington 25, D.C.
Att: Codes 2000   (1)
          2020   (1)
          2021   (6)

Chief, Bureau of Ships
Department of the Navy
Washington 25, D.C.
Att: Codes 300   (1)
          305   (1)
          335   (1)
          341   (1)
          342A   (1)
          345   (1)
          421   (1)
          440   (1)
          442   (1)
          634A   (1)
          420   (1)
          373   (1)

Chief, Bureau of Naval Weapons
Department of the Navy
Washington 25, D.C.
Att: Codes R   (1)
          R-12   (1)
          RAAD   (1)
          RR   (1)
          RRRE   (1)
          RU   (1)
          RUTO   (1)
          RU-222   (1)

Chief, Bureau of Yards and Docks
Department of the Navy
Washington 25, D.C.
Att: Codes D-202   (1)
          D-400   (1)
          D-500   (1)

Commander
Norfolk Naval Shipyard
Portsmouth, Virginia   (1)

Commander
New York Naval Shipyard
Naval Base
Brooklyn, New York   (1)

Commander
Boston Naval Shipyard
Boston 29, Massachusetts   (1)

Commander
Philadelphia Naval Shipyard
Naval Base
Philadelphia 12, Pennsylvania   (1)

Commander
Portsmouth Naval Shipyard
Portsmouth, New Hampshire
Att: Design Division   (1)

Commander
Charleston Naval Shipyard
U.S. Naval Base
Charleston, South Carolina   (1)

Commanding Officer
U.S. Naval Underwater Ordnance Station
Newport, Rhode Island
Att: Research Division   (1)

Commander
Long Beach Naval Shipyard
Long Beach 2, California   (1)

Commander
Pearl Harbor Naval Shipyard
Navy 128, Fleet Post Office
San Francisco, California   (1)

Commander
San Francisco Naval Shipyard
San Francisco 24, California   (1)

Commander
Mare Island Naval Shipyard
Vallejo, California
Att: 370A   (1)

Office of Technical Services
Department of Commerce
Washington 25, D.C.   (1)

Defense Documentation Center
Cameron Station
Alexandria 12, Virginia   (10)

Fluid Mechanics Section
National Bureau of Standards
Washington 25, D.C.
Att: Dr. G.B. Schubauer   (1)

Director
Engineering Science Division
National Science Foundation
Washington, D.C.   (1)

Air Force Office of Scientific
Research
Mechanics Division
Washington 25, D.C.   (1)

National Academy of Sciences
National Research Council
2101 Constitution Avenue, NW
Washington 25, D.C.   (1)

National Research Council
Montreal Road
Ottawa 2, Canada
Att: E.S. Turner   (1)

Webb Institute of Naval Architecture
Glen Cove, Long Island, New York
Att: Professor E.V. Lewis   (1)
      Technical Library   (1)

Institute of Mathematical Sciences
New York University
25 Waverly Place
New York 3, New York
Att: Professor J.J. Stoker   (1)
      Professor A. Peters   (1)
      Professor J. Keller   (1)
      Professor R. Courant   (1)

New York University
Department of Oceanography
University Heights
New York 53, New York
Att: Professor W.J. Pierson, Jr.   (1)

The Johns Hopkins University
Baltimore 18, Maryland
Att: Professor S. Corrsin   (1)
      Professor F.H. Clauser   (1)
      Professor O.M. Phillips   (1)

Commanding Officer and Director
David Taylor Model Basin
Washington 7, D.C.
Att: Codes 142 (1)
500 (1)
513 (1)
521 (1)
522 (1)
526 (1)
530 (1)
550 (1)
563 (1)
580 (1)
585 (1)
591 (1)
600 (1)
800 (1)
520 (1)

Commander
Naval Ordnance Laboratory
Silver Spring, Maryland
Att: Dr. A. May (1)
Desk DA (1)
Desk HL (1)
Desk DR (1)

Commander
Naval Ordnance Test Station
China Lake, California
Att: Mr. J.W. Hicks (1)
Codes 5014 (1)
4032 (1)
753 (1)

Commander
U.S. Naval Ordnance Test Station
Pasadena Annex
3202 E. Foothill Boulevard
Pasadena 8, California
Att: Mr. J.W. Hoyt (1)
Research Division (1)
P508 (1)
P804 (1)
P807 (1)
P80962 (Library Division) (1)

Hydrographer
U.S. Navy Hydrographic Office
Washington 25, D.C. (1)

Superintendent
U.S. Naval Academy
Annapolis, Maryland
Att: Library (1)

Commanding Officer and Director
U.S. Navy Marine Engineering Laboratory
Annapolis, Maryland
Att: Code 750 (1)

Commander
U.S. Naval Weapons Laboratory
Dahlgren, Virginia
Att: Technical Library Division (AAL) (1)
Computation and Exterior Ballistics
Laboratory (Dr. A.V. Hershey) (1)

Commanding Officer
NROTC and Naval Administrative Unit
Massachusetts Institute of Technology
Cambridge 39, Massachusetts (1)

Commanding Officer
Underwater Sound Laboratory
Fort Trumbull
New London, Connecticut
Att: Technical Library (1)

Commanding Officer and Director
U.S. Navy Mine Defense Laboratory
Panama City, Florida (1)

Superintendent
U.S. Naval Postgraduate School
Monterrey, California
Att: Library (1)
Dept. of Meteorology and
Oceanography (1)

Commanding Officer
Naval Electronic Laboratory
San Diego 52, California
Att: Codes 4223 (1)
2201 (1)
2420 (1)

Commanding Officer and Director
U.S. Naval Civil Engineering Laboratory
Port Hueneme, California
Att: Code L54 (1)

Director
Applied Physics Laboratory
The Johns Hopkins University
8621 Georgia Avenue
Silver Spring, Maryland   (1)

California Institute of Technology
Pasadena 4, California
Att: Hydrodynamics Laboratory   (1)
        Professor T.Y. Wu   (1)
        Professor A. Ellis   (1)
        Professor A. Acosta   (1)
        Professor H.W. Leipmann   (1)
        Professor M. Plesset   (1)
        Dr. J. Laufer   (1)
        Professor C.B. Milliken   (1)

University of California
Berkeley 4, California
Att: Department of Engineering   (1)
        Professor H.A. Schade   (1)
        Professor J. Johnson   (1)
        Professor J.V. Wehausen   (1)
        Professor E.V. Laitone   (1)
        Professor S.A. Schaaf   (1)
        Professor P. Lieber   (1)
        Professor M. Holt   (1)

University of California
Los Angeles, California
Att: Professor R.W. Leonard   (1)
        Professor A. Powell   (1)

Director
Scripps Institution of Oceanography
University of California
La Jolla, California   (1)

Iowa Institute of Hydraulic Research
State University of Iowa
Iowa City, Iowa
Att: Professor H. Rouse   (1)
        Professor L. Landweber   (1)
        Professor P.G. Hubbard   (1)

Harvard University
Cambridge 38, Massachusetts
Att: Professor G. Birkhoff   (1)
        Professor G.F. Carrier   (1)
        Professor S. Goldstein   (1)
        Professor B. Budiansky   (1)

University of Michigan
Ann Arbor, Michigan
Att: Engineering Research Institute (1)
        Professor W.W. Willmarth   (1)
        Professor V. Streeter   (1)
        Professor F.G. Hammitt   (1)
        Professor R.B. Couch   (1)

Director
Ordnance Research Laboratory
Pennsylvania State University
University Park, Pennsylvania
Att: Dr. E.J. Skudrzyk   (1)
        Dr. G.F. Wislicenus   (1)
        Dr. M. Sevik   (1)

Michigan State College
East Lansing, Michigan
Att: Professor H.R. Henry   (1)
        Professor H. Elrod   (1)

Director
St. Anthony Falls Hydraulic Laboratory
University of Minnesota
Minneapolis 14, Minnesota   (1)
Att: Mr. J.N. Wetzel   (1)
        Professor B. Silberman   (1)
        Professor E.R.G. Eckert   (1)

Massachusetts Institute of Technology
Cambridge 39, Massachusetts
Att: Professor P. Mandel   (1)
        Professor M.A. Abkowitz   (1)
        Professor Mollo-Christensen   (1)
        Professor M. Landahl   (1)
        Professor A.H. Shapiro   (1)
        Professor A.T. Ippen   (1)
        Professor C.C. Lin   (1)
        Professor P. Griffith   (1)
        Professor H. Ashley   (1)
        Professor T.Y. Toong   (1)

Institute for Fluid Mechanics
and Applied Mathematics
University of Maryland
College Park, Maryland
Att: Professor J.M. Burgers   (1)
        Professor F.R. Hama   (1)
        Professor A. Weinstein   (1)
        Professor M.A. Martin   (1)
        Professor J.R. Weske   (1)

Brown University
Providence 12, Rhode Island
Att: Dr. R.E. Meyer   (1)
        Dr. W.H. Reid   (1)
        Professor P.J. Westervelt   (1)

Stevens Institute of Technology
Davidson Laboratory
Hoboken, New Jersey
Att: Mr. D.Savitsky   (1)
        Mr. J.P. Breslin   (1)
        Dr. D.N. Hu   (1)
        Dr. S.J. Lukasik   (1)
        Mr. H.W. MacDonald   (1)
        Mr. E. Numata   (1)

Director
Woods Hole Oceanographic Institute
Woods Hole, Massachusetts   (1)

Stanford University
Stanford, California
Att: Dr. Byrne Perry   (1)
        Professor D. Gilbarg   (1)
        Professor J.K. Vennard (1)
        Professor P. Garabedian (1)
        Mr. L.I. Schiff   (1)
        Dr. S. Kline   (1)
        Professor E.Y. Hsu   (1)

Princeton University
Princeton, New Jersey
Att: Professor W. Hayes   (1)
        Professor L.L. Crocco (1)
        Professor E.J. Brunelle (1)

Aeronautical Engineering Department
Catholic University of America
Washington, D.C.
Att: Professor M.M. Munk, Head (1)

Department of Mechanical Engineering
Syracuse University
Syracuse, New York
Att: Professor S. Eskinazi (1)

Department of Mathematics
Rensselaer Polytechnic Institute
Troy, New York
Att: Professor R.C. DiPrima (1)

Department of Aeronautical Engineering
University of Colorado
Boulder, Colorado
Att: Professor M.S. Uberoi   (1)

University of Delaware
Newark, Delaware
Att: Professor A.B. Metzner   (1)

Mr. L.M. White
U.S. Rubber Company
Research and Development Department
Wayne, New Jersey   (1)

Mr. G.W. Paper
ASW and Ocean Systems Department
Lockheed Aircraft Corporation
Burbank, California   (1)

Dr. B. Zarwyn
Airborne Instruments Laboratory
Division of Cutler-Hammer Inc.
Walt Whitman Road, Melville
Long Island, New York   (1)

Dr. L.L. Higgins
Space Technology Laboratories, Inc.
Canoga Park Facility
8433 Fallbrook Avenue
Canoga Park, California   (1)

Mr. Myron J. Block
Block Associates, Inc.
385 Putnam Avenue
Cambridge 39, Massachusetts   (1)

Dr. A. Ritter
Therm Advanced Research Division
Therm, Inc.
Ithaca, New York   (1)

Dr. Ira Dyer
Bolt, Beranek, and Newman, Inc.
50 Moulton Street
Cambridge, Massachusetts   (1)

Hydronautics, Incorporated
Pindell School Road
Howard County
Laurel, Maryland
Att: Mr. P. Eisenberg, President (1)
      Mr. M.P. Tulin, Vice President (1)

Dr. J. Kotik
Technical Research Group, Inc.
Route 110
Melville, New York   (1)

AiResearch Manufacturing Company
9851-9951 Sepulveda Boulevard
Los Angeles 45, California
Att: Blaine R. Parkin   (1)

Hydrodynamics Laboratory
Convair
San Diego 12, California
Att: Mr. H.E. Brooke   (1)
        Mr. R.H. Oversmith   (1)

Director
Hudson Laboratories
Dobbs Ferry, New York   (1)

Aerojet General Corporation
6352 N. Irwindale Avenue
Azusa, California
Att: Mr. C.A. Gongwer   (1)

Director, Special Projects Office
Department of the Navy
Washington 25, D.C.
Att: Codes SP-001   (1)
              SP-201   (1)

Commander
Puget Sound Naval Shipyard
Bremerton, Washington   (1)

Professor L.M. Milne-Thomson
Mathematical Research Center
1118 W. Johnson Center
Madison 5, Wisconsin   (1)

Mr. Richard Barakat
Optics Department
Itek Corporation
Lexington, Massachusetts   (1)

College of Engineering
University of California
Davis, California
Att: Professor S.R. Keim   (1)

Superintendent
U.S. Merchant Marine Academy
Kings Point, Long Island, New York
Att: Department of Engineering   (1)

Commandant
U.S. Coast Guard
1300 E. Street, NW
Washington, D.C.   (1)

Commander
Hdqs. U.S. Army Transportation
Research and Development Command
Transportation Corps
Fort Eustis, Virginia
Att: Marine Transport Division   (1)

Maritime Administration
441 G Street, NW
Washington 25, D.C.
Att: Division of Ship Design   (1)
         Research and Development   (1)

Director of Research
National Aeronautics and Space
Administration
1512 H Street NW
Washington 25, D.C.   (1)

Society of Naval Architects and
Marine Engineers
74 Trinity Place
New York 6, New York   (1)

New York State Maritime College
Engineering Department
Fort Schuyler, New York
Att: Professor J.J. Foody   (1)

Cornell School of Aeronautical Engineering
Cornell University
Ithaca, New York
Att: Professor W.R. Sears   (1)

Southwest Research Institute
8500 Culebra Road
San Antonio 6, Texas
Att: Dr. H.N. Abramson   (1)

Manchester University
Manchester, England
Att: Professor F. Ursell   (1)

Mr. C. Wigley
Flat 103
6-9 Charterhouse Square
London E.C.1, England   (1)

Oceanics, Incorporated
Plainview, Long Island, New York
Att: Dr. Paul Kaplan   (1)

Professor R.C. MacCamy
Department of Mathematics
Carnegie Institute of Technology
Pittsburgh 10, Pennsylvania   (1)

Dr. K. Eggers
Institut fur Schiffbau
University of Hamburg
Berliner Tor 21
Hamburg, Germany   (1)

Dr. R. Tinman
Department of Applied Mathematics
Technological University
Julianalaan 132
Delft, The Netherlands   (1)

Secretary Ship Structure Committee
U.S. Coast Guard Headquarters
1300 E Street NW
Washington 25, D.C.   (1)

Commander
Military Sea Transportation Service
Department of the Navy
Washington 25, D.C.   (1)

Oceanographer
U.S. Naval Oceanographic Office
Washington 25, D.C.
Att: Library (Code 1640)   (1)

Director
Coast and Geodetic Survey
U.S. Department of Commerce
Washington 25, D.C.
Att: Office of Oceanography   (1)

Mr. James Trumbull
U.S. Geological Survey
Washington 25, D.C.   (1)

Director
U.S. Army Engineers Waterways
Experiment Station
Vicksburg, Mississippi
Att: Research Center Library   (1)

Director
National Oceanographic Data Center
Washington 25, D.C.   (1)

Director
Narragansett Marine Laboratory
University of Rhode Island
Kingston, Rhode Island   (1)

Gulf Coast Research Laboratory
Post Office Box
Ocean Springs, Mississippi
Att: Librarian   (1)

Director
Lamont Geological Observatory
Torrey Cliff
Palisades, New York   (1)

Director
Hudson Laboratories
145 Palisade Street
Dobbs Ferry, New York   (1)

Director
Chesapeake Bay Institute
Johns Hopkins University
121 Maryland Hall
Baltimore 18, Maryland   (1)

Mr. Henry D. Simmons, Chief
Estuaries Section
Waterways Experiment Station
Corps of Engineers
Vicksburg, Mississippi   (1)

Director, Marine Laboratory
University of Miami
1 Rickenbacker Causeway
Virginia Key
Miami 49, Florida   (1)

Head, Department of Oceanography
and Meteorology
Texas A and M College
College Station, Texas   (1)

Allan Hancock Foundation
University Park
Los Angeles 7, California   (1)

Head, Department of Oceanography
Oregon State University
Corvallis, Oregon   (1)

Head, Department of Oceanography
University of Washington
Seattle 5, Washington   (1)

Department of Meteorology and
Oceanography
University of Hawaii
Honolulu 14, Hawaii
Att: Dr. H.M. Johnson   (1)

Department of Geodesy and Geophysics
Cambridge University
Cambridge, England   (1)

Applied Physics Laboratory
University of Washington
1012 NE Fortieth Street
Seattle 5, Washington   (1)